CONCRETE IN AUSTRALIA
VOLUME 40 ISSUE 1 MARCH 2014
$9.95 inc. GST

TECHNICAL FEATURE
Geopolymers

# Shear design and evaluation of concrete structures

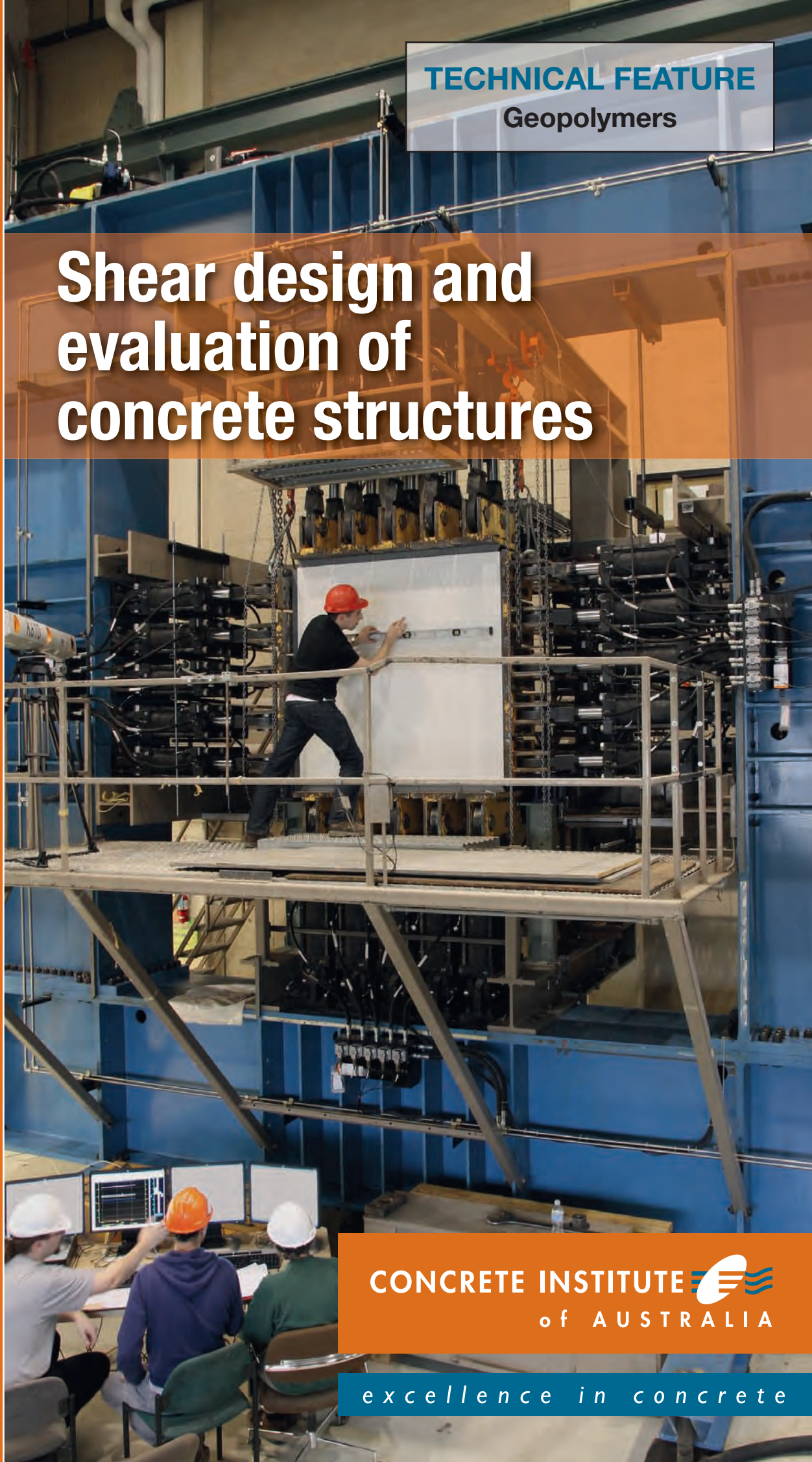

CONCRETE INSTITUTE of AUSTRALIA
excellence in concrete

# Design for shear, a work in progress

The history of the development of the theory of beam bending is a fascinating story, with many twists, turns, and dead ends on the way.

The story starts with Leonardo da Vinci in 1493, but it was Galileo in 1638 who published the first numerical theory, which over-estimated beam bending strength by a factor of 3. Edme Mariotte published a partially corrected theory in 1686, but through a calculation error this still gave double the correct bending strength.

This error was corrected by Antoine Parent in 1713, but was presented in a work so obscure that it had no influence. The first widely influential and correct theory was Euler's development of the work of the Bernoullis, published in 1744. Even this was not widely accepted in the field of practical engineering, and at the turn of the century Galileo and Mariotte's theories were still widely used. It was not until the mid-19th Century that the Euler-Bernoulli theory became widely accepted.

It might be expected that by now this story would be purely of historical interest, but if we look at the current state of design for shear in reinforced and pre-stressed concrete beams we find many parallels with the situation in the late 18th Century.

The provisions for shear design in modern concrete codes are mainly based on old empirical relationships intended to provide a simple design procedure covering complex interactions between shear, bending and torsion. This has resulted in significant differences between and within codes. For instance, the design shear strength of a section under combined axial load, bending and shear may be significantly different depending on whether the procedures for columns or pre-stressed sections are applied.

At the very forefront of more recent experimental and theoretical work have been Professor Michael Collins and his colleagues at The University of Toronto, whose work led to the development of the Modified Compression Field Theory, published in 1986 by Collins and his co-author Frank Vecchio. Development of this work has continued, in recent years with the collaboration of Professor Denis Mitchell, and the major concrete codes are now moving away from the empirical approach and towards more rational and consistent methods. This trend is now being followed in Australia, with major revisions proposed to the shear design provisions in the draft of the new Bridge Design Code (AS 5100).

It is vital that all practising engineers working in concrete design have a good understanding of the best current work on the shear behaviour of concrete, and to this end, the Concrete Institute is pleased to offer as our first National Seminar series for 2014, a full day seminar on Shear Design of Concrete Structures, presented by Professors Collins and Mitchell. This is a rare opportunity to attend detailed presentations from two of the world's leading researchers on this topic and I encourage all members to attend and inform their colleagues of these seminars.

Another source of information on current research work is the ACI Technical Journals which are available to Institute members through our discounted joint membership rates. The latest issue, for instance, includes papers by Mitchell and Vecchio, and others relevant to shear design. In addition, the membership agreement includes subscription to the ACI Concrete International journal and members' discount rates to the vast ACI library of technical publications.

The dissemination of recent research through seminars and access to international publications is one of the ways in which the CIA is able to provide value to its membership and I encourage all members to make use of these opportunities.

***Douglas Jenkins***
*President, Concrete Institute of Australia*
*president@concreteinstitute.com.au*

CONCRETE INSTITUTE of AUSTRALIA

# CONCRETE IN AUSTRALIA

VOLUME 40 ISSUE 1 MARCH 2014



**Concrete Institute of Australia**
PO Box 1227, North Sydney 2059
Tel: +61 2 9955 1744
Fax: +61 2 9966 1871
e-mail: help@concreteinstitute.com.au
web: www.concreteinstitute.com.au



**ISSN 1440-656X, VOL 40 No 1**

**EDITOR:**
Desi Corbett

**MANAGING EDITOR:**
Dr Tim Kannegieter

**ADVERTISING:**
**NSW/ACT:**
Dee Grant, dgrant@engineersmedia.com.au
phone 0435 758 081

**Vic, Tas, SA, WA:** David Sutcliffe,
dsutcliffe@engineersmedia.com.au
phone 0497 211 122

**Queensland:** MBL Media, Maree Fraser,
mblmedia@bigpond.com
phone 07 5580 9000

**DESIGN:** Stefan Novak, Michelle Watts

*Concrete in Australia* is produced
for the Concrete Institute of Australia
by Engineers Media
phone 02 9438 1533
email editorial@engineersmedia.com.au



*Average Net Distribution*
CIRCULATIONS AUDIT BOARD
*1713*
*October 2012 to March 2013*

# Contents



## 39 FEATURE: GEOPOLYMERS



## ALSO IN THIS ISSUE




*Shear design and evaluation of concrete structures by Michael P. Collins and Denis Mitchell.* *To read more on this turn to page 28.*

# Concrete Institute of Australia welcomes new CEO

In December 2013, the President of the Concrete Institute of Australia, Doug Jenkins, announced the appointment of David Millar as the new Chief Executive Officer of the Institute. A civil engineer and business graduate with over 20 years' experience, David is well known particularly through his previous role as Executive Director for the Concrete Pipe Association of Australasia, and from his long-standing involvement with the NSW Branch Committee of the Institute.

David formally commenced his role as CEO on 6 January.

Doug Jenkins said David offers an excellent combination of existing industry knowledge and contacts along with well-developed ideas for the continuing stability and growth of the Institute. And David said he is looking forward to continuing the Institute's drive towards its mission, promoting and developing excellence in concrete technology, application, design and construction throughout Australia, and working closely with members, committee members, and allied industry groups to achieve this.

"With a long standing involvement with the Institute I have seen, and been able to take advantage of, the many benefits the CIA has offered its members.

*David Millar*

"I'm hopeful that in my new role I'll be able to use this experience to get closer to our members and understand what's important to them and how we can provide greater value to the concrete industry," David said.

"Our main focus will be on delivering this value through quality education programs, technical events, and publications, as well as delivering added benefits through our alliances with the American Concrete Institute and *fib*. We're also in full-swing, organising the next biennial conference which will be held in Melbourne in September 2015, which includes hosting the international RILEM conference."

David went on to add that the CIA biennial conference will remain a focal point of the Institute's program for members, but other forms of providing education and information are always being considered.

"Social media, webinars, and online learning tools have become part of everyday life and part of understanding how our members work is finding out what tools they use for research, learning and being informed, and applying those to deliver the Institute's products," David said.

Doug welcomed David to his new position, saying the Institute is looking forward to working with him as the CIA Council, State Branches and various committee members continue to grow the Institute and maximise the benefits that are provided to members.

# AUSTRALIAN STANDARDS ON-LINE

By special agreement with SAI Global, the Concrete Institute of Australia is pleased to offer an ***Australian Standards On-line service,*** a new low cost service available to Individual Members of the Institute.

**This service has been specially developed by SAI Global to enable the Concrete Institute of Australia to provide a comprehensive Standards reference service to the Institute's current Individual Members, at a fraction of the cost of the full SAI Global On-Line Subscription Service.**

**This service will give you instant access via laptop and PDA to:**

- **All Australian Standards (AS)**
- **Joint Australia / New Zealand Standards (AS/NZS)**
- **Adoptions of International Organization for Standardization (ISO) and International Electrotechnical Commission (IEC) Standards**

**Subscribers to this service can also purchase Standards at a discounted rate of 20% off the hardcopy price (this offer excludes already discounted packages such as Reusable Electronic Contracts).****

The annual cost to subscribe to this service is **$220.00 (Incl. GST).***

**For more information on CIA membership, visit:**
**http://www.concreteinstitute.com.au/Membership**

*Subject to the term and other conditions of the agreement between SAI Global and the CIA
**Based on SAI Global's standard rates for a comparable service as at 04/10/2013

CONCRETE INSTITUTE of AUSTRALIA

SAI GLOBAL

*Fiona Stanley Hospital concrete core – formwork by PERI.*

# Formwork Seminar wrap up

The national technical program finished up 2013 with the Concrete Formwork Seminar held from 19 to 29 November in Brisbane, Sydney, Melbourne and Perth.

PERI, one of the largest manufacturers and suppliers of formwork and scaffolding systems worldwide, were the major sponsors of the event.

Delegates who attended the full day seminar were given the first opportunity to receive the draft Formwork Handbook, prepared and authored by Stephen Ferguson, and co-authored by Doug Crawford. The handbook was bundled with the notes package and was the first time a publication in draft format was given for peer review to non-members of the Institute.

The Formwork Handbook will be released for peer review to all members of the Concrete Institute of Australia in the first quarter of 2014. This will further provide an opportunity to those members involved in the formwork industry to provide the CIA Publications Committee and the Formwork Handbook review sub-committee some feedback before the document is published later in 2014.

The Institute would like to thank the presenters, Stephen Ferguson and Justin Smith, for sharing their knowledge and experience in design, construction, quality and safety.

# World first earth-friendly concrete airport

A new regional airport in southeast Queensland is not only the first privately built public airport in Australia in 50 years but it is the only airport in the world to be made with "earth-friendly concrete" (EFC).

Owned and developed by EFC maker, Wagners, the Wellcamp Airport, 17km west of Toowoomba, will be the largest geopolymer concrete pavement project in the world. EFC is a unique high performance and environmental concrete that can be produced and constructed like normal concrete in ambient curing conditions.

The material is a low carbon alternative to conventional concrete as it does not contain ordinary Portland cement (OPC). Instead, it is made from recycled slag and recycled fly ash in combination with chemical activators, which create a superior performing geopolymer binder. According to Wagners, the complete elimination of OPC from the concrete also results in "enormous carbon dioxide emission savings" and recycles two common waste by-products from industry.

"EFC is the lowest carbon concrete produced in the world and contains one of the highest levels of sulphate and chloride resistance," company director, Joe Wagner said.

Wagners estimates that 6,600t of $CO_2$ emission reduction will result from using EFC in the airport apron and taxiway pavements instead of conventional concrete. A high capacity wet-mix mobile batch plant has been set up at the airport project site and the 2.87km runway is on track to be completed in April this year.

Around 30,000m$^3$ of EFC will be used in the Wellcamp Airport as well as large volumes of the geopolymer concrete are to be used for buildings in the project as well as the adjacent business park precinct.

The airport's concrete pavements have a flexural tensile strength specification of 4.8MPa and typical depths will be 400-440mm. Due for completion in late 2014, the airport will be able to cater for Boeing 747s, 737s and Airbus A330s.

EFC evolved when Wagners began experimenting with geopolymer concretes composite fibre building products. The company spent more than eight years developing EFC and said many early projects were monitored under R&D conditions for producing the necessary material data to support structural commercial applications.

Two precast prestressed bridge beams were produced in EFC in December 2010 and have been continuously monitored since that time to assess both short term and long term deformations under load. The data shows that the structural performance of EFC is entirely predictable using the standard concrete design techniques enshrined in design codes.

This work along with many other EFC studies has been reported by Dr

*Approximately 30,000m³ of EFC will be used for the Wellcamp Airport's taxiways and apron.*

James Aldred of Aecom in "Engineering Properties of a Proprietary Premixed Geopolymer Concrete", Proceedings – Concrete 2013 Understanding Concrete, Concrete Institute of Australia, Sydney.

In his paper, Dr Aldred outlined significant benefits in terms of sustainability, drying shrinkage, temperature rise and chemical resistance that suggest EFC offers important technical benefits in certain applications.

He said it provided advantages in sulfate rich or acidic environments such as industrial and sewerage facilities, where Portland cement based products can be subject to significant attack.

The product recently won two major national awards: The 2013 *Building Product News* (BPN) sustainability award in the product innovation category and overall winner of the BPN awards. EFC was also a category winner for High Tech Manufacture and Design at the Australian Shell Innovation Awards. Wagner explained that EFC can also be used in a range of construction applications such as commercial precast, underground tunnels, gas plants and large commercial pavements.

The product has already been used in the floor panels of the $32 million Global Change Institute at the University of Queensland and has potential for commercial precast, underground tunnels, gas plants and large commercial pavements.

Wagners said there is already "strong interest" in Australia and internationally in EFC given its durability and structural performance advantages over normal concrete.

These include high resistance to sulphate attack and chloride ion ingress, very low heat of reaction, low shrinkage (typically 350 microstrain when tested using the AS drying shrinkage test) and high flexural tensile strength.

The company said EFC is cost competitive against other concretes that need to be of a similar performance level.

International®

# Intercrete™

## Advanced Concrete Repair and Protection

### Complete solutions for structural concrete infrastructure

- Rapid setting properties allow fast return to service
- Application on green concrete enables fast track construction
- Solutions for construction defects – low cover, slip-forming repairs
- Provides long term protection from carbonation, chloride attack and ingress of water
- Waterborne cement-based technology – zero VOC

**Contact us for your next project:**

**Toll Free Australia 131 474 | Toll Free New Zealand 0800 808 807**

**pc-australasia@akzonobel.com | www.international-pc.com**

AkzoNobel

# The changing future of cement and concrete: threat or opportunity

The Institute of Concrete Technology (ICT) in the UK is hosting a technical symposium to discuss a range of issues that it says will affect, and effect, the future of concrete and those who are involved in its manufacture, provision and use.

As a material capable of development in response to changes in design, demanded performance, environmental and sustainability issues, as well as social challenges, concrete has changed over time and will continue to change into the future, the ICT says.

Speakers at the ICT symposium on 27 March 2014 will include Dr Leon Black (University of Leeds) and John Gibbs (ERMCO) on the twin drivers of carbon pricing and legislation; Prof John Provis (University of Sheffield) on geopolymer concrete; and Prof Peter Hewlett and Dr Martin Liska (David Ball Group) on alternatives to Portland cement. Ian Gibb (Mott McDonald) will speak on changes in concrete specification, Martin Clarke will present on the new World Concrete Forum, and Prof Simon Austin will deliver the keynote lecture on 3-D printing in construction and its future.

The one-day event is part of the ICT's 42nd annual convention that includes a golf competition, annual members meeting and gala dinner. The program and registration form can be found at http://ict.concrete.org.uk/events.

# NSW company wins at World Concrete Awards

Honestone, an Australian floor and wall surfacing company, has received an award for a warehouse conversion in Sydney's inner city Paddington from the American Society of Concrete Contractors at the recent 2014 World Concrete Awards. The second place award in the Multiple Application <5000 square feet category was the third win for the NSW company at the Decorative Concrete Council Awards in the US which judges best practice application and the innovative use of concrete around the globe.

Honestone was recognised for its application of panDOMO Wall and Floor which the company chose to create "a balanced feeling of minimalism, industrial and home" throughout the residential warehouse. The cement-based composition creates smooth surfaces with a modern, reductionist look. Honestone said the product can be tinted or texturised with a wide array of specially-developed dyes and aggregate mixes. In this particular project, a range of bespoke modern and industrial greys was used.

Company director Rick Hendriks said using panDOMO allowed the project's collaborators to create concrete slab-looking features such as indentations and join lines with what is essentially a liquid product.

"We worked closely with the architect and homeowners to create the perfect spectrum of greys – modern and industrial, but not too cold or uninviting, as we had to work with original features being retained such as bare brick walls," Hendriks said.

# A PRODUCT AS STRONG AND ROBUST AS YOURS

CHILLERS FOR CONCRETE BATCH PLANTS

1300 CHILLERS

info@matsu.com.au

matsu.com.au

Summit Matsu Chillers

An AIR CHANGE Company

For Peak Performance

SUMMIT MATSU CHILLERS

Reliability Guaranteed

# The year ahead – CIA calendar for

| DATE | NSW | QLD | VIC | SA | WA | TAS |
|---|---|---|---|---|---|---|
| **Wed, 19 February** | Corrosion | | | | | Site Visit (TBA) |
| **Tues, 25 February** | | | | AEFAC joint seminar – Chemical Anchors in Construction | | |
| **Wed, 5 March** | | | | | **Shear Design National Seminar** | |
| **Fri, 7 March** | | | **Shear Design National Seminar** | | | |
| **Tues, 11 March** | | Cracking/Concrete Repair | | **Shear Design National Seminar** | | |
| **Wed, 12 March** | | **Shear Design National Seminar** | | | | |
| **Fri, 14 March** | **Shear Design National Seminar** | | | | | |
| **Tues, 18 March** | | | Rail Projects | | | |
| **Wed, 19 March** | | | | | | Chemical Anchors End Users, Hobart |
| **Tues, 1 April** | | Concrete Masonry | | | | |
| **Tues, 8 April** | | | | | Innovations in Design | |
| **Wed, 9 April** | | | | Precast/Corrosion | | |
| **Wed, 16 April** | Retaining Structures | | | | | |
| **Tues, 22 April** | | | | | | Piling, Retaining Walls & Foundation – Design Concepts, Hobart |
| **Wed, 23 April** | | | | | | Piling, Retaining Walls & Foundation – Design Concepts, Invermay |
| **Tues, 29 April** | | | Concrete Mix Design | | | |
| **Wed, 30 April** | | | | Fundamentals of Concrete Course week 1 | | |
| **Wed, 7 May** | | | | Fundamentals of Concrete Course week 2 | | |
| **Tues, 13 May** | | | | | Concrete Tanks | |
| **Wed, 14 May** | Boral Materials Services Laboratory Site Visit | | | Fundamentals of Concrete Course week 2 (Uni lab) | | |
| **Tues, 20 May** | | Developments in Concrete Technology | High Rise Design and Construction | | | |
| **Wed, 21 May** | Structural Strengthening of Concrete Structures | | | Fundamentals of Concrete Course week 4 | | Sponsors New Products for Concrete End Users, Invermay |
| **Wed, 28 May** | | | | Fundamentals of Concrete Course week 5 | | |
| **Wed, 4 June** | | | | Fundamentals of Concrete Course week 6 | | |
| **Tues, 10 June** | | **Steel Reinforcement Detailing National** | | | Concrete Pavements and Infrastructure | |
| **Wed, 11 June** | **Steel Reinforcement Detailing National** | | | | | |
| **Thurs, 12 June** | | | **Steel Reinforcement Detailing National** | | | |
| **Tues, 17 June** | | Deep Foundations | Durability in Concrete | **Steel Reinforcement Detailing National** | | |

# national and branch events 2014

| DATE | NSW | QLD | VIC | SA | WA | TAS |
|---|---|---|---|---|---|---|
| **Thurs, 19 June** | | | | | **Steel Reinforcement Detailing National** | |
| **Wed, 25 June** | | | | | | Corrosion Concrete Case Studies, Hobart |
| **Thurs, 26 June** | | | | | | Corrosion Concrete Case Studies, Invermay |
| **Tues, 8 July** | | | | | Concrete Repair | |
| **Tues, 15 July** | | | Torsion in Concrete Elements and Structures | | | |
| **Thus, 17 July** | Fire in Concrete Structures | | | | | |
| **Tues, 22 July** | | Architectural Concrete | | Reinforcing – What's new | | AS3850 Tilt and Precast Designers, Hobart |
| **Wed, 23 July** | | | | | | AS3850 Tilt and Precast Designers, Invermay |
| **Wed, 13 August** | Cracking in Concrete | | | | | |
| **Tues, 19 August** | | Seismic Design | Innovations in Precast Concrete Design and Construction | | | |
| **Wed, 27 August** | | | | | | Sponsors New Products for Concrete End Users, Hobart |
| **Tues, 16 Sept** | | Admixtures & Additives | Fire Resistance Levels in Concrete | | | |
| **Tues, 23 Sept** | | | | | | Latest Developments in Concrete Technologies, Hobart |
| **Wed, 24 Sept** | Mini Conference (topics TBC) | | | Hot Weather Concreting | | Latest Developments in Concrete Technologies, Invermay |
| **Tues, 14 October** | | | | | Hot Weather Concreting | |
| **Wed, 15 October** | Precast & Tilt up | | | | | |
| **Tues, 21 October** | | Standards Review Update | Major Project Case Studies | | | |
| **Wed, 22 October** | | | | | | Chemical Anchors End Users, Invermay |
| **TBC November** | **Durability National** OneSteel Sydney Steel Mill Site Visit | **Durability National** | **Durability National** | **Durability National** | **Durability National** | |
| **Tues, 11 November** | | | | | High Performance Concrete | |
| **Tues, 18 November** | | | Connection Performance in Concrete Structures | | | |
| **Tues, 25 November** | | Post-Tensioning | | | | Site Visit (TBA) |
| **Tues, 2 December** | | | | | | Members & Sponsors Networking End of Year Function, Hobart |
| **Wed, 10 December** | Major Project Case Studies | | | Sponsors Christmas breakfast | | |
| **Tues, 16 December** | | | Annual Sponsors Christmas Cocktail Party | | | |

Event dates and topics subject to change at any time. Please confirm with the Institute's national office and website.
For more information please visit http://www.concreteinstitute.com.au/Events-Seminars.aspx

# Early delivery for underpass despite challenges

The final stage of the Perth City Link rail project was opened in December 2013 and despite it being delivered six months ahead of schedule, the project was not without its challenges.

The Perth City Link Rail Alliance (Western Australian Public Transport Authority, John Holland and GHD) commenced work in early 2011 to build the new Fremantle Line tunnel and upgrade of Perth Station with two new features, an island platform for special events and the pedestrian underpass.

Perth train commuters are now using the underpass to connect between Perth and Perth Underground stations, significantly improving access and transfer times. However, its construction posed several challenges for the engineers involved as it sits four metres below the water table and runs underneath a major arterial road and the heritage-listed Perth Station building.

*Excavation works for the underpass below Wellington Street, Perth.*

Work to build the underpass began in November 2011 using a combination of bottom-up and top-down construction techniques.Top-down construction was used inside Perth Station so trains could continue operating, travelling over the roof of the underpass, while walls and base slabs were being built below.

Alliance Construction Manager Pat McCarthy explained the various challenges involved in pouring more than 7500 cubic metres of concrete to build the 162 metre long, seven metre wide, and three metre high underpass.

"Piling was the first stage of construction. Working inside an operating train station meant access and space were restricted, limiting the type of piling rigs that could be used.

"To form the structure of the

*The completed pedestrian underpass, December 2013.*

underpass 629 piles were installed using a combination of Continuous Flight Auger (CFA) piling inside Perth Station, and secant piling in Wellington Street forecourt," he said.

"Mini piling rigs were used to bore 300mm diameter piles up to 45 metres deep down to the Kings Park rock formation. CFA piling was the most efficient method to use and its major benefit was the minimum level of noise and vibration, which ensured the integrity of nearby structures and buildings was maintained."

Holcim Australia supplied a variety of special purpose concrete mixes that were engineered and tested to minimise concrete expansion, and to ensure the required 120 year design life would be achieved.

"Within the piled walls, 50MPa concrete was used and 40MPa structural concrete mix in other areas. In some sections the waterproofing additive caltite was mixed, supplied by Cementaid, where other means of waterproofing was not possible and to ensure the roof of the underpass remained water tight. Low heat concrete was also used for certain walls to prevent shrinkage during the base slab curing process," McCarthy said.

Some of the project challenges involved temporarily closing three traffic lanes on Wellington Street to build the connection from Perth Station to Perth Underground, and suspending the station building before excavating underneath.

Post-tensioned concrete underpinning beams supported by the piles were used to 'clamp' the existing Perth station building foundations to carry out the station underpinning. The technique was a success with zero settlement recorded. To 'breakthrough' into Perth Underground and link the two stations, a staged process was carried out to wire-saw through the existing 1.2metre thick diaphragm walls.

Features of the new underpass include architectural skylights at platform level inside Perth Station which provide natural light and air below ground. In addition, new lifts, stairs and escalators improve passenger flow and provide better access between the two stations.

Each day more than 9300 passengers transfer between Perth Station and Perth Underground. By 2031, this will increase to an estimated 22,600 people per day.

# Concrete 2015

Concrete 2015, the 27th Biennial National Conference of the Concrete Institute of Australia, will be held next year in conjunction with the 69th RILEM Week conference. This historic joint event will provide national delegates with valuable exposure to cutting edge research and development exchanges in the international forum of RILEM Week and will be held at the Pullman Albert Park in Melbourne, from 30 August to 2 September, 2015. Concrete 2015 will focus on the theme 'Research into Practice'. The conference is dedicated to bringing together global leaders in the concrete industry, covering all aspects of concrete design improvements, research, construction, maintenance and repair of concrete projects. Concrete 2015 will offer participants from around the world the opportunity to connect face to face and share innovative and interesting ideas on valuable research outcomes and latest construction practices. Papers are invited that are based on experimental work, research and development, practice or industry application, case studies, innovations and other relevant work of interest. The multidisciplinary theme of Concrete 2015 will provide an excellent forum for networking and education and an opportunity to meet and interact with practitioners, engineers, scientists, researchers, academics, and professionals, and also to engage with international delegates from RILEM technical committees. We hope you can join us in Melbourne in August next year. Save the date!

*Professor Jay Sanjayan, Conference Chair – Concrete 2015*
*Dr Kwesi Sagoe-Crentsil, Technical Committee Chair*

# SHEAR DESIGN

**Perth 5 March | Melbourne 7 March | Adelaide 11 March**

**Brisbane 12 March | Sydney 14 March**

*Michael P. Collins*

*Denis Mitchell*


## The presenters

The Concrete Institute is proud to have two world renowned experts on shear – Michael P. Collins and Denis Mitchell – visiting Australia in March 2014 for the shear design seminar series.

Collins, University of Toronto, and Mitchell, McGill University, have together researched the behaviour of concrete structures for about forty years. They are best known for developing new approaches for the design of reinforced concrete in shear and torsion. These approaches, the compression field theory, the modified compression field theory and compatible strut-and-tie modelling have been incorporated into codes of practice and design manuals in Canada and the United States.

For their research they have received prizes and awards from the American Concrete Institute, the Prestressed Concrete Institute, the American Society of Civil Engineers, the Canadian Society for Civil Engineering, the Institution of Structural Engineers, and the Royal Society of Canada. Their philosophy of basing design and evaluation on simple, rational behavioural models was explained in their influential textbook "Prestressed Concrete Structures" and will inform their teaching of this seminar. As active consulting engineers, they have been involved in a significant number of failure investigations and in evaluating and strengthening concrete structures in distress.

## Topics covered in the seminar will include:

- Basics of shear response; behaviour of reinforced concrete elements in pure shear; the Compression Field Theory (CFT) and the Modified Compression Field Theory (MCFT).
- Shear response of reinforced and prestressed concrete flexural members; the size effect and the strain effect; design with the simplified MCFT; evaluation with program Response.
- Shear response of deep beams and other disturbed regions. Design with strut-and-tie models which consider compatibility; evaluation with program VecTor2
- Punching shear in slabs.
- Detailed design examples of bridge girder, deep transfer girder, shear wall coupling beam, post-tensioned floor beam and large footing.
- Lessons from shear failures and from evaluating the shear safety of existing concrete structures.

CONCRETE INSTITUTE of AUSTRALIA

# of concrete structures



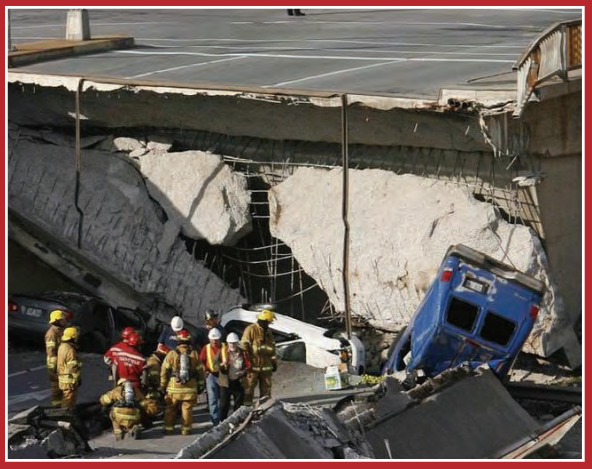

| | |
|---|---|
| 8.30AM | Welcome and Housekeeping: Day Chair |
| 8.45AM | Introduction and Overview: Michael Collins |
| 9.00AM | Basics of Shear Response: Michael Collins |
| 10.00AM | Morning Tea |
| 10.30AM | Design and Evaluation of Flexural Members: Michael Collins |
| 11.30AM | Design and Evaluation of Disturbed Regions: Denis Mitchell |
| 12.30PM | Lunch |
| 1.30PM | Punching Shear in Slabs: Denis Mitchell |
| 2.15PM | Examples of Design and Evaluation: Denis Mitchell |
| 3.00PM | Examples of Design and Evaluation: Michael Collins |
| 3.30PM | Afternoon Tea |
| 4.00PM | Lessons from Shear Failures: Denis Mitchell |
| 4.30PM | Lessons from Shear Failures: Michael Collins |
| 5.00PM | Close: Day Chair |

RECOGNISED FOR CPD BY ENGINEERS AUSTRALIA

**Ticket pricing: CIA Members $590.00 | CIA Student Members $295.00 | EA Members $640.00**
**Non-Members $795.00 | Seminar & Membership Package (incl. 12 month individual membership) $850.00**

**To register or to find out more please visit:**
**http://www.concreteinstitute.com.au/sheardesign.aspx**

# New solution makes crack widths almost invisible to the naked eye

The Admixture Systems business of BASF's Construction Chemicals division has announced the launch of a unique crack-reducing admixture technology in North America.

MasterLife CRA 007 admixture enhances the aesthetics and long-term durability of concrete by reducing the likelihood that cracking will occur and, if it does, minimises the crack width, according to BASF. The company said the MasterLife admixture will meet ASTM C494, Standard Specification for Chemical Admixtures for Concrete, Type S, Specific Performance Admixtures.

This patent-pending technology is a special class of shrinkage-reducing admixture that produces a maximum initial crack width of 175µm (.007 inches) in high-performance, crack-prone (HPCP) concrete mixtures tested in accordance with ASTM C1581 test method.

Photo: CC by Apasciuto (http://www.flickr.com/photos/apasciuto).

And the minimised crack width is almost invisible to the naked eye. Crack widths this small do not transport water and have the potential to self-heal over time, BASF explained, thus increasing concrete durability by minimising the ingress of chlorides, sulfates and other potentially harmful materials.

"Cracking is a major issue for the concrete industry, as it detracts from the aesthetics of concrete, can be a safety hazard, and may compromise durability or structural integrity," Juan Alfonso Garcia, vice president BASF – Admixture Systems said.

# Shear Rails: Pre-fabricated punching shear reinforcement

Gary Connah, Technical Manager, Ancon Building Products Pty Ltd

*The loads on a concrete slab supported on a concrete column induce shear stresses in the slab. Where additional reinforcement is not provided, this stress could result in the column 'punching' through the slab. Although this punching shear stress can be relieved by localised thickening of the concrete, such as downstand beams or enlarged column heads, the construction of a flat slab is often preferred. A consistent head space, a reduction in overall building height and significant savings in both time and materials are the main advantages of flat slab construction.*

## 1.0 SHEAR RAILS

Shear rails can be located around a column head or base to reinforce a flat slab against punching shear. The shear load from the slab is transferred through the studs and into the column.

A shear rail system comprises a number of stud and rail units which have been factory-produced to suit the specific requirements of a particular column. Each unit comprises double-headed studs, hot forged to 10 times the area of the bar, welded to a flat steel carrier rail. The rails are located around the column in the required layout.

The quantity and dimensions of studs and rails, the spacing and the layout are all determined by calculation. To simplify system design, shear rail manufacturers provide free calculation software and other technical support such as faxback design sheets.

The rails perform no structural function. They simply ensure stud alignment, spacing and vertical positioning within the slab. Studs are manufactured in a variety of diameters and in virtually any length to suit the load and depth of the slab.

## 2.0 SHEAR RAIL DESIGN

A shear rail reinforcement system is designed by calculating the stress at concentric perimeters around a column, in accordance with specifications set out in the Clause 9.2 of AS 3600: 2009[1], but the major part of the design is based on the research presented by F K Lim and B V Rangan from the School of Engineering, Curtin University of Technology, Perth.

The first stud is positioned 0.5 d from the face of the column, i.e. along critical shear perimeter, with the spacing between individual studs taken at 0.7 (D – top cover – bottom cover – 5) with a maximum limit of 500 mm. The maximum spacing between parallel rails is 600 mm or D whichever is less, where D is the overall depth of the slab and d is the effective depth of the slab. Rail layouts can be radial or orthogonal. Shear rail manufacturers provide free calculation software, which simplifies this design process.

A shear rail system is designed for all column shapes (rectangular, circular, L-shaped etc.) and locations (edge, corner, interior etc.). They can be installed either top down or bottom up – selection is based on user preference. When installed top

*Figure 1: Ancon shearfix stud welded to a flat rail.*

*Figure 2: Shear rails arranged around a column head.*

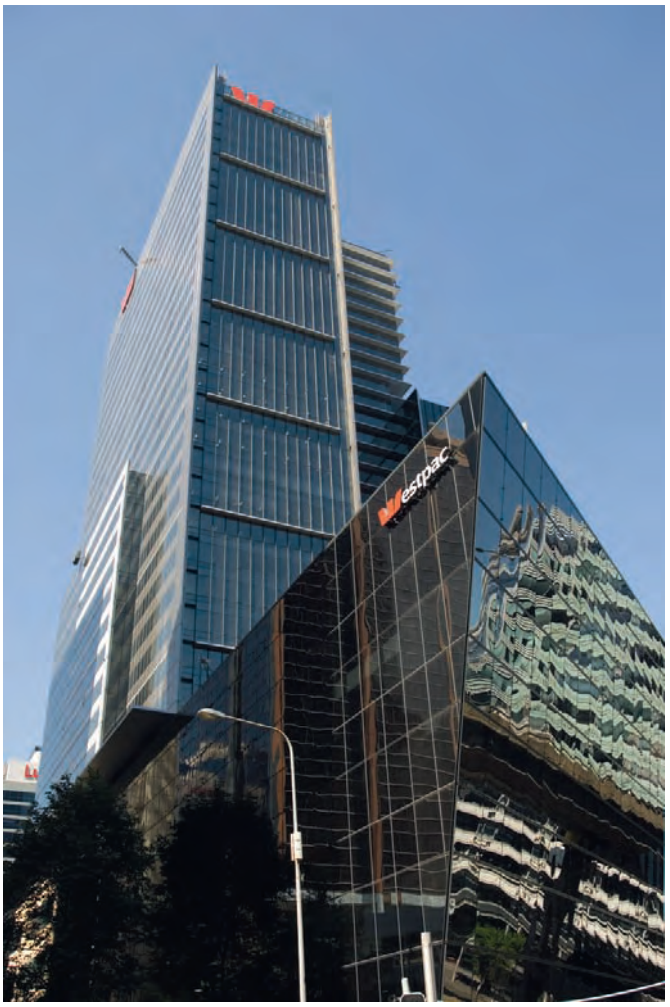


***Figure 3: A Shearfix stud rail system has been installed in the concrete frame of Westpac Place, the head office of the Westpac Banking Corporation in Sydney's CBD.*** PHOTOS COURTESY OF HYDER CONSULTING

down, the studs are installed after all other reinforcement. The rail rests on the top layer of reinforcement and is securely tied in position. Bottom up installation takes place before all other reinforcement. The rails are tied to spacers before being located around the column and nailed to the formwork.

Please note that AS 3600: 2009 does not have a specific clause on shear rail design, therefore the Ancon software is based on the research paper. We strongly recommend the shear rail design is verified against an alternate standard such as BS EN 1992-1-1 (Eurocode 2) or BS 8110.

## 3.0 COMPARISON WITH SHEAR LINKS

Loose shear links, formed on site from short lengths of rebar, can be used to reinforce a slab against punching shear. They are hooked around the top and bottom reinforcement, where calculated by the project engineer. When compared to loose shear links, the use of shear rails can accelerate both the design and the construction process.

With reinforcement being on the critical path to completing the structural frame, time savings are the major benefit of using shear rails. Research shows that the savings made from the significantly reduced fixing time far outweigh any additional material costs. A British Cement Association best practice guide[2] claims pre-fabricated solutions can be up to 10 times quicker to install than loose shear links. Shear rails are supplied to site welded to rails at the appropriate spacing, so a number of studs are installed simultaneously, unlike shear links which are formed on site and installed individually.

The software provided by shear rail manufacturers not only calculates the stud dimensions and spacing, it also generates a DXF file of the rail layout for each column, which is then easily inserted in to floor plans. Although shear rails are manufactured to order, they are available on a short lead time. Even sizeable shear rail systems are normally despatched one working week from receipt of order. To further enhance installation times, pallets can be packed in priority order, eg by pour number, and each rail is labelled with the particular column reference and product code. Codes normally comprise stud diameter, number of studs on rail, stud length and rail length and correspond directly with the layout drawing.

## 4.0 SUMMARY

Shear rails are an effective means of reinforcing flat concrete slabs against punching shear at column locations. They offer

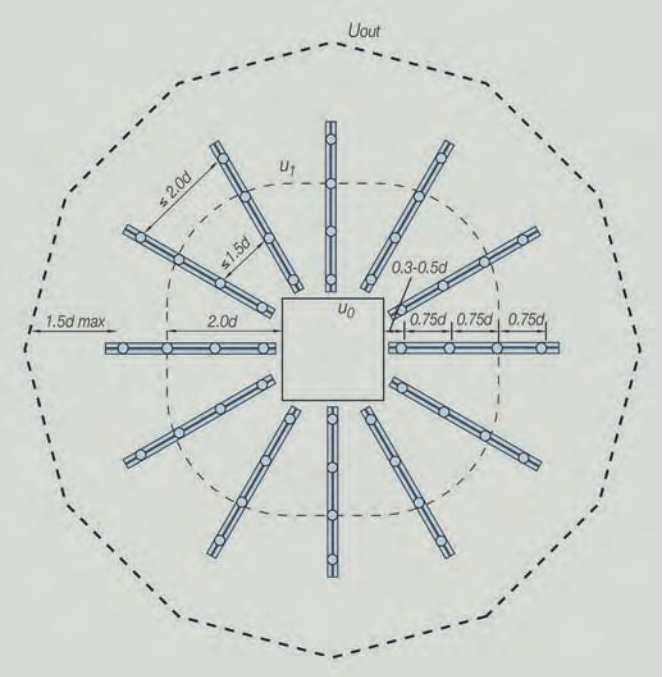


*Figure 4: Example of radial rail layout in accordance with Eurocode 2.*

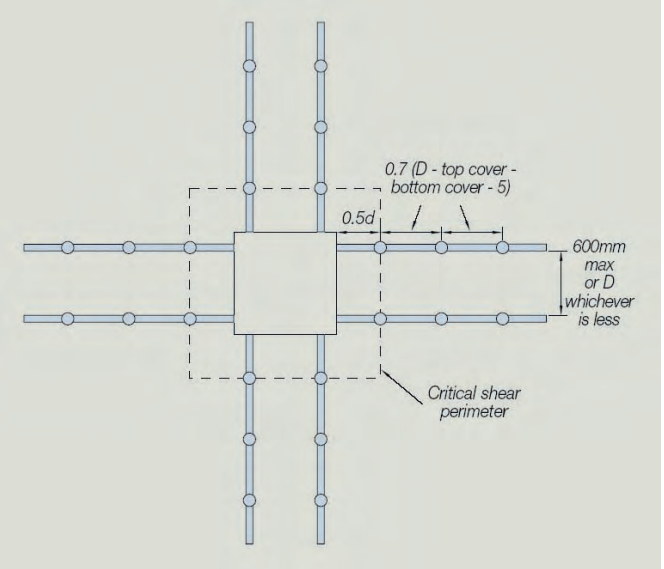


*Figure 5: Example Orthogonal Rail Layout in accordance with Lim and Rangan Approach.*

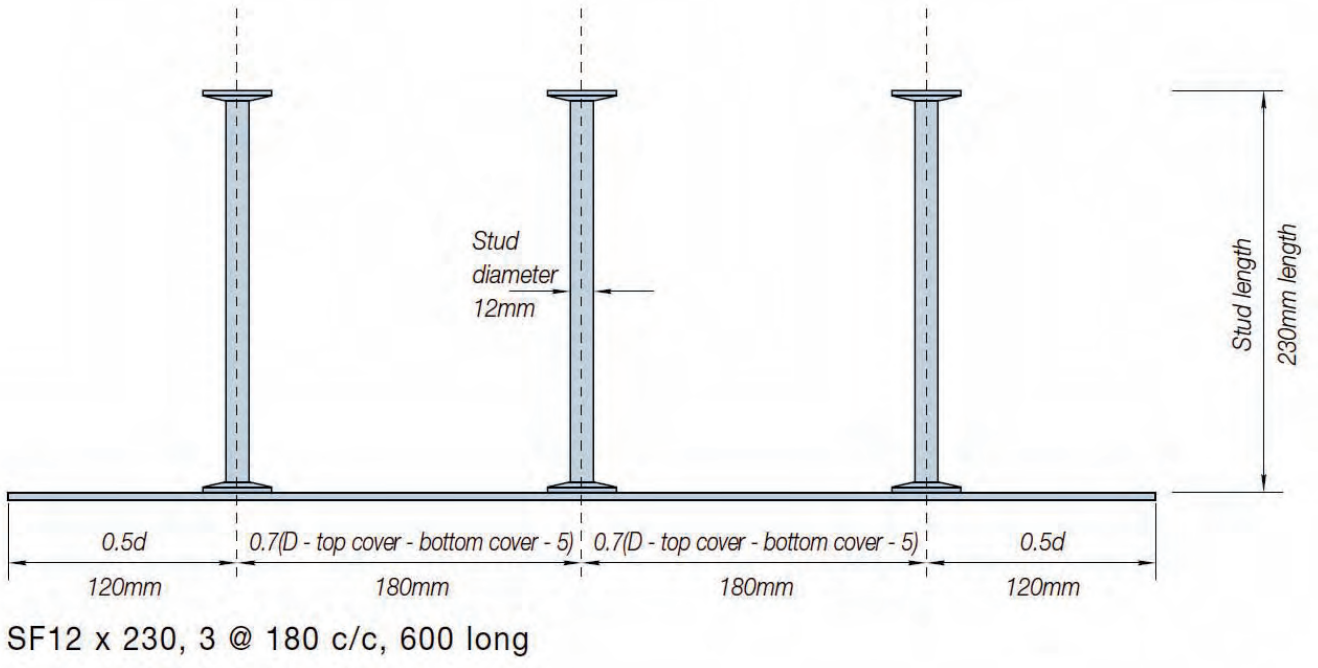


*Figure 6: Stud spacing.*

considerably reduced fixing times when compared to loose shear links and are designed using free calculation software available from shear rail manufacturers. Double-headed steel studs are supplied welded to flat steel rails at the designed centres. The rails ensure stud alignment and the accurate vertical positioning of the studs within the slab.

## REFERENCES

1. *AS3600: 2009 Concrete Structures.*
2. British Cement Association, *Prefabricated Punching Shear Reinforcement for Reinforced Concrete Flat Slabs,* 2001.

# Performance of concrete beam elements reinforced with polyvinyl alcohol (PVA) micro fibres

Amin Noushini, Bijan Samali and Kirk Vessalas
Centre for Built Infrastructure Research (CBIR)
School of Civil and Environmental Engineering
University of Technology Sydney

*The structural properties of reinforced concrete (RC) beams incorporating short-length monofilament polyvinyl alcohol (PVA) fibre addition as a form of intrinsic reinforcement are investigated in this current study. RC beams (measuring: 150 × 200 × 1900 mm) incorporating steel reinforcement of two strength grades ($f_{sy}$ = 250 and 500 MPa) and PVA fibres of two lengths (6 and 12 mm) and two volume fractions of 0.25% and 0.5% have been prepared and evaluated for their load-deflection behaviour using 4-point loading. Furthermore, compressive, indirect tensile strength, modulus of rupture and modulus of elasticity also have been evaluated following relevant Australian Standard testing methods. From the results, the inelastic behaviour and ductility of PVA fibre reinforced concretes (PVA-FRCs) were found to significantly improve by adding both 6 mm and 12 mm PVA fibres to concrete although no improvement to load bearing capacity of the concrete beams was noted. An increase of 40% in ductility was noted for the RC beam incorporating longitudinal steel reinforcement of low strength grade ($f_{sy}$ = 250 MPa) and 0.25% volume fraction of 6 mm PVA fibres. In addition, 30% increase was also found for the RC beam having high strength reinforcement with 0.50% volume fraction of 12 mm fibres.*

## NOMENCLATURE

| | |
|---|---|
| $E_{c,28}$ | concrete modulus of elasticity at the age of 28 days |
| $f'_c$ | characteristic compressive (cylinder) strength of concrete |
| $f_{c,28}$ | concrete compressive strength at the age of 28 days |
| $f_{ct.sp,28}$ | concrete indirect (splitting) tensile strength at the age of 28 days |
| $f_{ct.f,28}$ | concrete flexural strength (modulus of rupture) at the age of 28 days |
| $f_{sy}$ | yield strength of steel reinforcement |
| $F_u$ | ultimate load applied |
| $\mu$ | ductility factor |
| $\delta_y$ | yield displacement of reinforced concrete beam |
| $\delta_u$ | ultimate displacement of reinforced concrete beam |

## 1.0 INTRODUCTION

Low tensile strength and brittleness are the main weak points of concrete as a structural material. In fact, many deteriorations and failures in concrete structures are due to the brittle nature of this material (Hamoush et al., 2010). The addition of fibres may significantly enhance the mechanical properties of concrete such as ductility and residual load bearing capacity (toughness) (Radtke et al., 2012; Noushini et al., 2013b). Ductility is characterised as a dominant safety feature of a structure since it demonstrates the ability of a structural element to withstand inelastic deformation prior to failure without significant loss in resistance. Ductility acts in delaying local failure of statically indeterminate structures by permitting redistribution of stresses from one critical section to another (Jeong, 1994).

Adding fibres into a conventional concrete matrix significantly improves the post-peak behaviour by providing an enhanced residual strength which is also defined as toughness (Noushini et al., 2013a). At the structural level, fibre reinforced concrete (FRC) toughness allows smaller crack opening which results in a higher durability. This property is particularly significant at serviceability limit state. Furthermore, by using FRC, it may be possible to reduce (or even totally remove) the shear reinforcement (Meda et al., 2012).

When reinforced concrete is subjected to bending load, it is susceptible to cracks initiating from tensile stresses. Stress redistribution after initiation of cracks creates stress concentrations where the cracks meet the reinforcing steel bars, resulting in the plastic deformation of the bars. Addition of fibre to the concrete mix may suspend the steel bar yielding by bridging the cracks and restricting the crack development, which results in higher load bearing capacities. Furthermore, fibres may also act as secondary reinforcement in the plastic region of reinforced concrete (RC) beams and contribute to transferring the load through the cracks which leads to an increase in tensile ductility.

These disadvantages may be avoided by adding short discontinuous fibres to plain concrete which has been a major motivation for many research works in recent years (Wu & Sun, 2003). Fibres are added in to a brittle-matrix composite to help improve three major aspects; toughness, ductility and strength (tensile) (Arisoy, 2002). Fibres tend to increase toughness of the composite material by bridging the cracks and provide energy absorption mechanism related to de-bonding and fibre pull-out. Furthermore, they can increase the ductility of the composite by allowing multiple cracking. They may also help increase the strength by transferring load and stresses across the cracks.

The modern usage of fibres in construction industry goes back about 100 years ago (1900s) and the creation of asbestos

*Table 1: Properties of PVA fibres.*

| Specific gravity | Diameter | Thickness | Cut length | Tensile strength | Young's modulus | Elongation |
|---|---|---|---|---|---|---|
| [g/cm$^3$] | [mm] | [dtex] | [mm] | [MPa] | [GPa] | [%] |
| 1.29 | 0.014 | 1.8-2.3 | 6 and 12 | 1500 | 41.7 | 7 |

*Table 2: Mix proportions of reference concrete.*

| kg/m$^3$ | | | | | | Lit/m$^3$ | Water/C* |
|---|---|---|---|---|---|---|---|
| Cement | Fly ash | Sand | 10 mm aggregate | 20 mm aggregate | Water | HWR | |
| 301 | 129 | 635 | 390 | 700 | 151 | 1.215 | 0.35 |

cement. However, the first serious theoretical studies of fibre in concrete were developed in the early 1960s by Romualdi, Batson and Mandel when they published their research (Romualdi & Batson, 1963; Romualdi & Mandel, 1964; Zollo, 1997). It initially brought FRC to the attention of academic and industry research scientists around the world as a viable solution for improving post peak behaviour and ductility of concrete. Advancement of FRCs then continued in the 1970s when mostly glass fibre and steel fibre were investigated (Perumalsamy & Surendra, 1992). In the mid 1980s many new fibre types and fibre geometries (e.g. synthetic fibres) had been introduced which significantly altered FRC production techniques and influenced FRC strength and toughness (crack control) performance measures (Zollo, 1997).

The pioneering works (Zensveld, 1975; Hannant, 1980; Krenchel & Shah, 1986) on synthetic FRC and synthetic fibre reinforced cementitious composites emphasised the need to overcome disadvantages due to the low modulus of elasticity and poor bonding properties of synthetic fibres within the matrix. The latter is particularly a problem in reference to many of the synthetic fibres due to their chemical composition and their surface properties (Bentur & Mindess, 2007).

From among the many types of synthetic fibres used in concrete and cementitious composites, polyvinyl alcohol (PVA) fibre is a relatively new inclusion. PVA fibre is known to be stable and durable in the alkali environment present in the concrete matrix (Garcia et al. 1997). These fibres are characterised by their high tensile strength (0.9–1.6 GPa), high elastic modulus (23–40 GPa) and hydrophilic surface which creates a strong chemical bond with the cementitious material (Redon et al., 2004). PVA fibre serves several advantages when used in concrete or cementitious composites. The high tensile strength of PVA fibres contributes by sustaining the first crack stress and resisting pull out force due to the strong bond present between the fibre and cementitious matrix. Contrary to this the low lateral resistance of the fibres may also lead to fibre rupture before being pulled out of the matrix (Atsuhisa et.al, 2006). PVA fibres elongate and transfer the load to different parts of the matrix and as a result the load applied is distributed more evenly between the loading surfaces.

Although a considerable amount of research has been done so far on the concept of using PVA fibre in cementitious composites, limited studies are performed on structural properties of PVA-FRC. Most of the previous works on PVA fibre have focused on PVA engineered cementitious composites (PVA-ECC). This research work shall therefore aim to strengthen the knowledge of using PVA-FRC in structural applications. The main objective of this study is to investigate how the mechanical and structural characteristics of concrete are affected by addition of a certain amount of PVA fibres into the concrete.

## 2.0 EXPERIMENTAL PROGRAM

### 2.1 Materials

Shrinkage limited Portland cement (PC) and fly ash (FA) were used as the binder for all concrete mixes. Shrinkage limited PC was used in this study to minimise concrete drying shrinkage. The fineness of FA by 45 µm sieve was determined to be 94% passing (tested in accordance with AS 3583.1–1998). A maximum nominal size of 20 mm aggregate was used in all mixes. All aggregates used in mix design were sourced from Dunmore, Australia, which includes 50/50 blended fine/coarse manufactured sand and 10 mm and 20 mm crushed latite gravel. The grading of all aggregates complies with Australian Standard AS 2758.1 specifications and limits. All aggregates were prepared to saturated surface dry condition prior to batching. Drinking grade tap water was used for all mixes after conditioning to room temperature (23±2 °C). Furthermore, in order to improve the workability, a polycarboxylic-ether based high range water reducing admixture (HWR) was used. Non-coated PVA fibre of two different geometries, 6 and 12 mm, with specifications mentioned in Table 1, were used in all FRC mixes.

### 2.2 Mixing and samples preparations

Mixes were prepared to obtain characteristic compressive strength at 28 days ($f'_c$) of 60 MPa to conform to AS 3600 requirements as structural concrete (ranging from 20 MPa to 100 MPa) even after adding fibres which may cause strength reduction, along with a slump of 80±20 mm. In order to obtain the desired slump HWR dosage was varied. Details of the mix proportions for control concrete (no fibres) are presented in Table 2. Mix ingredients were all measured and added to the mix by weight. All FRCs also followed the same proportioning and only fibres were added to the mixture by 0.25% and 0.5% of volume fraction of the mix.

For control mix, mixing was performed in accordance with AS 1012.2. However, for FRC mixes, due to the presence of

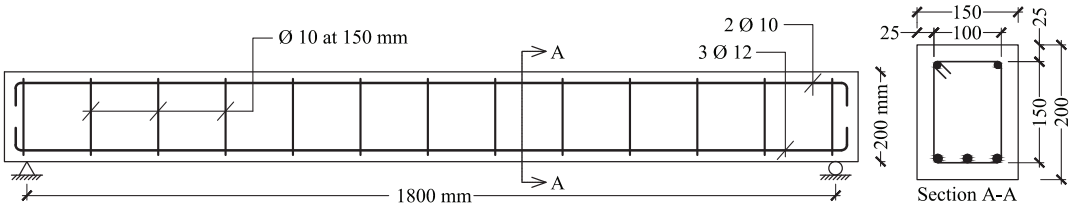


*Figure 1: Schematic of RC beam.*

*Table 3: Steel reinforcement arrangements.*

| | Tension steel reinforcement | | | Compression steel reinforcement | | |
|---|---|---|---|---|---|---|
| | Diameter [mm] | No. | $f_{sy}$ (nominal) [MPa] | Diameter [mm] | No. | $f_{sy}$ (nominal) [MPa] |
| Type A | 12 | 3 | 250 | 10 | 2 | 250 |
| Type B | 12 | 3 | 500 | 10 | 2 | 250 |

the fibres, the standard mixing regime suggested in Australian Standard for conventional concrete was modified. Accordingly, the mixing time was increased to three minutes to achieve a completely homogeneous concrete. Modifying the standard mixing sequences in order to achieve a more uniform mix has also previously been investigated by different researchers. For instance, Manolis et al. have suggested a 3-5 minutes of mixing after fibre addition to achieve a proper fibre dispersion. Slump was taken to check the workability and, thereafter, freshly mixed concrete was placed into moulds and compacted.

In order to prepare the RC beams, fabricated steel cages were placed into the steel moulds using plastic bar chairs and wheel spacers to provide a uniform concrete cover in all directions of the concrete beam. Thereafter, concrete was cast and compacted by means of an internal (poker) vibrator. Finally, the concrete surface was levelled using a concrete trowel. Moulds were covered with plastic sheets to retain moisture. RC beam samples were wet-cured in moulds for seven days and after that demoulded and air cured until the test dates. Curing of other test specimens (concrete cylinders and prisms) was carried out in accordance with AS 1012.8. At 24 h for cylindrical specimens and 48 h for prismatic samples, specimens were demoulded and placed in lime-saturated water at a temperature of 20±2 °C until the test date.

The RC beams used for this test are designed in accordance with AS 3600 (2009). All specimens were 1.9 m long with a span of 1.8 m and a depth of 200 mm (effective depth ($d$) = 159 mm). A concrete cover of 25 mm was also used for all the beams. Figure 1 shows the beam geometry and the reinforcement details. In order to investigate the fibre contribution to flexural behaviour of RC beams, two different types (A and B) of steel reinforcement arrangements as shown in Table 3 was utilised. All beams of series A (made with steel arrangement of type A) and series B (made with steel arrangement of type B) were provided with 10 mm diameter stirrups (Ø10) with a constant spacing of 150 mm (centre-to-centre) over the whole of their length in order to avoid shear failure and have a reinforcement ratio ($\rho_s$) of 1.42%.

For concrete beams of series A, both fibre volume fractions of 0.25% and 0.50% were used in order to make FRC beams. However, for making the concrete beams of series B, the volume fraction of 0.50% was only utilised since it is believed (Kim et al, n.d.) to achieve more improved performance by using higher volume fractions of fibre. Accordingly, five RC beams made out of three different concrete mix designs and two different steel reinforcement arrangements as introduced further in details in Table 4, are tested for 4-point static flexure.

## 2.3 Testing methods

For each concrete type, in order to evaluate the material characteristics, the mechanical properties of concrete are assessed using indirect tensile strength, modulus of rupture (MOR) and modulus of elasticity (MOE) tests. Uniaxial compression tests are also conducted for each concrete beam using cylindrical specimens of 100 × 200 mm at the age of 28 days and at the beam test day, in accordance with AS 1012.9. Splitting tensile tests were performed on cylindrical specimens of 100 × 200 mm at the age of 28 days in accordance with AS 1012.10 specifications and method. Cylindrical specimens were tested under load rate control condition in an 1800 kN universal testing machine with a load rate equivalent to 20±2 MPa per minute for compressive test and 1.5±0.15 MPa per minute for indirect tensile test. Flexural tensile strength or MOR is obtained from four-point bending tests on 100 × 100 × 400 mm prisms at a loading rate of 1±0.1 MPa/min until fracture following AS 1012.11. MOE test was also carried out on 150 × 300 mm cylinders following AS 1012.17. All tests were conducted at 28 days of ageing and each of the following mentioned results is the average of three test specimens.

Literature offers some specific information and research

*Table 4: Concrete beam designations.*

| Beam label | Reinforcement arrangement | Fibre length [mm] | $V_f$ [1] [%] |
|---|---|---|---|
| Control (A) | Type A | – | – |
| Control (B) | Type B | – | – |
| 6 PVA-0.25% (A) | Type A | 6 | 0.25 |
| 12 PVA-0.50% (A) | Type A | 12 | 0.50 |
| 12 PVA-0.50% (B) | Type B | 12 | 0.50 |

[1] Fibre volume fraction.

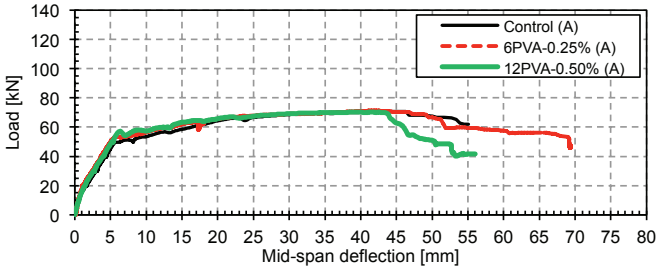


*Figure 2: Load-defection curves of PVA-FRCs and control beams of series A.*

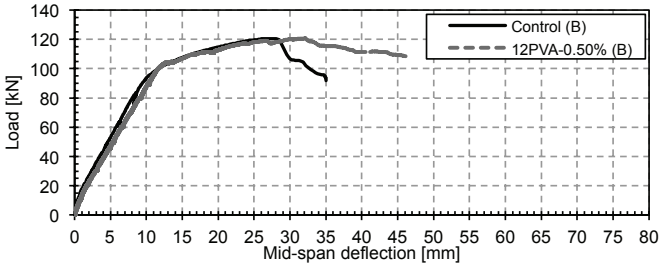


*Figure 3: Load-defection curves of PVA-FRC and control beams of series B.*

outcomes on the evaluation of RC beams. The best test methodology to evaluate the post-cracking and toughness properties of RC beam is the bending test. Design codes recommend one of two bending test configurations: the three-point or the four-point bending test (Bencardino et al., 2012). In this study, 4-point static flexural test method has been utilised. This test was performed after a minimum of 56 days of curing age to make sure that sufficient strength is gained due to the pozzolanic reaction of FA which mostly decreases the concrete strength development rate.

This procedure was also recommended in previous investigations (Felekoğlu et al., 2009). Besides recording values of the applied load, the deflection was also taken using linear variable differential transducers (LVDTs) mounted along the beam axis in middle section and one-fourth spans. The test set-up is arranged in a way to make sure that the simply supported beam condition is satisfied. Thus, supports allow the beam to rotate freely and minimise the friction which may impose bending moment at the end of the beam (in the supports location). The supports are also designed in a way, so that the vertical displacement at both supports is removed but horizontal displacement at one end can take place. The specimens are loaded at one-third span by the means of two hydraulic jacks.

## 3.0 RESULTS AND DISCUSSION

The compressive strength of concrete beams measured at the age of 28 days and at the beam test day, in addition to the other concrete mechanical properties are summarised in Table 5. The compressive test samples were collected from the same batch as the concrete beams were cast and the test was performed for each individual beam. However, the other samples, for indirect tensile, MOR and MOE tests, were prepared from separate batches with exactly the same mix design as of the concrete beams for each concrete series of control, 6PVA-0.25% and 12PVA-0.50%.

The load-deflection curves as shown in Figure 2 and Figure 3 are calculated from the data captured by two load-cells which were mounted on loading jacks and an LVDT placed at mid-span to measure the deflection.

The term ductility in seismic design is used to explain the ability of a structure to withstand large amplitude cyclic deformations in the inelastic range without a considerable strength reduction (Park, 1988). Ductility factor, which is defined as the maximum deformation divided by the corresponding deformation when yielding occurs, permits the maximum deformation to be expressed in non-dimensional terms. This can be used as indices of inelastic deformation for seismic design and analysis. Ductility factor is generally known as the various response parameters related to deformations, namely displacement, rotation and curvature (Park, 1988).

The displacement ductility factor ($\mu$), which is usually determined in inelastic time history dynamic analysis, may vary between one for elastically responding structures to as high as seven for ductile structures. However, it is typically ranging from three to six (Park, 1988). The displacement ductility factor can be calculated using the below mentioned equation where $\delta_u$ is the ultimate (maximum) displacement and $\delta_y$ is the yield displacement.

$$\mu = \frac{\delta_u}{\delta_y} \quad (1)$$

The definition of yield displacement often causes difficulty since the load-displacement relationship may not have a well-defined yield point. This may happen because of several reasons such as non-linear behaviour of materials, various moment levels needed for longitudinal bars at different depths in a reinforced concrete section to reach yield, and different load levels required to form plastic hinges in different parts of a structure (Park, 1988). Figure 4 demonstrates different variations of definitions used by researchers to estimate the yield displacement. Figure 4a shows the displacement when yielding first occurs and Figure 4b illustrates the yield displacement of the equivalent elastoplastic system with the same elastic stiffness and ultimate load as the real system. Figure 4c and Figure 4d explain the yield displacement of the equivalent elastoplastic system with the same energy absorption as the real system and the yield displacement of the equivalent elastoplastic system with reduced stiffness found as the secant stiffness at 75% of the ultimate load of the real system, respectively (Park, 1988).

The latter definition (Figure 4d) takes the secant stiffness as explained before, taking into account the reduction in stiffness due to cracking which happens near the end of the elastic range. This description may count as the most realistic definition of the yield displacement for reinforced concrete structures (Park, 1988). The ultimate (maximum) displacement has also been estimated using divergent assumptions, some of which are shown in Figure 5. These possible estimates as explained by Park (1988) involve the displacement corresponding to a particular limiting value for the concrete compressive strain (Figure 5a), the displacement corresponding to the peak of the load-displacement relation (Figure 5b), the post-peak displacement when the load bearing capacity has undergone a small reduction

*Table 5: Concrete mechanical properties of RC beams.*

| Beam label | $f_{c,28}$ [MPa] | $f_{c,test\ day}$ [MPa] | $f_{ct.sp,28}$ [MPa] | $f_{ct.f,28}$ [MPa] | $E_{c,28}$ [GPa] |
|---|---|---|---|---|---|
| Control (A) | 68.0±5.9 | 84.0±6.4 | 3.7±0.5 | 5.6±0.2 | 39.3 |
| Control (B) | 58.0±3.5 | 80.0±3.1 | 3.7±0.5 | 5.6±0.2 | 39.3 |
| 6PVA-0.25% (A) | 72.0±5.1 | 85.5±6.0 | 4.9±0.2 | 6.8±0.2 | 40.1 |
| 12PVA-0.50% (A) | 61.5±3.9 | 80.5±5.1 | 4.1±0.4 | 6.2±0.5 | 33.2 |
| 12PVA-0.50% (B) | 66.5±4.8 | 75.0±3.3 | 4.1±0.4 | 6.2±0.2 | 33.2 |

(Figure 5c), and the displacement when the transverse or longitudinal reinforcing steel fractures or the longitudinal compression reinforcement buckles (Figure 5d).

In order to consider the most appropriate definition, it is noteworthy to take into account the fact that most structures have some capacity to withstand deformation beyond the peak load without considerable reduction in strength. It would be reasonable to recognise at least part of this post-peak deformation capacity. Therefore, the most accurate and realistic definition for the ultimate displacement would be the criteria shown in Figures 5c and d (Park, 1988). And in order to calculate the ductility factor, displacement at yield point ($\delta_y$) and ultimate displacement ($\delta_u$) of all RC beams are calculated, using above mentioned definitions. For beams of series A, having low strength longitudinal tensile reinforcement, the secant modulus at 75% ultimate load is observed not to be the best fit representing the stiffness prior to yield.

It has been found that secant modulus at about 70% ultimate load provides the best achievable estimation of stiffness. Accordingly, this value (70% ultimate load) is selected for further calculations. However, in the case of series B beams including high strength longitudinal tensile reinforcement, secant modulus at 75% ultimate load is used to measure displacement at yield. The ultimate displacement ($\delta_u$) in this study is taken as the displacement of the beam when the load has dropped to 70% of the peak load, after reaching the peak, for series A beam and 85% for RC beams of series B. The summary of all above calculations are presented in Table 6. The results show that among all concrete beams of series A, 6PVA-0.25% (A) beam ranked first in terms of ductility and post-peak behaviour. A 40% higher value of ductility factor is recorded for this beam including 0.25% volume fraction of 6 mm fibre compared to the control. However, beam number three having 0.50% volume fraction of 12 mm PVA fibres demonstrates almost the same ductility as control. In concrete beams of series B, FRC beam including 0.50% volume fraction of 12 mm fibre showed approximately 30% higher ductility compared to control beam.

## 4.0 CONCLUSIONS

From the results, the inelastic behaviour and ductility of PVA-FRCs were found to significantly improve by adding both 6 mm and 12 mm PVA fibres to concrete although no improvement to load bearing capacity of the concrete beams was noted. An increase of 40% in ductility was noted for the RC beam incorporating longitudinal steel reinforcement of low strength grade ($f_{sy}$ = 250 MPa) and 0.25% volume fraction of 6 mm PVA fibres. In addition, 30% increase was also found for the RC beam having high strength reinforcement with 0.50% volume fraction of 12 mm fibres.

## ACKNOWLEDGEMENTS

The authors would like to express their gratitude to Mr Rami Haddad, Civil Engineering Laboratories Manager at the University of Technology Sydney (UTS), for his assistance with the experimental testing program.

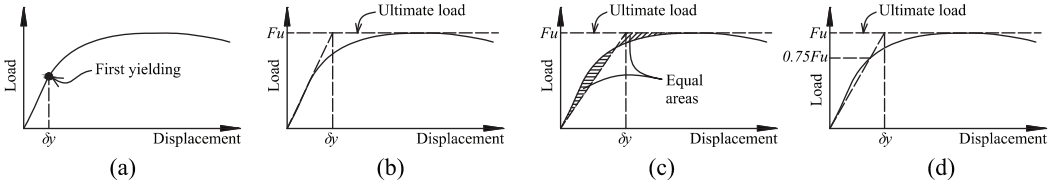


*Figure 4: Alternative definitions of yield displacement (Park, 1988).*

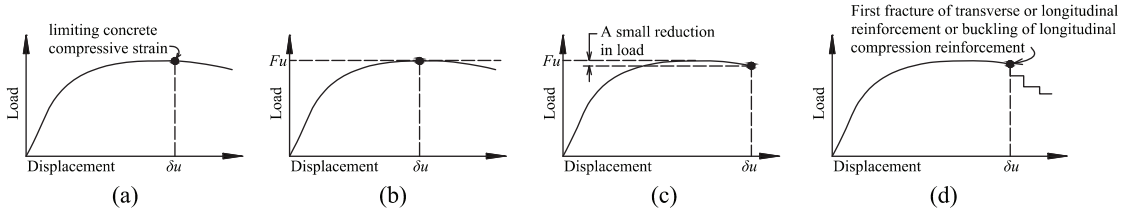


*Figure 5: Alternative definitions of ultimate (maximum) displacement (Park, 1988).*

*Table 6: Ductility factor of control and FRC beams.*

| No. | Beam label | Reinforcement [1] | Fibre $L_f$ [mm] | $V_f$ [%] | $f_c$ [2] [MPa] | $F_u$ [3] [kN] | $\delta_y$ [mm] | $\delta_u$ [mm] | $\mu$ |
|---|---|---|---|---|---|---|---|---|---|
| 1 | Control (A) | $f_y$ = 250 MPa | – | – | 84.0 | 70.8 | 8.0 | 55.1 | 6.9 |
| 2 | 6PVA-0.25% (A) | $f_y$ = 250 MPa | 6 | 0.25 | 85.5 | 71.3 | 7.1 | 69.2 | 9.7 |
| 3 | 12PVA-0.50% (A) | $f_y$ = 250 MPa | 12 | 0.50 | 80.5 | 70.2 | 7.2 | 50.4 | 7.0 |
| 4 | Control (B) | $f_y$ = 500 MPa | – | – | 80.0 | 120.5 | 12.7 | 32.0 | 2.5 |
| 5 | 12PVA-0.50% (B) | $f_y$ = 500 MPa | 12 | 0.50 | 75.0 | 120.6 | 13.9 | 46.1 | 3.3 |

[1] Longitudinal tensile reinforcement.
[2] Compressive strength of concrete beam (cylindrical samples) at test day (> 56 days).
[3] Ultimate (maximum) load applied.

## REFERENCES


Arisoy, B. 2002. Development and fracture evaluation of high performance fiber reinforced lightweight concrete. PhD, Wayne State University.

Bencardino, F., Rizzuti, L., Spadea, G. & Swamy, R. N. 2012. Implications of test methodology on post-cracking and fracture behaviour of Steel Fibre Reinforced Concrete. *Composites Part B: Engineering*.

Bentur, A. & Mindess, S. 2007. *Fibre Reinforced Cementitious Composites,* Abingdon, England, Taylor & Francis.

Felekoğlu, B., Tosn, K. & Baradan, B. 2009. Effects of fibre type and matrix structure on the mechanical performance of self-compacting micro-concrete composites. *Cement and Concrete Research,* 39**,** 1023-1032.

Hamoush, S., Abu-Lebdeh, T. & Cummins, T. 2010. Deflection behavior of concrete beams reinforced with PVA micro-fibers. *Construction and Building Materials,* 24**,** 2285-2293.

Hannant, D. J. Polymer fibre reinforced cement and concrete. *In:* Roy, D. M., Majumdar, A. J., Shah, S. P. & Manson, J. A., eds. *Advances in Cement-Matrix Composites*, 1980 Materials Research Society, Pittsburgh, PA. 171-180.

Jeong, S. M. 1994. Evaluation of ductility in prestressed concrete beams using fibre reinforced plastic tendons. PhD, University of Michigan.

Kim, S. B., Yi, N. H., Kim, H. Y., Kim, J.-H. J. & Song, Y.-C. n.d. Material and structural performance evaluation of recycled PET fiber reinforced concrete. *Cement and Concrete Composites,* 32**,** 232-240.

Krenchel, H. & Shah, S. P. 1986. Synthetic fibre for tough and durable concrete. *In:* Swamy, R. N., Wagstaffe, R. L. & OAKLEY, D. R. (eds.) *Developments in Fibre Reinforced Cement and Concrete.* Sheffield: RILEM Symp.

Manolis, G. D., Gareis, P. J., Tsonos, A. D. & Neal, J. A. 1997. Dynamic properties of polypropylene fiber-reinforced concrete slabs. *Cement and Concrete Composites,* 19**,** 341-349.

Meda, A., Minelli, F. & Plizzari, G. A. 2012. Flexural behaviour of RC beams in fibre reinforced concrete. *Composites Part B: Engineering,* 43**,** 2930-2937.

Noushini, A., Samali, B. & Vessalas, K. Flexural toughness and ductility characteristics of polyvinyl-alcohol fibre reinforced concrete (PVA-FRC). In: 8th International Conference on Fracture Mechanics of Concrete and Concrete Structures, FraMCoS-8, 2013a Toledo; Spain. 1110-1121.

Noushini, A., Vessalas, K., Ghosini, N. & Samali, B. 2013b. Effect of polyvinyl alcohol fibre and fly ash on flexural tensile properties of concrete. In: 22nd Australasian Conference on the Mechanics of Structures and Materials, ACMSM 2012, Sydney, NSW; Australia. 1165-1170.

Park, R. Ductility evaluation from laboratory and analytical testing. In: The 9th world conference on earthquake engineering, 1988. 605-616.

Perumalsamy, N. B. & Surendra, P. S. 1992. *Fiber-Reinforced Cement Composites,* New York, McGraw-Hill.

Radtke, F., Simone, A. & Sluys, L. 2012. A computational model for failure analysis of fibre reinforced concrete with discrete treatment of fibres. *Engineering Fracture Mechanics,* 77**,** 597-620.

Redon, C., Li, V. C., Wu, C., Hoshirio, H., Saito, T. & Ogawa, A. 2004. Measuring and modifying interface properties of PVA fibers in ECC matrix. *ASCE Journal of Materials in Civil Engineering*.

Romualdi & Batson 1963. Mechanics of crack arrest in Concrete. *ASCE Journal of Engineering Mechanics,* 89**,** 147-168.

Romualdi & Mandel 1964. Tensile strength of concrete affected by uniformly distributed closely spaced short length of wire reinforcement. American Concrete Institute, 61.

Wu, H. C. & Sun, P. 2003. High performance masonry units from 100% fly ash: synergistic approach. *Report: Advanced Infrastructure Materials Laboratory.* Wayne State University.

Zensveld, J. J. Properties and testing of concrete containing fibres other than steel. In: NEVILLE, A., ed. *Fibre Reinforced Cement and Concrete,* 1975 Lancaster, England. The Construction Press, 217-226.

Zollo, R. F. 1997. Fiber-reinforced concrete: an overview after 30 years of development. *Cement and Concrete Composites,* 19**,** 107-122.

# Shear design and evaluation of concrete structures

Michael P. Collins, University of Toronto and Denis Mitchell, McGill University

*Deficiencies in the shear design of concrete structure are inherently more dangerous than deficiencies in flexural design because shear failures can occur with no prior warning and with no possibility for redistribution of internal forces. While accurate assessment of the shear capacity of a reinforced concrete structure is critically important for public safety, the traditional techniques available for this task are open to dispute. For determining flexural capacity engineers can use the simple, accurate, general and internationally accepted "plane sections theory". However, for finding shear strength engineers typically rely on restricted empirical equations whose applicability and accuracy are sometimes very questionable. The purpose of this paper is to summarise some research aimed at understanding the basic mechanisms of shear transfer and to introduce simple, rational and general shear design and evaluation procedures.*

## 1.0 INTRODUCTION

A well-designed reinforced concrete structure, if subjected to extreme overloads, should fail in flexure rather than shear. Such structures are tough, give ample warning of approaching failure and are often capable of resisting surprisingly large loads. Unlike flexural failures, shear failures are relatively brittle and, particularly for members with inadequate stirrups, can occur without warning. Because of this, the prime objective of shear design is to identify where shear reinforcement is required and how much reinforcement must be provided to prevent such failures. Shear reinforcement links together the flexural tension and flexural compression sides of a member and ensures that the two sides act as a unit. Shear failures involve the breakdown of this linkage and typically are accompanied by the opening of a major diagonal crack, see Figures 1 and 2. Shear design and evaluation procedures which are based on rational models rather than empirical equations enable the engineer to develop a better understanding of actual structural behaviour and to more clearly appreciate situations where shear will be a critical safety issue. Developing more rational models for shear has been the objective of a long-term worldwide research effort and considerable progress has been made over the last 20 years. This paper will concentrate on procedures for modelling shear behaviour developed by the authors and their colleagues.

## 2.0 RELATIVE ACCURACY OF FLEXURE AND SHEAR DESIGN PROVISIONS

In designing for flexure, engineers have available a simple, general, rational method called the "plane sections theory", capable of predicting not only the flexural strength, but also the complete load-deformation response of reinforced concrete sections. Because of this there is little disagreement between different international design codes as to the flexural strength of a given reinforced concrete section or the quantities of reinforcement needed to ensure ductile flexural behaviour. There is, however, substantial disagreement as to the magnitude of the shear strength of structural elements and the reinforcement requirements needed to ensure ductile shear response. Further, rather than the simple, general, behavioural theory available for flexural design, the building code procedures for shear design typically consist of a collection of complex, restricted empirical equations for shear strength. In view of the disparity between the state-of-the-art in flexure, and the state-of-the-art in shear, it is perhaps not surprising that while failures of reinforced concrete structures due to deficiencies in flexural design are extremely rare, failures due to deficiencies in shear design occur much more frequently.

As an illustration of the inconsistencies between current shear design provisions, consider the results of the four slab-strip specimens[2] shown in Figure 3. Two of these specimens were

***Figure 1: Failure of slab strip without shear reinforcement[1].***

***Figure 2: Catastrophic shear failure of Concorde Overpass Sept. 2006.***
PHOTO: COURTESY OF *LA PRESSE*, MONTREAL/ROBERT SKINNER

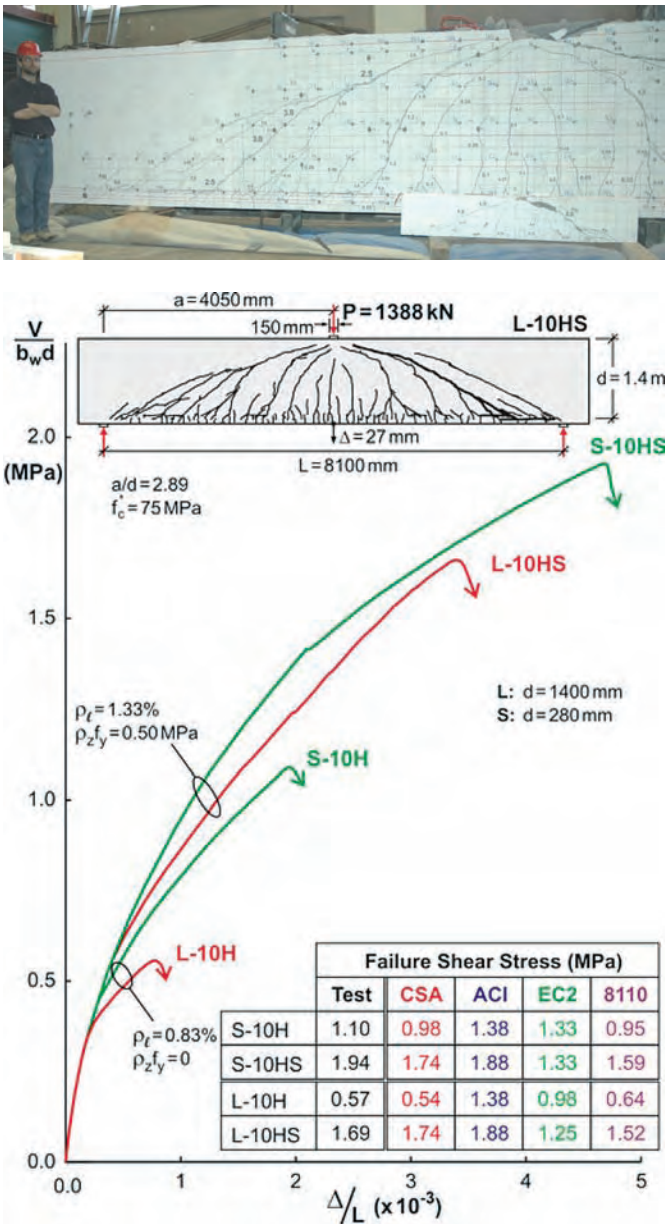


| | Failure Shear Stress (MPa) | | | | |
|---|---|---|---|---|---|
| | Test | CSA | ACI | EC2 | 8110 |
| S-10H | 1.10 | 0.98 | 1.38 | 1.33 | 0.95 |
| S-10HS | 1.94 | 1.74 | 1.88 | 1.33 | 1.59 |
| L-10H | 0.57 | 0.54 | 1.38 | 0.98 | 0.64 |
| L-10HS | 1.69 | 1.74 | 1.88 | 1.25 | 1.52 |

***Figure 3: Four high-strength concrete slab strips failing in shear.***

large (L) with a thickness comparable to that of the failed bridge slab[3] shown in Figure 2 while the other two were small (S) with thickness similar in size to traditional laboratory specimens. For each pair of specimens, one (like the bridge slab) contained no shear reinforcement and 0.83% of longitudinal reinforcement ($A_s/b_w d$ = 0.0083) while the other contained 0.50 MPa of shear reinforcement ($A_v f_y/b_w s$ = 0.50 MPa). To avoid flexural failures, the specimens with shear reinforcement contained somewhat more longitudinal reinforcement (1.33%). All four specimens were constructed with 75 MPa concrete and failed in shear. The table in Figure 3 compares the observed failure shear stresses with the failure shear stresses predicted by current Canadian (CSA[4]), American (ACI[5]), European (EC2[6]), and British, (BS8110[7]) codes. For AS3600[8] the four predicted failure shear stresses are 1.24, 1.88, 0.66, and 1.28 MPa. Note that for each slab strip, there are considerable differences between the five code predictions. Thus for the large specimen without stirrups, L-10H, the highest predicted failure shear stress is 2.56 times the lowest predicted failure shear stress. Further, the codes give very different estimates as to how the failure shear stress will change as the depth is made larger or shear reinforcement is added. The ACI code predicts the same failure shear stress for the thick slabs as for the thin slabs and predicts that adding 0.50 MPa of stirrups will increase the failure shear stress by 0.50 MPa thus predicting that the shear strength of slabs with stirrups will be 1.36 times the shear strength of slabs without stirrups. EC2 predicts that this shear strength ratio for the thick slabs will be 1.28; AS3600 predicts 1.94, BS8110 predicts 2.38 and CSA predicts 3.22. The experimentally determined value was 2.96.

In contrast to the major inconsistencies that exist between the shear strength predictions of these codes, the predictions for flexural failure loads are remarkably consistent. If the magnitude of the shear stress at flexural failure of the large specimen without shear reinforcement (L-10H) is calculated, the different codes all predict a value of 1.26 MPa within plus or minus 0.5%. Hence while the ratio of highest to lowest shear failure load is 2.56, the ratio of highest to lowest predicted flexural failure load is only 1.01. Thus ranking of structures in terms of susceptibility to flexural failures using any of these codes should give very similar results. However rankings in terms of susceptibility to catastrophic shear failures may change significantly depending on the shear provisions used.

## 3.0 MECHANISMS OF SHEAR RESISTANCE

Consider the simplified version of a flexurally cracked beam or slab strip not containing shear reinforcement shown in Figure 4. The depth of the flexural compression zone is $kd$ and the flexural lever arm is $jd$. Because the compressive stresses under the loading plate fan out into the beam, the tension force in the longitudinal reinforcement will be nearly constant over a region about $2d$ long. Near the bottom face of the beam the spacing of the vertical cracks will be controlled by the bond characteristics of the reinforcement. Near mid-depth of the beam, crack spacing will be controlled by the distance required for tensile stresses in the concrete to spread out from the reinforcement or from the stiff uncracked compression zone. Assuming a dispersion angle of 45°, see Figure 4, the horizontal spacing of the cracks in the upper region of the web will be about $(1\text{-}k)d$. A free body diagram of a 'tooth' of concrete is shown on the bottom left of Figure 4 and labelled Case 1. It is bounded on the top by the neutral axis and on the sides by two of the widely spaced vertical cracks. Horizontal equilibrium requires that the average shear stress on the top horizontal plane is $Vl/(bjd)$ if the tension force in the longitudinal reinforcement is to increase linearly with the moment (beam action). If the vertical cracks are narrow enough to be able to transmit this shear stress by aggregate interlock, then the concrete in the tooth between the two vertical cracks will be in pure shear. This means the principal tensile stress is also equal to $Vl/(bjd)$ which will cause a diagonal crack at an angle of 45° (destroying beam action) when the shear stress equals the cracking stress of the concrete, $f_{cr}$. The ACI[5] traditional value of principal tensile stress to cause diagonal cracking is $0.33\sqrt{f_c'}$.

Case 2 in Figure 4 shows the situation for a beam where

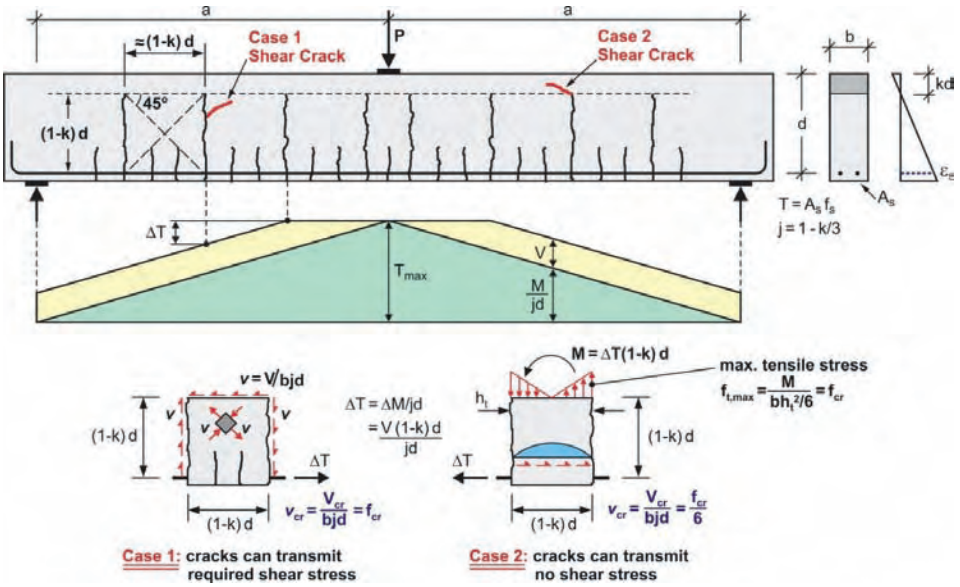


*Figure 4: Bounds on shear stress at which diagonal cracks will form*[9].

the vertical cracks are so wide that no shear stresses can be transmitted across the cracks. Again horizontal equilibrium requires the average shear stress on any horizontal plane across the tooth must equal $Vl(bjd)$ but now these horizontal shear stresses must reduce to zero at the crack locations. In this case in order to change the force in the longitudinal reinforcement as required by beam action, bending moments causing vertical stresses must develop in the concrete tooth. The highest tensile stress in concrete tooth shown will occur at the top right corner and will equal $6Vl(bjd)$. Thus, for Case 2, the concrete must resist a tensile stress six times higher than that for Case 1 to maintain beam action. In Case 2, a nearly horizontal inclined crack is predicted to form when the shear stress $Vl(bjd)$ equals about $0.055\sqrt{f_c'}$. Thus depending on the width of the cracks in the web of the beam the shear stress to cause flexural shear cracking can be expected to vary from about $0.055\sqrt{f_c'}$ to about $0.33\sqrt{f_c'}$. As crack width depends on crack spacing and as crack spacing in the upper region of the web is proportional to beam depth, as beam depths increase the shear stresses at which beam action breaks down will become closer to the lower limit.

After beam action breaks down, it is possible that a strut-and-tie mechanism can carry even higher loads provided that the distance from the load to the support is not too great. This point is illustrated in Figure 5 which shows the results of 14 experiments[10] where the only significant variables were the shear span to depth ratio, a/d, and the size of the bearing plates, $l_b$. It is of interest that the bearing plate size had no influence on the failure load of the longer specimens but strongly influenced the strength of the shorter specimens. The strut-and-tie model used to determine the carrying capacity after breakdown of beam action is shown on the figure. Strut-and-tie provisions were introduced in the 1984 edition of the CSA code[11] and similar provisions now appear in EC2 and ACI. The predictions from these three codes are also shown on the figure. These strut-and-tie provisions differ principally in the definition of the limiting compressive stress in the diagonal strut. For EC2 and ACI, this limiting compressive stress is a function only of the concrete strength though ACI also places a lower limit of 25° on the angle, $\theta_s$, between the strut and the reinforcement. For CSA, the limiting stress is a function of the angle $\theta_s$ and the strain in the reinforcement that crosses the strut. It should be noted that the predicted shear strength for any given a/d ratio, is taken as the larger of the beam action strength or the strut-and-tie strength. For these particular beams, it might be noted that the shear capacities of the longer beams which are governed by breakdown of beam action are more accurately predicted by the ACI and CSA provisions than by EC2. For the shorter spans, the increase in shear capacity as the shear span length decreases is more accurately predicted by the CSA provisions than by ACI or EC2. The theory upon which the CSA provisions are based will be outlined next.

## 4.0 MODIFIED COMPRESSION FIELD THEORY (MCFT)

The earliest shear design procedures for reinforced concrete, the truss analogies of Ritter and Mörsch[12] assumed that after concrete cracked, shear stresses would be resisted only by diagonal compressive stresses inclined at 45° to the longitudinal axis of the member. Equilibrium then dictates that the failure shear stress, $Vl(bjd)$, will equal the transverse tensile stress, $(A_v f_y / b_w s = \rho_z f_{yz})$, that can be applied by the stirrups. Thus as member L-10HS in Figure 3 contains 0.50 MPa of shear reinforcement the 45° truss model predicts that the shear stress at failure will be 0.50 MPa. Taking $jd$ as $0.9d$ it can be seen that the actual failure stress was 1.69/0.9 or 1.88 MPa a value 3.76 times the predicted value of the 45° truss model. Because members with small amounts of shear reinforcement usually resist shear stresses much higher than $\rho_z f_{yz}$ many international codes have included an empirical correction term called the "concrete contribution". Rather than accounting for contributions related to the tensile strength of concrete, European researchers[6] concentrated on improving the estimate of the angle of inclination, θ, of the principal compressive stresses in the concrete after diagonal cracking. The predicted failure shear stress then becomes $\rho_z f_{yz}$ cot $\theta$. For cot $\theta$ to reach 3.76 the inclination of the compression diagonals needs to reduce to 15°. The photograph of L-10HS taken just at failure, Figure 6, shows a failure crack inclination of more than 30°. Examination of Figure 6 also shows slip of the crack at failure and local crushing of the concrete at the crack caused by shear transfer across the crack.

The Modified Compression Field Theory (MCFT) [13, 14] was developed to account for both the contributions of the concrete tensile stresses in the cracked concrete and the variable angle of principal compressive stresses. Figure 7 shows the 15 equations of the MCFT. Across the width of the figure the equations are divided into three sets: five equilibrium equations, five geometric conditions and five stress-strain relationships. In the

upper part of the figure the equations deal with average stresses, average strains and the relationships between average stresses and average strains. Average stresses (eg, $f_{sx}$) and average strains (eg, $\varepsilon_x$) correspond to stresses and strains averaged out over lengths long enough to damp out the local variations that occur at cracks and between cracks. The bottom five relationships in the figure are concerned with stresses at a crack (eg, $f_{sxcr}$), the crack width and the maximum shear stress that can be transmitted across the crack. The term $v_{ci}$ stands for shear stress transmitted across the crack interface. The two small inset stress-strain figures represent the standard bilinear stress-strain relationship assumed for reinforcing bars and the uniaxial compressive stress-compressive strain relationship obtained from a standard cylinder test. The average stress-average strain relationships for cracked concrete given by Equation 13 and Equation 14 in Figure 7 are the result of experiments on elements of reinforced concrete loaded in pure shear or combined shear and biaxial compression or tension in special testing frames. See Figure 8. The relationship used for determining the ability of the crack surfaces to transmit the interface shear, Equation 15 in Figure 7, was derived from the aggregate interlock experiments of Walraven[15]. Note that this shear stress limit is a function of crack width, $w$, maximum aggregate size, $a_g$, and concrete cylinder strength, $f_c'$. While solving these 15 equations by hand is tedious, it is straightforward using an appropriate computer program such as Membrane-2000, available on the web[16]. As the name implies, the MCFT is a modified version

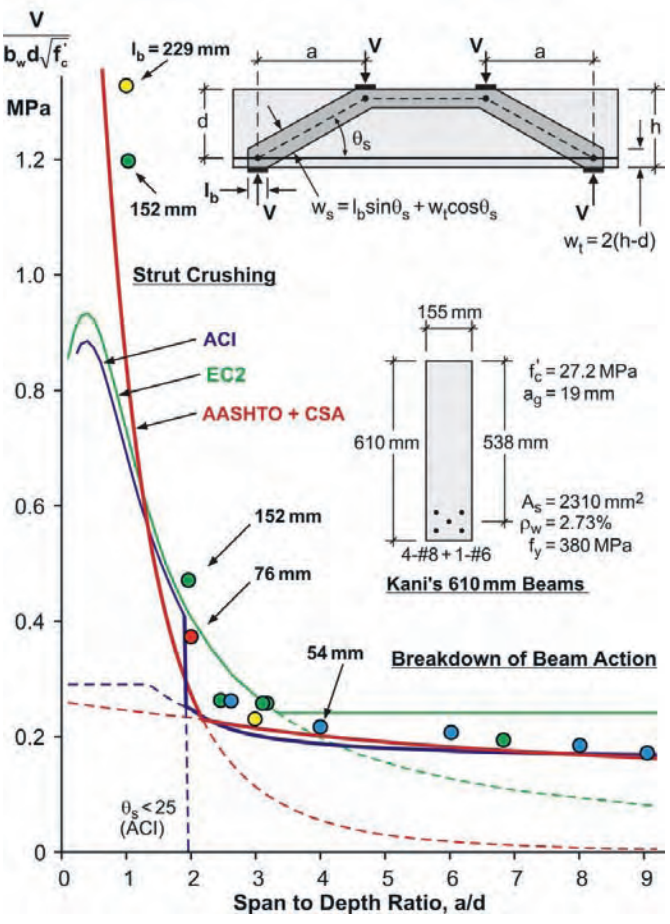


*Figure 5: Beam action and strut-and-tie action.*

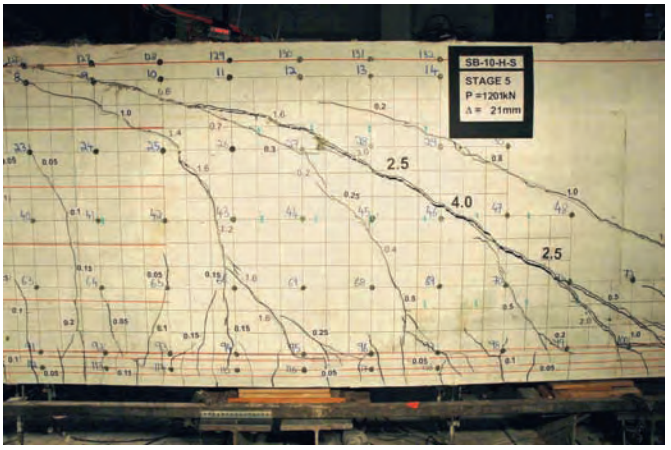


*Figure 6: Failure of 1.5 m thick slab strip with minimum shear reinforcement.*

of the compression field theory (CFT)[17, 18] which neglected the influence of tensile stresses in the cracked concrete. For specimens with at least minimum transverse reinforcement the simpler CFT provides a suitable lower bound to expected shear response. In this case, the 15 equations in Figure 7 reduce to nine equations: three equilibrium equations (1, 2 and 3 with $f_1$ taken as zero); three compatibility equations (6, 7 and 8); and three stress-strain relationships (11, 12 and13).

One of the key relationships for both the CFT and the MCFT is Equation 13 in Figure 7 which captures the experimental observation that cracked reinforced concrete cannot transmit high levels of compressive stress. As the concrete becomes more cracked the average principal tensile strain, $\varepsilon_1$, becomes larger and the concrete principal compressive stress, $f_2$, which can be transmitted becomes smaller. Figure 9 compares the predictions from this now 30 year old relationship with the results from 12 recent experiments[19]. In these 355 mm thick shell elements the grid of reinforcing bars are at 45° to the specimen edges with the stronger x reinforcement going from bottom left to top right. The vertical actuators apply compression while the horizontal actuators apply tension. It took a shear of 8600 kN on the main diagonal planes to fail Specimen 3 which ranks as one of the largest shear forces ever applied to a laboratory specimen. Specimens with biaxial compression in addition to shear were stronger but more brittle than specimens tested in pure shear.

## 5.0 LEVELS OF APPROXIMATION IN MCFT ANALYSES

To use the MCFT to predict the load-deformation response of a reinforced concrete beam or slab strip such as one of those shown in Figure 3, the beam could be represented as a two dimensional grid of elements with the response of each element being predicted by the MCFT. This is the basis of non-linear finite element programs such as VecTor2 [20, 21] which have been developed at the University of Toronto over the past 25 years. If such a program is used to analyse the beam it will be found (see Figure 10) that in zones extending for a distance of about $d$ away from the point loads and the reactions there will be significant vertical compressive stresses in the concrete. These clamping stresses will enhance the shear

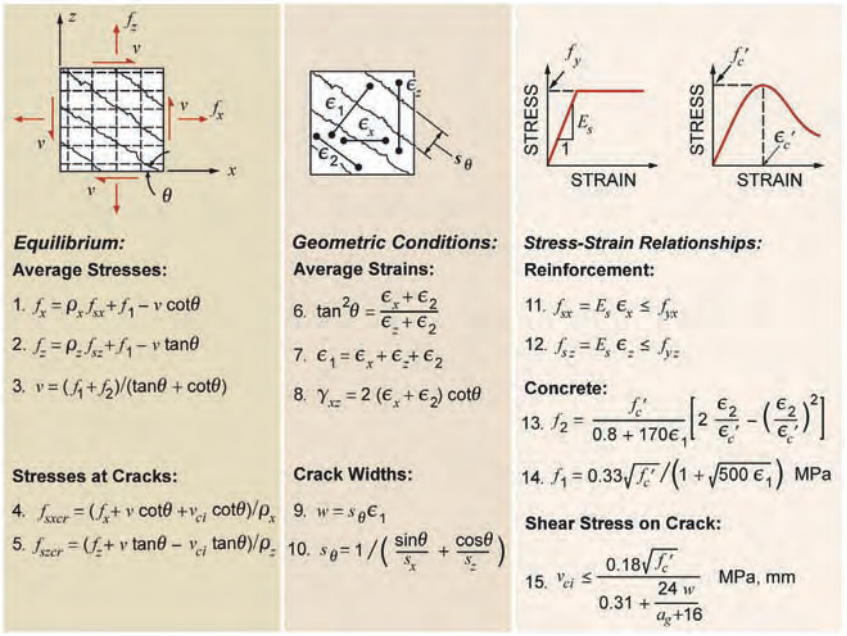


*Figure 7: The Modified Compression Field Theory (MCFT).*

*Figure 8: Shell element tester with 60 computer controlled actuators.*

strength of the elements in these zones making it probable that the shear failure will occur outside of these zones. For beams with short shear spans the zones with significant clamping stresses will overlap and the shear strength of the beam will be considerably increased. It is important to recognise that in these "disturbed regions" the shear stress distribution over the depth of the beam is influenced by the distribution of the clamping stresses and near the loads and reactions, plane sections do not remain plane.

Outside of the disturbed regions it is appropriate to assume that plane sections remain plane and that the clamping stresses are negligible. With these two assumptions a beam cross-section can be modeled as a stack of biaxially stressed elements with the response of each element being predicted by the MCFT. This is the basis of program Response-2000 [22, 23] which can be used to predict the shear stress distribution over the depth of the beam and the complete load-deformation response of concrete sections subjected to shear, flexure and axial load; see Figure 10. If only the shear strength of a beam cross-section is required then the web of the beam can be approximated by just one biaxial element located at mid-depth and the shear stress on the element can be assumed to be $V/(b_w d_v)$ where $b_w$ is the web width and $d_v$ is the flexural lever arm which can be taken as $0.9d$. The longitudinal strain, $\varepsilon_x$, at mid-depth of the beam can be found from the calculated strain in the longitudinal flexural reinforcement and the assumption that plane sections remain plane. For a given value of $\varepsilon_x$ the failure shear stress can then be calculated from the MCFT as the sum of two terms, $V_c$ and $V_s$, see Figure 10. This simplified MCFT [24, 25] sectional design model for shear is the method used in the current Canadian Standards Association (CSA) document "Design of Concrete Structures" A23.3-04[4].

Based on the MCFT, the CSA shear provisions provide a set of equations that depend on geometric terms, material properties, and a measure of the average longitudinal strain at mid-depth of the beam at shear failure. The reliable shear strength ($V_r$) of a beam with partial safety factors ($f_c$=0.65, $f_s$ = 0.85) can be taken as:

$$V_r = V_c + V_s \quad \le 0.25\phi_c f_c' b_w d_v$$
$$V_r = \phi_c \beta \sqrt{f_c'} \cdot b_w d_v + \phi_s \frac{A_v}{s} f_y d_v \cot\theta \qquad (1)$$

where, $b_w$ is the web width (mm), $d_v$ is the shear depth taken as 0.9d (mm), $f_c'$ is the concrete cylinder strength (MPa), $A_v$ is the area of shear reinforcement (mm$^2$) at a spacing of $s$ (mm) and a yield strength of $f_y$ (MPa). For higher strength concretes the square root of $f_c'$ in the $V_c$ term should not be taken as greater than 8.0 MPa.

Two parameters are needed to solve this equation, the first, $\beta$, is a measure of the ability of the cracked reinforced concrete to transmit shear stresses across cracks. The second, $\theta$, indicates the direction of principal compression and governs the contribution of the stirrups. Derived from the MCFT equations, the following equation is included in the code to determine $\beta$:

$$\beta = \frac{0.40}{(1 + 1500\varepsilon_x)} \cdot \frac{1300}{(1000 + s_{xe})} \qquad (2)$$

where $\varepsilon_x$ is a measure of the average longitudinal strain at mid-depth of the section under the combined loading, see below. The term $s_{xe}$ defines the effective crack spacing of the member and is taken as 300 mm for members with at least minimum stirrups or $d_v$ = 0.9d for other members with normal strength concrete and 19 mm coarse aggregate size. In general, $s_{xe}$ is given as:

$$s_{xe} = \frac{35 d_v}{16 + a_{ge}} \ge 0.85 d_v \qquad (3)$$

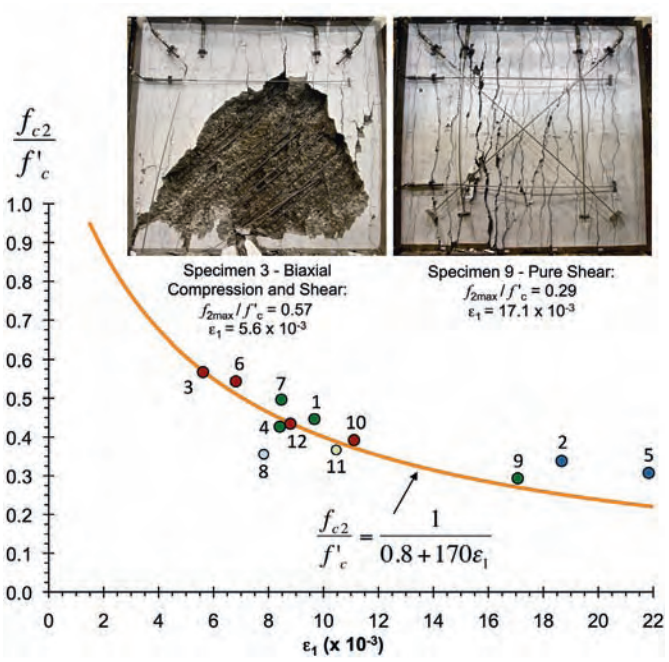


***Figure 9: Reduction of compressive strength with principal tensile strain.***

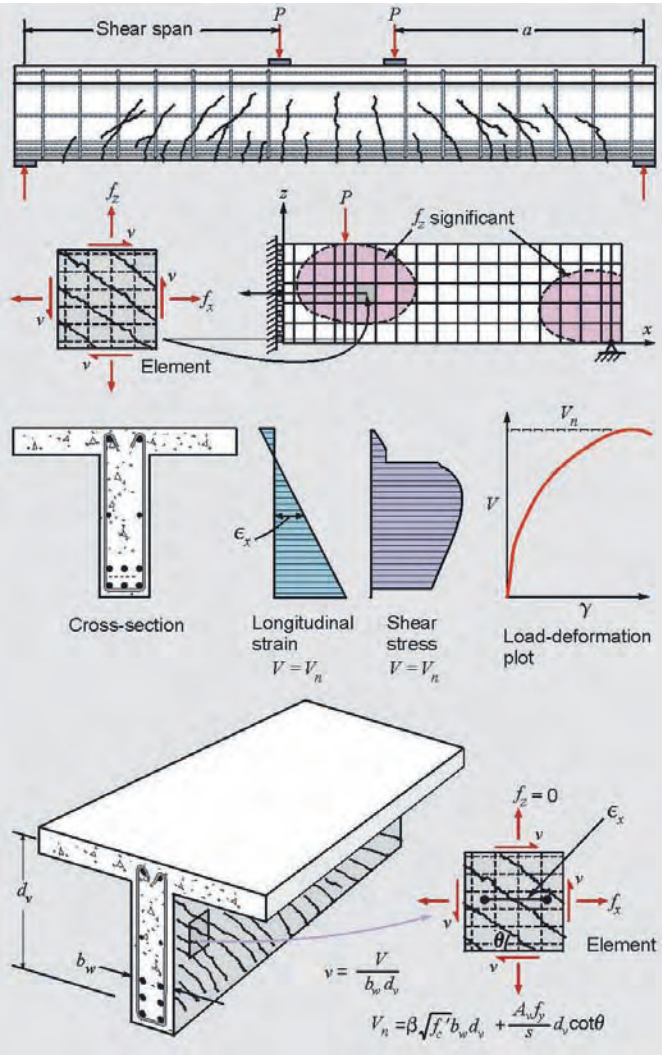


***Figure 10: Levels of approximation in MCFT analysis.***

The effective aggregate size, $a_{ge}$, is the maximum aggregate size except it is taken as zero for concrete strengths greater than 70 MPa.

The first term in Equation 2 for $\beta$ accounts for the detrimental effect of increasing longitudinal strain on shear capacity (the strain effect), while the second term accounts for the detrimental effect of increasing crack spacing on shear strength (the size effect). Note that if high-strength reinforcement or low stiffness reinforcement (FRP) is used, the longitudinal strains will likely be considerably higher resulting in lower shear capacities.

To estimate the longitudinal strain at mid-depth, the following general equation is used:

$$\varepsilon_x = \frac{M_f / d_v + V_f + 0.5N_f - A_p f_{p0}}{2(E_s A_s + E_p A_p)} \quad (4)$$

Where the terms $M_f$, $V_f$, and $N_f$ are the moment and shear (both taken as positive) and the axial force (tension positive) at the section of interest. While $A_s$, $E_s$, $A_p$, $E_p$, are the areas and Young's moduli of the regular and bonded prestressed reinforcement respectively. The term $f_{p0}$ is the stress in the prestressing reinforcement when loaded to an extent that the strain in the surrounding concrete is equal to zero. Note that axial load and prestressing are considered in a compatible way in the CSA code shear provisions.

While the MCFT equations indicate that a variable angle truss model could be used for the shear design of members with stirrups, the following equation is provided in the CSA code to directly calculate the appropriate value of $\theta$:

$$\theta = 29° + 7000\varepsilon_x \quad (5)$$

To demonstrate the use of the above design equations, consider the high-strength concrete large member without stirrups (L-10H) in Figure 3. It has the following parameters: $b_w$ = 300 mm, $d$ = 1400 mm, $f'_c$ = 75 MPa, $a_{ge}$ = 0 mm, $A_s$ = 3500 mm$^2$, $E_s$ = 200 GPa, and a shear span of 4050 mm. The critical section for shear for this beam is indicated by the CSA code to be a distance of $d_v = 0.9d$ = 1260 mm away from the edge of the loading plate. At this location, a shear of 1 kN will result in a moment of (4.050-0.075-1.26) = 2.720 kNm. This M/V ratio can be taken as constant. The crack spacing term in this case is

$s_{xe}$ = 1260 × 35/(16+0) = 2760 mm.

While design of a section for shear is a direct calculation, predicting the shear strength of a given section requires some iteration. It is usually best to assume a value of $\varepsilon_x$ to allow Equations 1 and 2 to be evaluated, and then check the assumed value of $\varepsilon_x$ using Equation 4. With $\varepsilon_x$ assumed equal to 1.0 × $10^{-3}$, Equation 2 gives a value for $\beta$ of 0.0553. Substituting this into Equation 1 indicates a shear strength estimate of 167 kN. This will have a corresponding moment of 167 × 2.720 = 454 kNm. Substituting these force values into Equation 4 produces a calculated strain of 0.377x$10^{-3}$. Thus the assumption of a strain of 1.0×$10^{-3}$ was conservative. An appropriate next iteration could be taken as $\varepsilon_x$ = (2.0 × 0.377 × $10^{-3}$+1.0 × $10^{-3}$)/3.0 = 0.585 × $10^{-3}$ producing a shear strength of 223 kN and a calculated strain from Equaton 4 of $\varepsilon_x$ = 0.50 × $10^{-3}$.

Convergence is reached with $\varepsilon_x = 0.527 \times 10^{-3}$ and a shear strength of 234 kN. The test specimen failed at a shear of 240 kN for a test-to-predicted ratio of 1.03.

For the large high-strength concrete member with shear reinforcement (L-10HS) the same process is applied, but Equation 5 is also used to determine θ from the assumed strain and this too contributes to the total shear strength. When these calculations are performed, the beam is found to have a predicted shear strength of 732 kN versus an observed strength of 710 kN for a test-to-predicted ratio of 0.97. As already noted, the addition of just minimum shear reinforcement has increased the shear strength of the member by a factor of about 3.0. The stirrups results in a pattern of more closely spaced cracks, see Figure 6, which justifies the use of the assumed $s_{xe}$ = 300 mm. The reduction in the size effect caused by stirrups is clear in Figure 3 where the ratio of failure shear stress of the large members to the small members goes from 0.52 for members without stirrups to 0.87 for members with stirrups.

The inset diagrams near the bottom of Figure 11 compare two simply supported beams without shear reinforcement subjected to uniformly distributed loads. The 1000 mm thick specimen (SP1)[26] was tested in 2011 at the University of Toronto and forms part of the eight specimen series shown in the plot. The small 325 mm thick specimen shown below SP1 was tested 50 years earlier at the University of Stuttgart[27] and forms part of a ten specimen series. With clear-spans-to-overall-thickness ratios of 4.65 and 4.38 neither specimen is classified as a deep beam by the ACI[5] limit of 4.0. However the small specimen acted as a deep beam carrying loads many times greater than the diagonal cracking load and failing at a shear stress 4.91 MPa. The large specimen, however, failed when the first major diagonal crack formed at a shear stress of 1.31 MPa demonstrating again the vulnerable nature of large members without shear reinforcement. Because of this it is advisable to use the more conservative strut-and-tie model shown in Figure 11 in the design of such members

## 6.0 EXAMPLES OF STRUCTURAL EVALUATION USING THE MCFT

### Cracked reinforced bridge girders in Oregon

About two hundred reinforced concrete deck-girder bridges in Oregon along major interstate highways[28] were found to have diagonal tension cracks which appeared to be increasing in width with time. Most of these bridges were designed and built in the 1950s using shear design procedures that are now known to be significantly unconservative. After placing weight restrictions on the cracked bridges a major research program was launched to develop procedures to more accurately assess the safety of all these bridges. See Figure 12. As part of this study 40 full scale bridge girder segments were fabricated and tested at Oregon State University. It was found that the observed response of these large specimens matched very closely the behaviour predicted by program Response-2000[23]. Because of this the assessment methodology developed involved using Response-2000 calculations to estimate shear failure strengths for the different bridge girders.

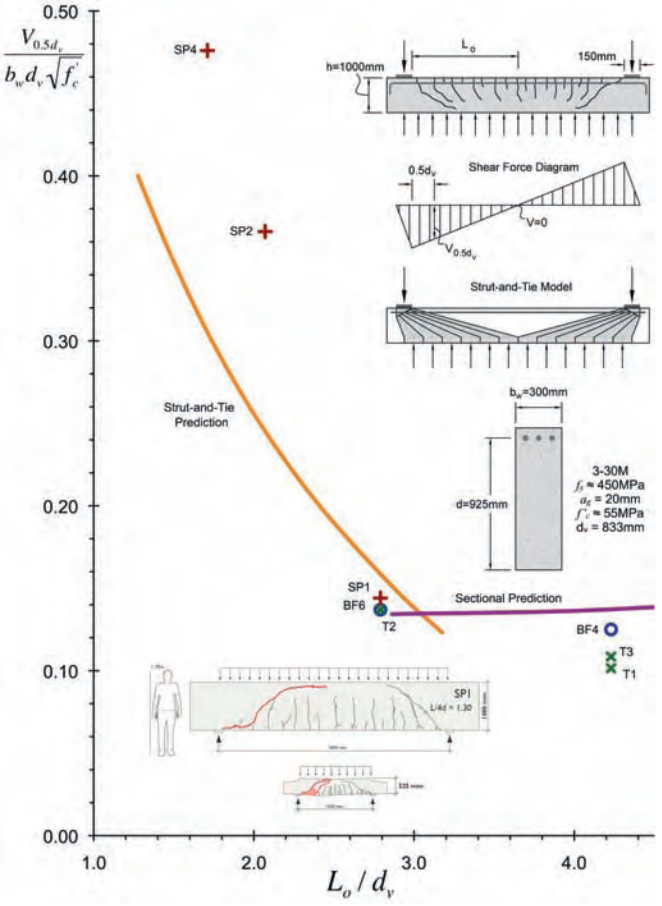


*Figure 11: Large footing strips under uniform loads.*

### Transfer girder supporting forty stories in high rise building

As part of an investigation of the safety of six metre deep transfer girders supporting forty stories in a high rise building a one-fifth scale model of a significant portion of a girder was constructed and loaded to failure. The girder, which had a large opening at mid-span, was loaded by an off-centre vertical load. See Figure 13 in which the shear force resisted by the girder is plotted against the measured mid-span deflection. It can be seen that failure occurred by crushing of the concrete in the lightly reinforced web of the girder with the shear stress at failure reaching 28% of the cylinder strength of the concrete. Both the load-deflection response and the failure load were well predicted by the MCFT based VecTor2[21] non-linear finite element analysis.

### Post-tensioned girder with larger openings

Figure 14 shows the Habitat'67 structure in Montreal. One of the special features of this structure was the presence of long-span post-tensioned "street girders" to provide walkways in the complex. The street girders span 22 m between precast concrete columns and contain three large openings in each of the two webs. The girders provide an upper and a lower walkway for pedestrians. A non-linear analysis using program VecTor2[21] was used to predict the response of the girder. It was found that the areas just inside the outermost openings


***Figure 12: Large bridge girders predicted response and observed response.***

were the most critical, with horizontal cracking predicted that matched the observed cracking. Insufficient vertical reinforcement was provided to "lift" the shear to the top of the girder near the inner face of the outermost openings. In addition, the anchoring of inclined tendons in this region contributed to the vertical tensile stresses. The strengthening measures consisted of adding a total of four pairs of post-tensioned high-strength threaded rods in this critical region, with two additional pairs of tendons added on both sides of the central opening. The added tendons were anchored with thick stainless steel anchor plates and the exposed stainless steel ducts were grouted.

## Transfer girder in a 14 storey apartment building

The Toronto apartment building shown in Figure 15 developed wide diagonal cracks in major girders visible from the outside of the building. The width of the cracks and the extent of the cracking were both increasing with time. Analysis of the structure and the supporting soil, revealed that the prime cause of these shear cracks was the differential settlement of the raft foundation which in turn was caused by a significant layer of clay beneath the building. The "outrigger" part of the girders, in which the cracks were visible, was carrying an increasingly large portion of the building weight. It was calculated that under high wind loads these outrigger girders had an unacceptably high risk of failing. A detailed VecTor2[21] analysis of the 1.2 m deep transfer girder system at the second floor level predicted that an even more dangerous situation existed in parts of the girders that were not visible. When the ceiling was removed and these portions examined, wide shear cracks were discovered in the locations and in the orientations predicted. A temporary support system was immediately provided until more permanent repairs could be completed.

## The Concorde Overpass collapse

On September 30, 2006, the south half of the Concorde Overpass in Laval, Québec, suddenly failed in shear, killing five people and injuring six others; see Figure 2 and Figure 16. A major public enquiry followed the collapse to determine the causes of the collapse. The six lane bridge consisted of precast pretensioned hollow box girders spanning 27.4 m that were supported by thick cast-in-place slabs that cantilevered 3.96 m from an inclined wall support at each end. The reinforcement details in the thick slab cantilever that failed in the south east corner of the structure are shown in Figure 16. A major shortcoming of the reinforcement detailing was that the #8 Ushaped hanger reinforcement was not properly anchored around the top and bottom longitudinal reinforcement. It is noted that this thick slab had an effective depth of 1.2 m and did not contain stirrups. Investigations revealed that, in addition to the inadequate anchorage of the hanger reinforcement, the reinforcement in the beam seat region had been misplaced. The resulting gap between the hooks of the hanger reinforcement and the top longitudinal reinforcement created a tensile zone of weakness in the concrete between the hooks and the #14 top bars. In addition, the #14 bars, which were spaced at 152 mm, were not properly anchored at the end of the full-depth section, resulting in high bond stresses in the tensile zone of weakness.

After 36 years in service, the thick slab cantilever failed suddenly, under essentially its own weight, with an inclined crack occurring immediately above the hooks of the #8 U-shaped hanger reinforcement and the hooks of the #6 inclined bars . At the time of the design, in 1969, codes did not address the design of disturbed or D-regions. Failure was attributed[3] to several contributing factors including: improper anchorage of the #8 U-shaped hanger reinforcement, misplaced hanger reinforcement and degradation of the concrete due

*Figure 13: Testing one-fifth scale model of transfer girder.*

primarily to freeze-thaw deterioration in the presence of deicing salts. An additional major factor affecting the failure was the "size effect" in shear for this thick slab without stirrups. Figure 16 illustrates the shear stress at service load for the cantilever, the shear stress limit under working stress design and the shear failure stresses of two series of beams[1]. These beams did not contain shear reinforcement and had varying effective depths, d. It is evident that for the Concorde Overpass these earlier shear design provisions resulted in a totally inadequate factor of safety against a catastrophic shear failure. Had the current Canadian shear provisions been used the thick slabs would have required shear reinforcement and failure would have been prevented.

## 7.0 CONCLUSIONS

This paper has summarized the shear design procedures developed by the authors and their colleagues over the past 40 years. These procedures are based on the MCFT which is capable of predicting accurately the shear behaviour of cracked reinforced concrete under general biaxial loading conditions. The paper has summarised the 2004 Canadian shear provisions based on the MCFT and shown how they can be used to calculate the shear strength for a wide variety of members and structures.

It has been demonstrated that while the predicted flexural capacities given by different internationally respected design codes agree very closely, the predicted shear capacities may differ by factors as high as 2.56. The difficulty is that shear strength is influenced by many more parameters than flexural strength and most laboratory experiments have been conducted on rather small specimens with a rather narrow range of parameters. Because of this, the traditional empirically-based shear provisions can give unsafe predictions when applied to large, lightly-reinforced members or to members made with new materials such as high strength concrete, self- compacting concrete, FRP reinforced concrete or members reinforced with high strength steel.

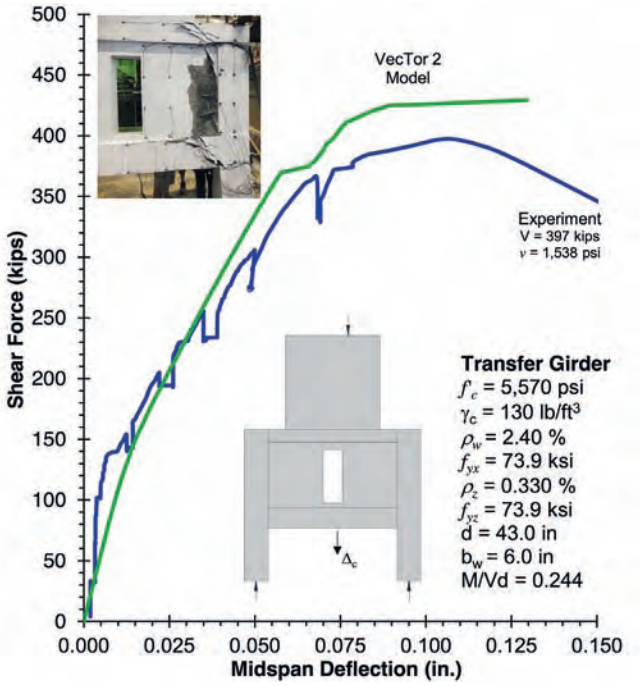


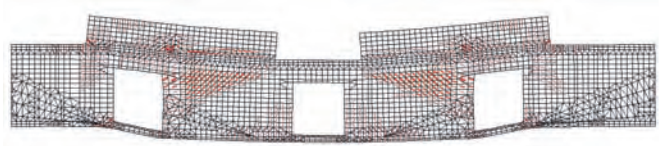

*Figure 14: Post-tensioned girder with large openings.*

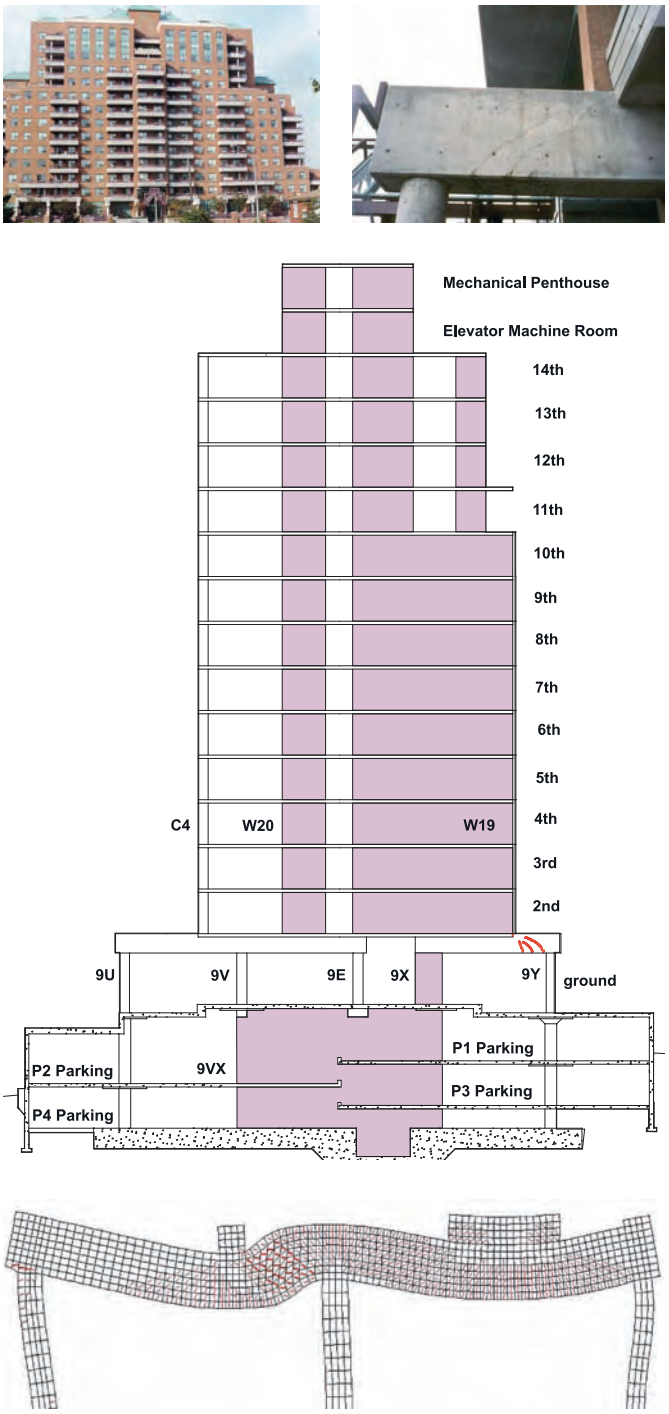


*Figure 15: Shear distress in 14 storey apartment building.*

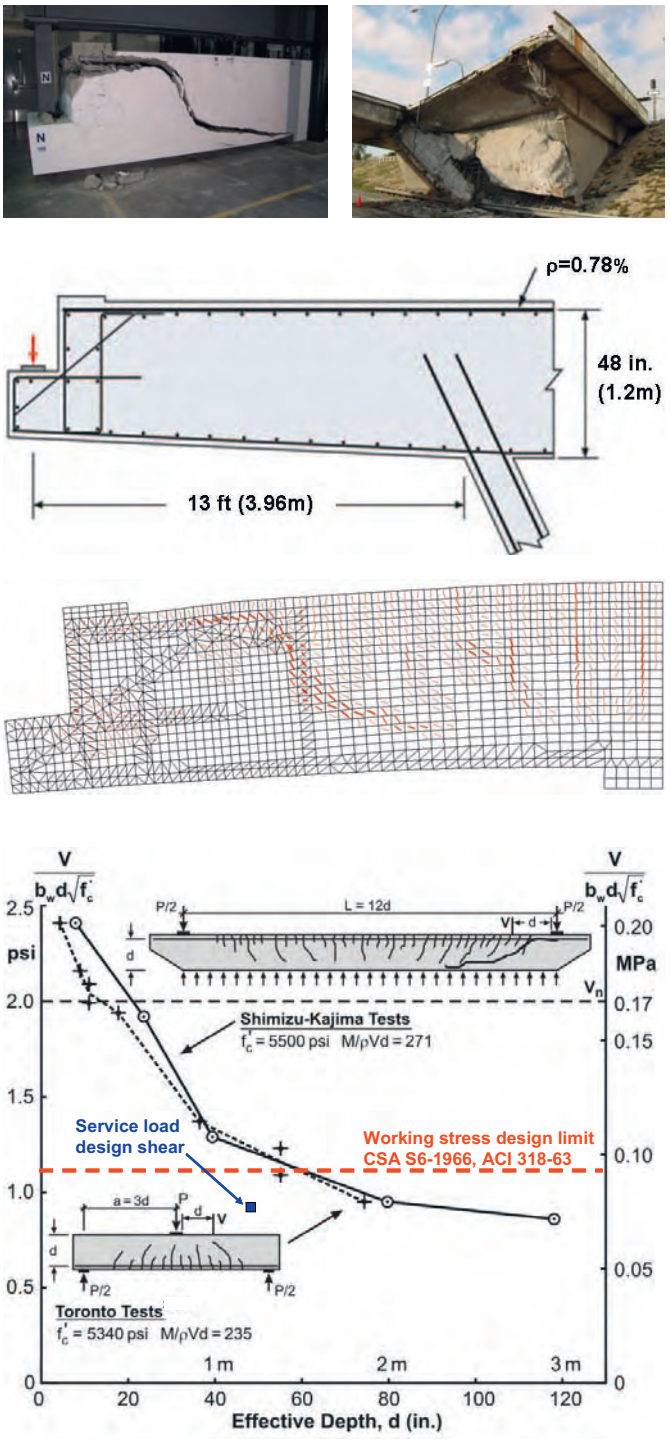


*Figure 16: Investigating collapse of Concorde Overpass[29].*

Given the large number of existing concrete structures designed using shear provisions now known to be unconservative, and the limited resources available to increase public safety, it is essential that the shear design procedures used to evaluate these structures be as accurate as possible. It is evident from the comparisons made in this paper that of the five codes studied the shear provisions of the CSA code provide estimates with the least scatter. This low scatter is despite, or perhaps, because of the fact that these Canadian provisions are theoretically based, not fitted to the experimental database. It is hoped that the methods presented in this paper will allow wiser decisions to be made in allocating available resources to improve the resilience and safety of concrete structures.

## ACKNOWLEDGEMENTS

The authors would like to express their gratitude to the Natural Sciences and Engineering Research Council of Canada for a series of grants that have made possible the long-term research projects on shear design at the University of Toronto and at McGill University.

## REFERENCES


1. Collins, M.P., Bentz, E.C., and Sherwood, E.G., "Where is Shear Reinforcement Required? Review of Research Results and Design Procedures", *ACI Structural Journal*, Vol. 105, No.5, Sept.-Oct. 2008, pp. 590-600.
2. Sherwood, E.G., Bentz, E.C., and Collins, M.P., "Effect of Aggregate Size on Beam-Shear Strength of Thick Slabs", *ACI Structural Journal*, Vol. 104, No. 2, March-April 2007, pp 180-190.
3. Johnson, P.-M., Couture, A. and Nicolet, R. (2007), "Commission of Inquiry into the Collapse of a Portion of the de la Concorde Overpass", Library and National Archives of Quebec. http://www.cevc.gouv.qc.ca/UserFiles/File/Rapport/report_eng.pdf
4. CSA Committee A23.3, "Design of Concrete Structures", Canadian Standards Association, Mississauga, Ontario, Canada, 2004, 214 pp.
5. ACI Committee 318, "Building Code Requirements for Reinforced Concrete (ACI 318-11) and Commentary (318R-11)," American Concrete Institute, Farmington Hills, Michigan, USA, 2011, 509 pp.
6. European Committee for Standardization, CEN, "EN 1992-1-1:2004 Eurocode 2: Design of Concrete Structures – Part 1-1: General rules and rules for buildings," Brussels, Belgium, 2004, 225 pp.
7. BSI, "BS 8110-1:1997 Structural Use of Concrete – Part 1: Code of Practice for Design and Construction," 1997, British Standards Institute, London, 159 pp.
8. Australian Standards, "Concrete Structures, AS3600-2009", Standards Australia, Sydney, pp.
9. Collins, M.P., Bentz, E.C., Sherwood, E.G., and Xie, L., "An Adequate Theory for the Shear Strength of Reinforced Concrete Structures", *Magazine of Concrete Research*, Vol. 60, No. 9, Nov. 2008, pp. 635-650.
10. Kani, M.W., Huggins, M.W., and Wittkopp, R.R., "Kani on Shear in Reinforced Concrete", Department of Civil Engineering, University of Toronto, Toronto, 1979, 225 pp.
11. Collins, M.P. and Mitchell, D., "A Rational Approach to Shear Design – The 1984 Canadian Code Provisions", *Journal of the American Concrete Institute*, Vol. 83, No. 6, Nov.-Dec. 1986, pp. 925-933.
12. Mörsch, E., "Der Eisenbetonbau", translated to English as *Concrete-Steel Construction*, McGraw Hill, New York, 1909, 387 pp.
13. Vecchio, F.J. and Collins, M.P., "The Modified Compression Field Theory for Reinforced Concrete Elements Subjected to Shear", *Journal of the American Concrete Institute*, Vol. 83, No. 2, March-April 1986, pp. 219-231.
14. Collins, M.P. and Mitchell, D. "Prestressed Concrete Structures", Prentice Hall, Englewood Cliffs, New Jersey, 1991, 766 pp.
15. Walraven, J.C., "Fundamental Analysis of Aggregate Interlock," *Journal of the Structural Division*, American Society of Civil Engineers, Vol. 107, No. 11, Nov. 1981, pp. 2245-2270.
16. Bentz, E. C., Membrane-2000, http://www.ecf.utoronto.ca/~bentz/m2k.htm.
17. Mitchell, D. and Collins, M.P., "The Compression Field Theory – A Rational Model for Structural Concrete in Pure Torsion," *Journal of the American Concrete Institute*, Vol. 71, No. 8, August 1974, pp. 396-408.
18. Collins, M.P. "Towards a Rational Theory for RC Members in Shear," *Journal of the Structural Division*, American Society of Civil Engineers, Vol. 104, No. ST4, April 1978, pp. 649-666.
19. Bae, G. M., Proestos, G. T., Lee, S.-C., Bentz, E. C., Collins, M. P., and Cho, J. -Y., "In-Plane Shear Behavior of Nuclear Power Plant Wall Elements with High-Strength Reinforcing Bars," *Transactions*, SMiRT-22 San Francisco, California, August 18-23, 2013 Division VI, pp. 510-519.
20. Vecchio, F. J., "Nonlinear Finite Element Analysis of Reinforced Concrete Membranes," *ACI Structural Journal*, V. 86, No. 1, Jan.-Feb. 1989, pp. 26-35.
21. Vecchio, F.J., VecTor2, 2013, http://www.civ.utoronto.ca/vector
22. Bentz, E.C., "Sectional Design of Concrete Structures," PhD Thesis, Department of Civil Engineering, University of Toronto, 2000, 310 pp.
23. Bentz, E.C., Response-2000, 2013, http://www.ecf.utoronto.ca/~bentz/r2k.htm
24. Bentz, E.C., Vecchio, F.J., and Collins, M.P., " The Simplified MCFT for Calculating the Shear Strength of Reinforced Concrete Elements", *ACI Structural Journal*, V.103, No. 4, July-Aug. 2006, pp.614-624.
25. Bentz, E.C. and Collins, M.P., " Development of the 2004 CSA A23.3 Shear Provisions for Reinforced Concrete", *Canadian Journal of Civil Engineering*, Vol. 33, No. 5, May 2006, pp 521-534.
26. Perkins, S.M.J, "Shear Behaviour of Deep Reinforced Concrete Members Subjected to Uniform Load", MASc Thesis, Department of Civil Engineering, University of Toronto, 2011, 129 pp.
27. Leonhardt, F., and Walther, R., "The Stuttgart Shear Tests, 1961," A translation of the articles that appeared in *Beton und Stahlbetonbau*, Vol. 56, No. 12, 1961, and Vol. 57, No. 2, 3, 6, 7 and 8, 1962, Cement and Concrete Association Library Translation No. 111, Dec. 1964, 134 pp.
28. Higgins, C., Miller, T.H., Rosowsky, D.V., Yim, S.C., Potisuk,T., Daniels,T.K., Nicholas, B.S., Robelo, M.J., Lee, A.Y., and Forrest, R.W., "Assessment Methodology for Diagonally Cracked Reinforced Concrete Deck Girders", Final Report for Oregon Department of Transportation and the Federal Highway Administration, Final Report SPR 350, SR 500-091, October 2004, 340 pages plus appendices.
29. Mitchell, D., Marchand, J., Croteau, P. and Cook, W.D. "The Concorde Overpass Collapse – Structural Aspects", *ASCE Journal of Performance of Constructed Facilities*, Nov/Dec. 2011, pp. 545-553.

# Development of geopolymer precast floor panels for the Global Change Institute at the University of Queensland

Rod Bligh, Bligh Tanner, Brisbane

Tom Glasby, Wagner, Toowoomba

*Wagners EFC (Earth Friendly Concrete) has been successfully utilised for construction of 11 m span precast panels in what is believed to be an Australia first use of suspended geopolymer concrete in the building industry. The design team (Bligh Tanner Consulting Engineers, Lead Consultant Hassell Architects and Arup Sustainability), with the support of University of Queensland worked closely with Wagners to fast track the testing and certification phase of EFC to enable use on this exemplar sustainability project. Adoption of geopolymer to minimise the carbon footprint of this 6 star Greenstar rated project necessitated precasting of the floor panels to ensure quality control of the concrete placement. Use of precast provides opportunities for shaping a vaulted soffit, which improves the efficiency of the cooling systems incorporated in the panels as well as enhancing the space architecturally. The project required close collaboration between the design team, Wagners, the precast fabricator, Precast Concrete, and the builder, McNab, to achieve high quality panels, which are an important visual element in the project. The concrete mix has performed very well with low shrinkage, no visible cracking and good performance in relation to testing of cylinders and load testing of the full panels. The project is very significant in the conference categories of design, sustainability, precast/geopolymer, architecture, and project case study. This paper was presented at the Concrete 2013 conference on the Gold Coast.*

## 1.0 INTRODUCTION

This paper is written from a design process perspective to demonstrate how recent innovations in material technology can be incorporated into a construction project. The chief author is a director of Bligh Tanner, a medium sized civil, structural and environmental consulting engineering business that has always sought to develop and utilise new technologies, particularly in relation to positive environmental outcomes.

***Figure 1: The completed Global Change Institute.***

The Global Change Institute (GCI) is a University of Queensland organisation researching global sustainability issues including resource security, ecosystem health, population growth and climate change. The conceptual design of a new building to house the institute was undertaken by the project architects, Hassell and Arup Sustainability, commencing in 2009. At this time UQ was undertaking a number of new building projects utilising principles of sustainable design. The GCI building was to be the exemplar project being benchmarked using the Green Building Council Greenstar rating (at 6 Greenstar level) as well achieving an Australia first Living Building Challenge compliance. The Living Building Challenge is an international rating system based in North America that looks to a broader basis of sustainability, assessing the seven performance areas of site, water, energy, health, materials, equity and beauty. Further design parameters set for the project were zero net carbon emission for building operation, carbon neutral with carbon offset. The building is designed to use only 40% of the benchmark Green Building Council energy benchmark for an educational building.

At the commencement of the schematic design phase of the project, a study tour of recent leading sustainable construction projects in Sydney and Melbourne was undertaken. Buildings visited included University of Sydney Law School, Surry Hills Library, Green Building Council, the Macquarie Bank building in Sydney, and Council House 2, The Gauge and Vic Urban

in Melbourne. One interesting finding was that success of the building passive and low energy thermal systems was greatly influenced by the engagement of the building occupants in the operation of the systems. With the Global Change Institute occupying this key university building, the potential for pushing boundaries in the building design from materials to passive energy systems seemed high. The building aims to be in natural ventilation mode for 88% of the year and this goal can only be achieved if the building occupants embrace the opportunities that are afforded by the built-in operational systems.

## 2.0 DESIGN PROCESS

Use of geopolymer concrete was one of many potential ideas mooted in the preliminary concept study by Arup Sustainability, although the nature of its use was not conceived. The material was put forward due to its substitution of Portland cement, which has a high carbon/energy footprint in its production. The general feeling at that early stage was that its development was too immature and that the most likely uses would be in the manufacture of concrete blocks or for landscaping pavements and the like. We were aware that geopolymer had been trialled by some local council engineers for pavements and that some bridge girders had been manufactured for the purposes of testing. Our initial discussions with industry experts indicated that although it was recognised that geopolymer concrete had a number of potential benefits such as low shrinkage, the required testing for compliance with AS 3600 and the ability to control quality of batches had a long way to go. One significant question about substituting 100% of OPC was whether the product was even concrete within the intent of AS 3600. It was recognised that the material compliance aspects of AS 3600 were largely performance requirements and as such could potentially be applied to geopolymer concrete.

Early in the design, we explored the potential for incorporation of structural timber. The work at UTS developing and testing Timber-Concrete Composite (TCC) floors was of interest and was proposed as a potential floor system that combined the benefits of timber (LVL) framing with the acoustic, fire separation and wearing properties of concrete. It was at this stage that we identified the strong potential for use

*Figure 2: Timber concrete composite floor panel.*

*Figure 3: Global Change Institute – vaulted panel soffit.*

of geopolymer concrete in the system, as the structural topping would be working at low stress and precasting of the TCC panels would enable quality control in a factory environment. Use of precast was also recognised as advantageous considering very limited site access off Staff House Road and a site bounded by existing buildings on three sides.

The design of the passive and low energy thermal control systems was developing at the same stage and this was pushing the floor systems towards high thermal mass with active heat exchange through pumping of air or water through a concrete slab system. The next logical iteration of the design was to precast geopolymer concrete floor panels with hydronic pipes coils incorporated. To maximise the effectiveness of the radiant heat transfer from the concrete, the soffit needed to be exposed with maximum surface area. This then led to the development of vaulted soffit panels, which were both visually appealing, of high thermal efficiency and reflected light down on to functional spaces. Suspended ceiling panels below the panels contain lighting, comms and sprinklers. Various forms of the 11 m span panels were explored, which allowed for air distribution in a plenum/services void above the panels. The exposed concrete frame, which supports the precast geopolymer concrete panels, was designed to incorporate the air distribution system, which supplies the plenum.

By this stage we had made contact with Wagners, based in Toowoomba, who were developing a geopolymer concrete product branded Earth Friendly Cement (EFC). Wagners had undertaken some preliminary testing and had engaged Dr James Aldred, who worked for GHD's Sydney office at the time, to produce an initial summary engineering report that would ultimately lead to further verification testing for compliance with AS 3600. Wagners was extremely interested to be involved with the GCI, which was to be a leading sustainability driven project. Although the use of geopolymer was so novel that it would not gain any additional Greenstar points in the Material category, UQ as the client understood the significance of the innovation which went beyond Greenstar rating. Wagners was asked to fast track the reporting and testing with a critical cut off date for the interim research report to be delivered to give confidence that use of geopolymer concrete on the project

*Figure 4: Support at the panel end during the full scale test.*

*Figure 5: Full scale load test at Precast factory.*

was viable. The Greenstar submission which is currently being assessed does include up to four points for the use of the geopolymer concrete on the basis of being a world first innovation and exceeding the Greenstar benchmarks. To us, a critical factor was the acceptance by Dr Aldred who would ultimately be certifying that the EFC could be considered as concrete in accordance with the design rules of AS 3600 and the associated material properties that they are based on. A positive interim report was delivered during the design period and indicative supply costs were entered into the project cost plan. The only issue that was identified as a potential concern relative to normal concrete was carbonation resistance; however, this was not considered to be of significance for our case with internal use only. Subsequent testing has shown that rate of carbonation for the mix design adopted is similar to normal concrete incorporating blended cement. At this point the project consultants accepted EFC geopolymer concrete as the preferred option for the precast floor beams used in the three suspended floors.

A further critical consideration was the ability to supply the EFC concrete to the precast fabricator and also for the precast fabricator to be willing to take on the risk of working with a new product. The design team and Wagners worked closely with Precast Concrete at this stage of the project to ensure that the process was feasible. Bligh Tanner stipulated that a full-scale load test (up to maximum working load) could be undertaken on a panel to confirm the strength and deflection were as predicted. This was considered prudent considering the world first application of modern geopolymer concrete for suspended construction.

Following receipt of the interim GHD report which was generally positive, Bligh Tanner developed a detailed list of testing that was required to enable our final recommendation of acceptance for use of geopolymer concrete on the GCI project. This recommendation was required regardless of the 3rd party Certification in accordance with AS 3600 which Wagners were required to provide in support of the EFC mix design.

## 3.0 COMPLIANCE TESTING

Wagners EFC geopolymer concrete was included in the design for the 33 no. precast floor beams (volume 320 $m^3$) that formed three suspended floors in the building. Bligh Tanner built a specification for the geopolymer concrete in these beams that relied on:

- testing key material properties referenced in the Australian Standard for Concrete Structures, AS 3600
- having independent engineering verification that the tested properties showed that the structural performance properties were complementary to the design basis for design of reinforced concrete enshrined in AS 3600.

All tests were undertaken by Wagners Technical services, in some cases using external laboratories. The results were independently assessed by Dr Aldred who Wagners commissioned to provide the independent certification on the EFC geopolymer concrete as supplied. At the end of the supply period Dr Aldred provided certification to the effect that all EFC supplied was in compliance with the project specification, the details of which are presented by Dr Aldred in a separate paper at this conference.

The range of compliance tests covering structural performance included:

- 28 day compressive strength
- density
- 28 day flexural strength
- 28 day indirect tensile strength
- modulus of elasticity
- stress strain curve
- Poisson's ratio
- 56 day drying shrinkage
- creep
- tensile development lengths for reinforcement bar bond
- chloride content
- sulfate content
- alkali aggregate reaction

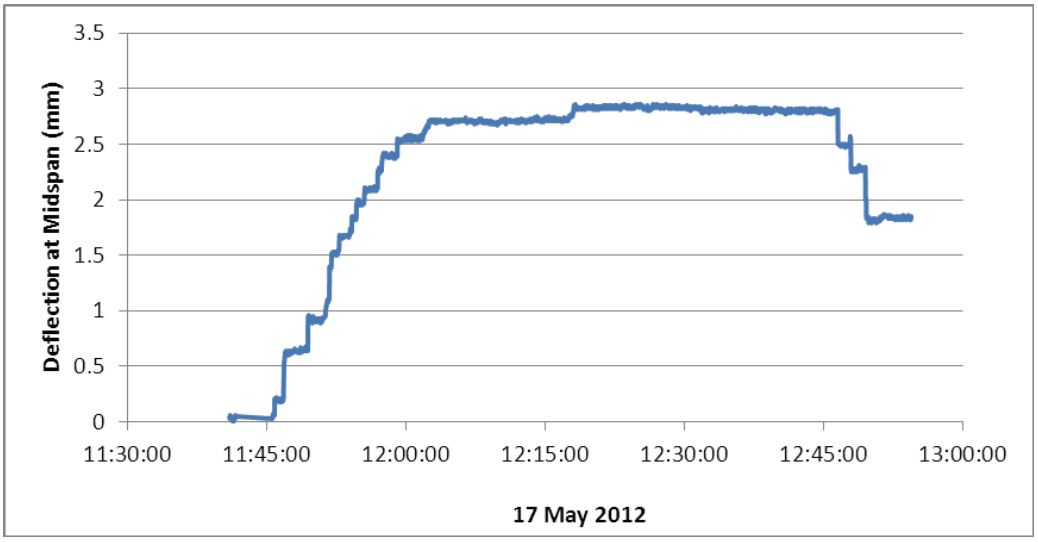


*Figure 6: Prototype EFC geopolymer beam load test.*

- load testing of a prototype beam
- fire testing of a loaded floor element.

All of the test samples, with the exception of creep and the fire and load tests, were cast and made from EFC geopolymer concrete supplied during the supply phase of the project. The relevant Australian Standard test method was used in all cases. Creep was assessed via full scale prestressed beams which were made in 2010 and have been monitored under load via the use of internal vibrating wire strain gauges. A fire test was conducted at the CSIRO fire testing station at North Ryde, Sydney prior to project commencement. The first floor beam panel produced acted as the prototype to be load tested. Figure 6 shows the test undertaken where the measured deflection under an equally distributed 10 t load was 2.85 mm, slightly less than the predicted 3 mm using an uncracked section analysis. The testing program revealed a number of beneficial properties of the geopolymer concrete compared to normal GP based concrete, most notably:

- half the typical 56 day drying shrinkage, at an average value of 320 microstrains
- 30% higher flexural tensile strength than a comparison standard concrete
- extremely low heat of reaction.

These properties would indicate that an improved level of performance would be achieved in a range of typical structural applications.

*Figure 7: EFC geopolymer concrete being vibrated into the beam moulds at the Precast Concrete factory in Brisbane.*

## 4.0 PRACTICAL ASPECTS

Apart from the design and specification details, the geopolymer concrete was required to meet all of the usual handling requirements involved in batching and delivering concrete. This project had the added complication of dealing with a 2-3 hour travel time from a Toowoomba batching facility to a Brisbane precast factory. At the time, the only Wagners batch plant set up to produce EFC was located in Toowoomba. While EFC can be produced in normal concrete batching facilities, it is a requirement that no general purpose (GP) cement contaminate the mix because it causes rapid setting, particularly at higher temperatures. If weigh bins and the like are shared with normal concrete production in a batch plant then it is possible that the fines of GP cement dust will enter the EFC geopolymer mix in enough quantity to cause variable set times.

Based on several years of EFC supply to a range of external projects and trials, Wagners was able to demonstrate that the geopolymer concrete could be handled and finished similarly to normal concrete. In the case of filling and compacting precast molds the methods are the same. Curing is required to

*Figure 8: Precast geopolymer beams installation.*

be carried out for a period of seven days under ambient curing conditions in order to ensure full strength development as well as produce a sound durable surface. Methods for curing include:

- leaving the forms in place
- covering the hardened surface with plastic sheet
- misting with water, or
- chemical curing compound of not less than 90% efficiency for a minimum period of 7 days. Insufficiently cured geopolymer surfaces will display a weak dusting surface.

On unformed surfaces that are hand placed, an initial mist with water should precede covering with the chosen curing method to ensure there is sufficient available moisture for the ongoing geopolymer binder reaction. During placing operations up until final set, exposed surfaces should not be allowed to dry out. EFC geopolymer has very little bleed, which means on exposed surfaces there will typically be required the application of an evaporative retardant spray during placing operations to ensure the surface does not dry out. Care needs to be taken to ensure any sprays applied to the surface are not subsequently worked into the concrete and increase water content of the geopolymer paste at the surface.

Under ambient temperature conditions of 22–33 °C EFC has a similar set time to normal GP based concrete. Accelerated strength development can be achieved by the application of low heat, keeping the EFC at 38 °C. The GCI beams were specified by the project architects to have an off-white colour. The natural colour of EFC after it has fully cured and achieved full strength is off-white, an attribute given by the amount of slag powder contained in the mix as one of the alumino-silicate source powders. In the days immediately following setting and stripping the surface colour of EFC will appear a strong greenish hue, which is due to the slag based geopolymer reaction. After several days exposure to the atmosphere the EFC colour becomes a consistent off-white. This aspect will be a cost effective benefit on architecturally themed work requiring off-white colour.

A practical beneficial aspect of geopolymer concrete in relation to travel time is that loads can be batched with all ingredients except the activating chemicals and transported up to 12 hours or more to a remote destination in a completely dormant non-reactive state. At the destination the chemicals are added in a dry powder form directly into the agitator bowl and mixed on site. Using this method the geopolymer concrete was transported from Toowoomba to Brisbane and activated when the Precast factory was ready for casting.

The finished precast geopolymer beams were installed into the building structure during the period August to October 2012.

Following installation, sealing of the precast EFC geopolymer beams was undertaken on site. Several patch trials were carried out to ensure compatibility between the geopolymer concrete and proprietary sealers. In regards to proprietary sealer products that have a dust inhibiting or surface repair characteristic, it should be noted that they may not have that effect on geopolymer concrete due to its different chemistry.

Proprietary dust inhibiting sealers are generally designed to penetrate and react with leftover by-products from the Portland cement hydration reaction which occurs in normal concrete. Trials should be conducted to establish the compatibility of sealers with any particular geopolymer concrete prior to application.

## 5.0 CONCLUSION

Geopolymer concrete has now moved beyond an emerging technology into the space of a structural concrete that can be designed and used in structures and other applications, as long as the necessary verification and testing is undertaken. The term geopolymer is very broad and encompasses a range of different concretes which may have quite different structural properties. The proprietary geopolymer concrete used in the GCI building proved to be fully compliant with the structural performance parameters that AS 3600 is based on.

The use of geopolymer concrete in the multi-storey GCI building provides an example of how a medium sized engineering consultancy went about assessing a new technology's 'fit for purpose' suitability. It is hoped that this example may provide a path for others to explore new and innovative approaches to building that improve the sustainability of our built environment. In association with a range of other sustainability innovations utilised in this building, the geopolymer concrete floor beams help make the GCI building project be an outward communication of its inner purpose.

# Corrosion durability of geopolymer concretes containing different concentrations of alkaline solution

Faiz U.A. Shaikh and Ali Afshang, Curtin University, Perth, Western Australia

*This paper presents the chloride induced corrosion durability of reinforcing steel in geopolymer concretes containing different contents of sodium silicate ($Na_2SiO_3$) and molarities of NaOH solutions. Seven series of mixes are considered in this study. The first series is ordinary Portland cement (OPC) concrete and is considered as the control mix. The rest six series are geopolymer concretes containing 14 and 16 molar NaOH and $Na_2SiO_3$ to NaOH ratios of 2.5, 3.0 and 3.5. In each series three lollypop specimens having one 12 mm diameter steel bar cast in a 100ϕ × 200 mm cylinder are considered. The specimens are subjected to cyclic wetting and drying regime for eight weeks. In wet cycle the specimens are immersed in water containing 3.5% (by wt.) NaCl salt for four days, while in dry cycle the specimens are placed in open air for three days. The corrosion activity is monitored by measuring the copper/copper sulphate ($Cu/CuSO_4$) half-cell potential according to ASTM C-876. The chloride penetration depth and sorptivity of all seven concretes are also measured. Results show that the geopolymer concretes exhibited better corrosion resistance than OPC concrete. The higher the amount of $Na_2SiO_3$ and higher the concentration of NaOH solutions, the better the corrosion resistance of geopolymer concrete is. Similar behaviour is also observed in sorptivity and chloride penetration depth measurements. Generally, the geopolymer concretes exhibited lower sorptivity and chloride penetration depth than that of OPC concrete.*

## 1.0 INTRODUCTION

Concrete is one of the most widely used construction materials in the world. However, the concrete industry contributes between 5-7% of total global $CO_2$ emission into the atmosphere. Research efforts are continuing to make the concrete more sustainable by reducing the amount of cement in the concrete. Partial replacement of cement by various cementitious materials such as fly ash, slag, silica fume, etc. in concrete is now common practice in the industry as their use improves the properties. However, their use as partial replacement of cement in concrete is limited to 25-30% for fly ash and slag and up to 5-10% for silica fume.

The development of a new type of inorganic cementitious binder called "geopolymeric binder" is the newest development in recent years. Geopolymer binder is a 'new' material that does not require OPC. Instead, a source material, such as fly ash, that is rich in silica (Si) and aluminium (Al), is reacted by alkaline solutions [1]. It has been estimated that the manufacture of geopolymeric cement emits about 80% less $CO_2$ than the manufacture of OPC [2,3], primarily because the limestone does not need to be calcined to produce the geopolymeric binder. Fly ash based geopolymers have extremely low embodied energies. In geopolymer based concrete (produced from fly ash and a soluble silica like activator, and cured under mild heating), Tempest et al [3] estimated that 70% less energy is consumed when compared to OPC based concrete of similar strength.

Considerable research has been conducted on the mechanical properties of fly ash based geopolymer concrete. Geopolymer concrete exhibits comparable or even, in some instances, superior mechanical properties than ordinary concrete. It also exhibits superior durability properties in terms of acid, sulphate, fire and corrosion resistance. Chloride induced corrosion of reinforcing steel in concrete is an important durability issue for reinforced concrete (RC). Better corrosion resistance is always a sought after property in the RC. Different techniques are also used to protect the reinforcing steel in the concrete. Among different techniques the use of high performance concrete that exhibits superior corrosion resistance in terms of low permeability, less porosity, etc. are used to design the RC.

Corrosion durability of geopolymer concrete is studied by limited researchers [4-9]. Miranda et al [4] studied the corrosion resistance of fly ash based geopolymer mortar and reported similar corrosion resistance of geopolymer mortar to cement mortar. The molarities of sodium hydroxide (NaOH) alkali solution used in their study were 8 M and 12.5 M. Bastidas et al [5] also reported similar corrosion resistance of fly ash based geopolymer mortars to ordinary cement mortars and the molarity of NaOH solution was 12.5 M. Oliva and Nikraz [6] studied corrosion resistance of two geopolymer concrete mixes containing 14 M NaOH alkali solution in accelerated corrosion environment. Superior corrosion resistance of both geopolymer concretes are reported compared to OPC concrete of similar compressive strength. Reddy et al [7] also studied the corrosion resistance of geopolymer concretes containing 8 M and 14 M NaOH solution under accelerated corrosion environment at very high external DC potential of 30 V to a 500 mm long 13 mm diameter bar. Better corrosion resistance of geopolymer concretes in terms of lower corrosion current than OPC concrete is also reported in their study. Superior corrosion resistance of geopolymer concrete is also reported recently by Patil and Allouche [8]. The molarity of NaOH solution in their study was also 14 M.

It can be seen that in all of the above studies the highest molarity of NaOH solution was 14 M and the ratio of

*Table 1: Chemical analysis and physical properties of materials.*

| Chemical Analysis | Cement (%) | Class F Fly Ash (%) |
|---|---|---|
| $SiO_2$ | 20.2 | 51.80 |
| $Al_2O_3$ | 4.9 | 26.40 |
| $Fe_2O_3$ | 2.8 | 13.20 |
| CaO | 63.9 | 1.61 |
| MgO | 2.0 | 1.17 |
| MnO | – | 0.10 |
| $K_2O$ | – | 0.68 |
| $Na_2O$ | – | 0.31 |
| $P_2O_5$ | – | 1.39 |
| $TiO_2$ | – | 1.44 |
| $SO_3$ | 2.4 | 0.21 |
| **Physical Properties** | | |
| Particle size | 25-40% ≤ 7 μm | 40% of 10 μm |
| Specific gravity | 2.7 to 3.2 | 2.6 |
| Surface area ($m^2/g$) | – | – |
| Loss on ignition (%) | 2.4 | 0.5 |

sodium silica ($Na_2SiO_3$) to NaOH was as high as 2.5. NaOH and $Na_2SiO_3$ are commonly used to activate the fly ash in geopolymer concretes. The concentrations of NaOH solution and the amount of $Na_2SiO_3$ affect the properties of concrete [9]. It is generally believed that the higher the molarity of NaOH solution for a given amount of $Na_2SiO_3$ the faster the geopolymerisation process and higher the compressive strength of concrete. The same is also valid for the $Na_2SiO_3$, where higher compressive strength of geopolymer concrete can be achieved by increasing its content. The passivity of geopolymer concrete is also affected by the high molar NaOH solution and high $Na_2SiO_3$ content as it affects the alkalinity of the geopolymer concrete [10]. However, no such study on the effect of high molar NaOH solution and the high content of $Na_2SiO_3$ on the corrosion durability of reinforcing steel in geopolymer concrete is reported. Moreover, no study on the associated durability properties such as chloride penetration and sorptivity of such geopolymer concretes is reported in the literature. Therefore, this study is designed to evaluate the effects of high molar NaOH solutions such as 14 M and 16 M and $Na_2SiO_3$/NaOH ratios of 2.5, 3 and 3.5 on the corrosion durability of geopolymer concretes. The effects of above parameters on two associated durability tests such as chloride penetration and sorptivity that directly relates the chloride induced corrosion resistance of concrete are also evaluated in this study.

## 2.0 MATERIALS

General purpose (GP) Portland cement and class F fly ash is used in the control and geopolymer mixes, respectively. Chemical compositions and properties of GP cement and class F fly ash are shown in Table 1. The activating solutions for geopolymer consist of sodium silicate ($Na_2SiO_3$) and sodium hydroxide solutions. The chemical composition of sodium silicate is (wt.%): $Na_2O$ = 14.7, $SiO_2$ = 29.4 and water = 55.9. The other characteristics of the sodium silicate solution are specific gravity of 1.53 g/cc and viscosity at 20 °C of 400 cp. The sodium hydroxide (NaOH) solution is prepared from analytical grade sodium hydroxide pellets. The mass of the NaOH solids in the solution varied depending on the concentration of the solution expressed in terms of molarity, M. In this study, the NaOH solution with concentrations of 14 M and 16 M are considered. The NaOH is first mixed with de-ionised water. During the mixing of sodium hydroxide solution, the white sodium hydroxide pellets were slowly dissolved by the addition of de-ionised water. A rise of temperature occurred as the sodium hydroxide pellet slowly dissolved in the solutions. And then the sodium hydroxide solution is mixed with $Na_2SiO_3$ (Sodium Silicate) at desired ratios and produced the alkali activator solution. The alkali activator solutions are then used for the mixing of geopolymer concretes.

## 3.0 EXPERIMENTAL PROGRAM AND MIX PROPORTIONS

In this study, seven series of mixes were considered. Table 2 shows the detail of the experimental program and mix proportions of all seven series. The first series was the control series where ordinary concrete was used and was designated as OPC mix. The remaining six series were geopolymer concretes and contained different concentrations of NaOH solution and ratios of $Na_2SiO_3$/NaOH. The second, third and fourth series contained 14 M NaOH solution and three different $Na_2SiO_3$/NaOH ratios of 2.5, 3 and 3.5, respectively. They are designated as GP-14-2.5, GP-14-3 and GP-14-3.5, respectively. The fifth, sixth and seventh series were similar to the second, third and fourth series in every respect except the concentration of NaOH solution, where the molarity of NaOH solution was 16 M. They were designated as GP-16-2.5, GP-16-3 and GP-16-3.5, respectively. The alkali activator solution to fly ash ratio of geopolymer concrete was similar to water/cement ratio of OPC mix.

Conventional mixing was used to prepare both OPC and geopolymer concretes. The geopolymer concretes were subjected to steam curing at 60 °C for 24 hours immediately after casting. The specimens were then demoulded and cured in the laboratory in open air until the date of testing. The OPC concrete specimens were demoulded after 24 hours and stored in the curing tanks where they were subjected to standard wet curing conditions. Concrete cylinders 100 mm in diameter and 200 mm in height were cast to measure the 28 days compressive strength. At least three cylinders were cast and tested for each mix. Lollypop cylinder specimens of 100 mm in diameter and 200 mm in height with a 16 mm diameter steel bar at the centre were prepared for the corrosion test.

## 4.0 DURABILITY TESTS

### 4.1 Monitoring of corrosion of reinforcing steel in concrete

The corrosion of reinforcing steel in geopolymer and ordinary concretes is evaluated by half-cell potential measurements according to ASTM C876 standard [11]. It is a non-

*Table 2: Mix proportions of OPC concrete and geopolymer concretes.*

| Series | Mix type/ designation | Fly ash (kg/m³) | Cement (kg/m³) | Aggregate (kg/m³) | Alkaline activator solution (kg/m³) | | Superplasticiser (kg/m³) | Water (kg/m³) |
|---|---|---|---|---|---|---|---|---|
| | | | | | Sodium silicate, ($Na_2SiO_3$) | Sodium hydroxide (NaOH) | | |
| 1 | OPC | – | 422 | 1788 | – | – | – | 190 |
| 2 | GP-14-2.5 | 422 | – | 1788 | 135.7 | 54.3 | 6.3 | – |
| 3 | GP-14-3 | 422 | – | 1788 | 142.5 | 47.5 | 6.3 | – |
| 4 | GP-14-3.5 | 422 | – | 1788 | 147.7 | 42.2 | 6.3 | – |
| 5 | GP-16-2.5 | 422 | – | 1788 | 135.7 | 54.3 | 6.3 | – |
| 6 | GP-16-3 | 422 | – | 1788 | 142.5 | 47.5 | 6.3 | – |
| 7 | GP-16-3.5 | 422 | – | 1788 | 147.7 | 42.2 | 6.3 | – |

destructive electro-chemical method used to find out the corrosion tendency of rebar in concrete. This technique directly measures the potential of rebar using a high-impedance voltmeter as shown in Figure 1. The voltmeter has two terminals, one is connected to the rebar in the concrete, while the other is connected to a copper/copper sulphate reference cell with a porous sponge at the end. During the measurement, the sponge is guided to slide over the surface of the concrete, and readings from the voltmeter are registered. ASTM C 876 has provided guidelines on the relationship between half-cell potential and the tendency of rebar corrosion as follows [11]:

- If potentials over an area are more positive than -200 mV, there is greater than 90% probability of no corrosion in that area at the time of measurement.
- If potentials over an area are in the range of -200 mV to -350 mV, corrosion activity of the reinforcing steel in that area is uncertain.
- If potentials over an area are more negative than -350 mV, there is greater than 90% probability of corrosion in that area at the time of measurement.

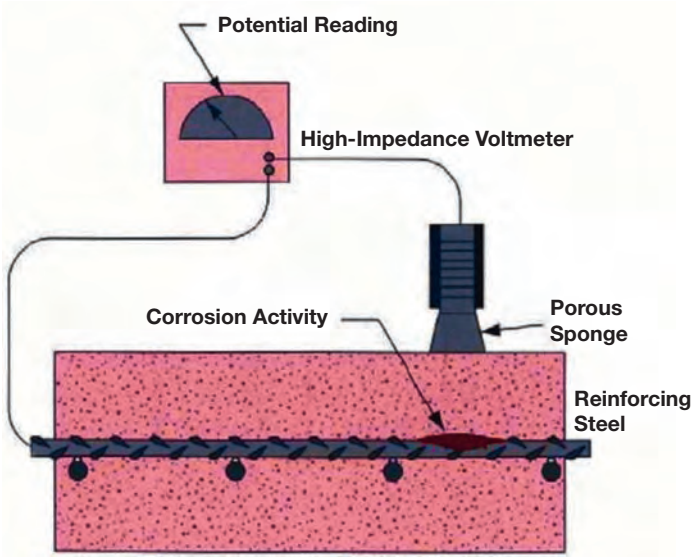


*Figure: 1. Half-cell potential measurement setup [12].*

### 4.2. Sorptivity of concrete

Sorptivity of both ordinary and geopolymer concretes is measured according to ASTM C1585 standard [13]. In this test 50 mm thick and 100 mm diameter discs are used. The curved surface and one flat surface of each disc is epoxy coated for this test.

### 4.3 Chloride penetration test

Chloride penetration of ordinary and geopolymer concretes is determined according to the ASTM C1543 [14]. The sample dimensions are similar to that used in a sorptivity test. Epoxy is also used to coat the curved surface and one plain surface of the specimen in this test. This is done in order to restrict the chloride flow in one direction only. The epoxy coated samples are then immersed in water containing 3.5% sodium chloride for four days and then allowed to dry for three days. This wetting-drying cycle is applied for eight weeks.

After the wetting-drying cycles the specimens are broken into two pieces and 0.1 N $AgNO_3$ solution is sprayed on the broken surface in order to observe the chloride penetration depth. The light pink colour on the surface indicates the chloride penetration depth in the specimen.

In all of the above durability tests at least three specimens are used and the results averaged.

## 5.0 RESULTS AND DISCUSSION

### 5.1 Effect of molarity of NaOH and amount of $Na_2SiO_3$ on the compressive strength

The effects of two different molarities of NaOH solution and three different $Na_2SiO_3$/NaOH ratios on 28 days compressive strength of geopolymer concretes are shown in Figure 2. It can be seen that the compressive strength of geopolymer concrete increases with increase in $Na_2SiO_3$ content for a given concentration of NaOH solution. The rate is much higher in the geopolymer concretes containing 16 M NaOH solution. The higher compressive strength of geopolymer concrete

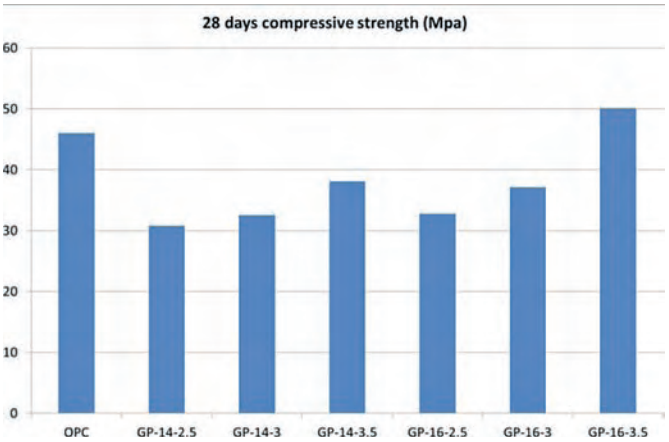


*Figure: 2 Effects of molarity of NaOH and amount of $Na_2SiO_3$ on the compressive strength.*

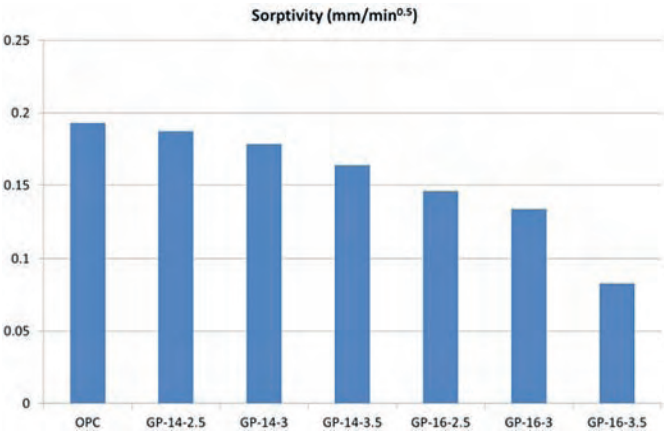


*Figure: 3 Effects of molarity of NaOH and amount of $Na_2SiO_3$ on water sorptivity.*

containing 16 M NaOH compared to that containing 14 M NaOH is due to faster and higher dissolution rate of silicate and aluminate in fly ash [9]. During the geopolymerisation process the silicate and aluminate in fly ash is dissolved by the NaOH and form sodium-alumina-silicate geopolymerisation product which contributed to the strength of the geopolymer matrix. Similar results are also reported by other researchers [15].

### 5.2 Effect of molarity of NaOH and amount of $Na_2SiO_3$ on water sorptivity

The water sorptivity values of different geopolymer concretes and ordinary concrete are shown in Figure 3. It can be seen that the water sorptivity of geopolymer concretes is lower than that of ordinary concrete. Results also show that the water sorptivity of geopolymer concrete decreases with increase in $Na_2SiO_3$ contents for a given concentration of NaOH solution. The rate is even higher for higher concentration of NaOH in geopolymer concretes. The significant reduction of sorptivity of geopolymer concretes containing high molar NaOH and high amount of $Na_2SiO_3$ solutions can be attributed to the formation of an increasing amount of sodium-aluminasilicate gel in the matrix. The low sorptivity value of geopolymer concrete is also an indication of disconnected fine pore structures in the matrix. Research shows that the water absorption and sorptivity of concrete are significantly reduced in disconnected pore system [16]. The positive effect of low sorptivity is also observed on chloride penetration and corrosion resistance of geopolymer concretes and is discussed in the following sections.

### 5.3 Effect of molarity of NaOH and amount of $Na_2SiO_3$ on chloride penetration

The effects of different molarities of NaOH and $Na_2SiO_3$ contents on chloride penetration of geopolymer concretes are shown in Figure 4. A linear decreasing trend of chloride penetration in geopolymer concretes can be seen with increasing concentrations of NaOH solution and amount of $Na_2SiO_3$ contents. The results are consistent with those of water sorptivity values. As discussed before the low water sorptivity of geopolymer concrete might be attributed to the better chloride penetration resistance.

### 5.4 Effect of molarity of NaOH and amount of $Na_2SiO_3$ on chloride induced corrosion resistance

Among many corrosion monitoring and measuring techniques, the half-cell potential measurement method is the most convenient and quickest method of monitoring the corrosion of reinforcing steel in the concrete. However, this method only provides the probability of corrosion activity of steel bar in the concrete. The half-cell potential readings shown in Figures 5 and 6 are based on a copper/copper sulphate reference electrode. The effects of two different molarities of NaOH solution on the corrosion resistance of geopolymer concretes in terms of half-cell potential readings are shown in Figure 5 and compared with that of ordinary concrete. The half-cell potential readings shown in the figures are the average of three specimens. It can be seen that all geopolymer concretes exhibited better corrosion resistance in terms of lower negative potential readings than their counterpart ordinary concrete.

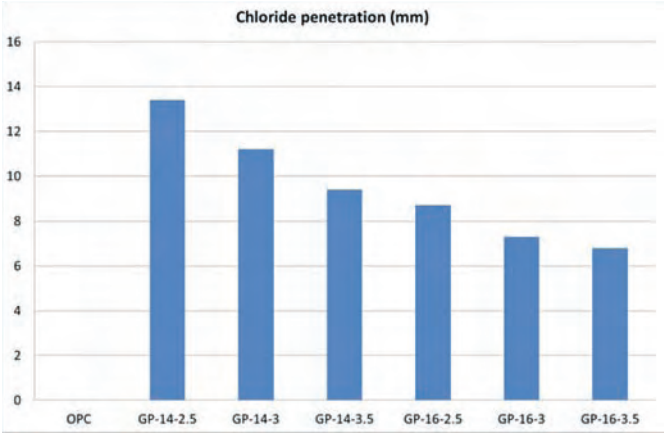


*Figure: 4 Effects of molarity of NaOH and amount of $Na_2SiO_3$ on chloride penetration.*

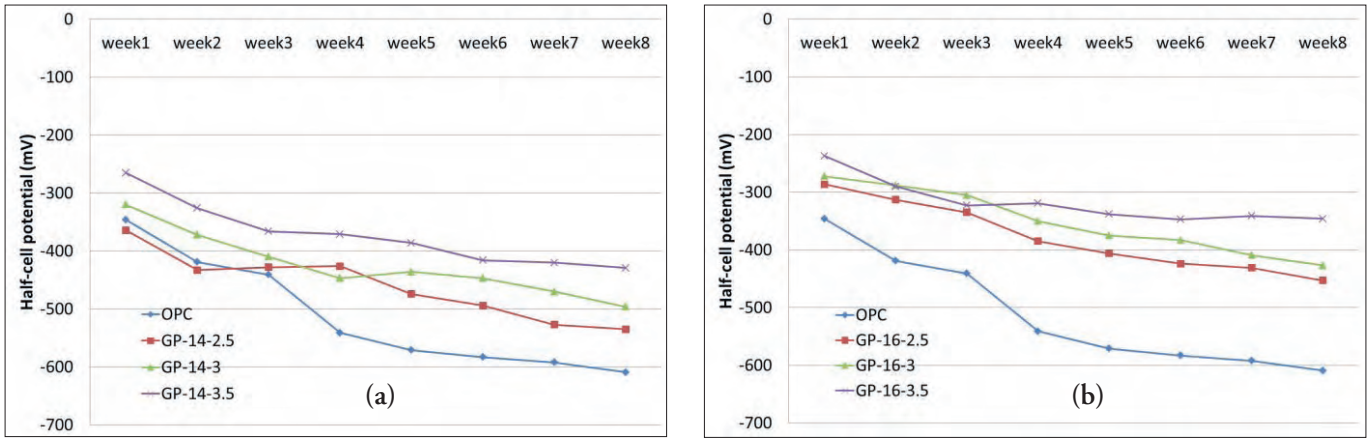


*Figure: 5 Effect of amount of $Na_2SiO_3$ solution on corrosion resistance of geopolymer concrete: (a) concrete containing 14 M NaOH and (b) concrete containing 16 M NaOH.*

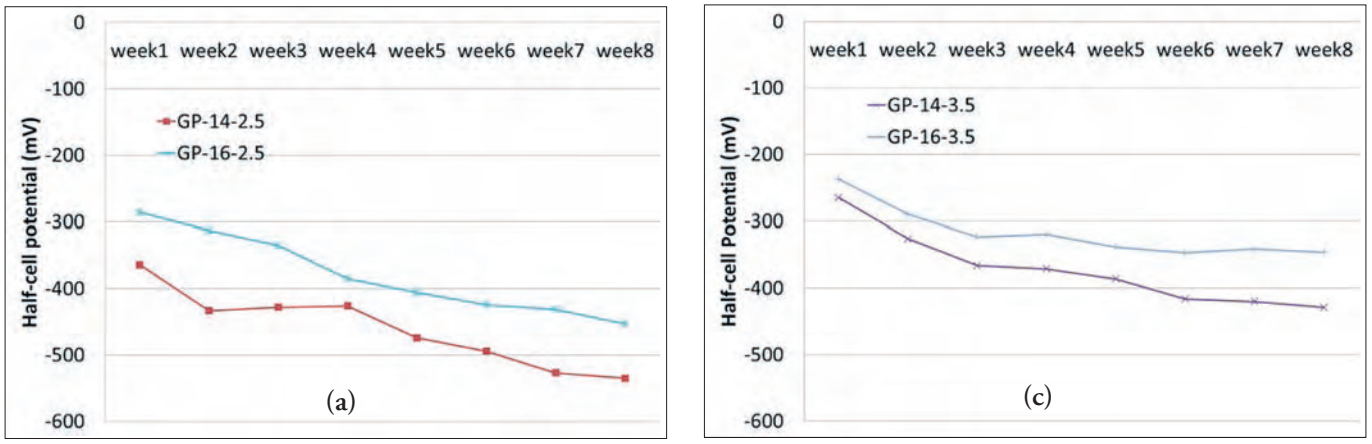


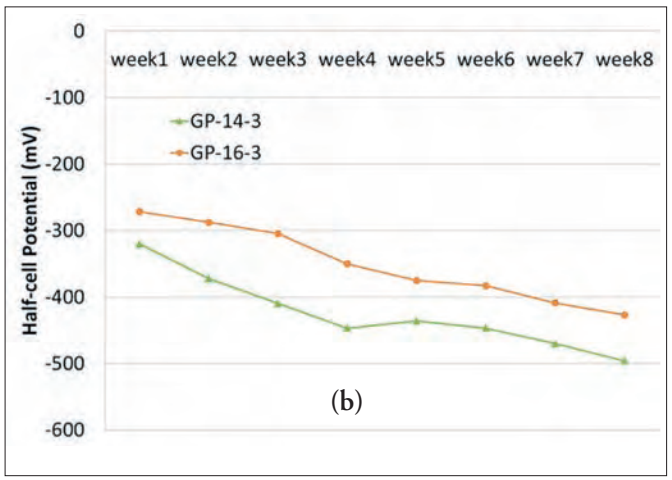


*Figure 6: Effect of molarity of NaOH solution on corrosion resistance of geopolymer concrete: (a) concrete containing $Na_2SiO_3$/NaOH=2.5, (b) concrete containing $Na_2SiO_3$/NaOH=3, (c) concrete containing $Na_2SiO_3$/NaOH=3.5.*

The potential readings of all concretes increase to more negative readings with the progress of time. However, the rate of increase of negative readings of geopolymer concretes is slower than that of ordinary concrete. The geopolymer concrete made with 16 M NaOH solution exhibited better corrosion resistance in terms of lower negative potential values than that containing 14 M NaOH solution. According to ASTM C876 [11] the smaller the negative potential readings the lower the probability of corrosion of steel in the concrete.

The better corrosion resistance of geopolymer concretes containing
16 M NaOH solution is also consistent with the sorptivity and chloride penetration resistance results observed in this study.

The effects of different quantities of $Na_2SiO_3$ on the corrosion resistance of geopolymer concrete are also shown in Figure 6. It is observed that the negative potential readings become less by increasing the $Na_2SiO_3$/NaOH ratios. The rate of increase of negative potential values of geopolymer concrete containing $Na_2SiO_3$/NaOH ratio of 3.5 is very slow and reached towards an almost constant rate at 16 M NaOH. This is believed to be due to simultaneous increase in molarity of NaOH and quantity of $Na_2SiO_3$ solutions in geopolymer concrete. The superior corrosion resistance of geopolymer concretes over ordinary concrete can also be seen in Figure 7.

The sodium silicate is also believed to act as a corrosion inhibitor in geopolymer concrete. Research shows that the sodium silicate is used as a corrosion inhibitor in many applications e.g. in metallic water pipe protection. Silicate inhibits the corrosion of steel bar in geopolymer concrete by

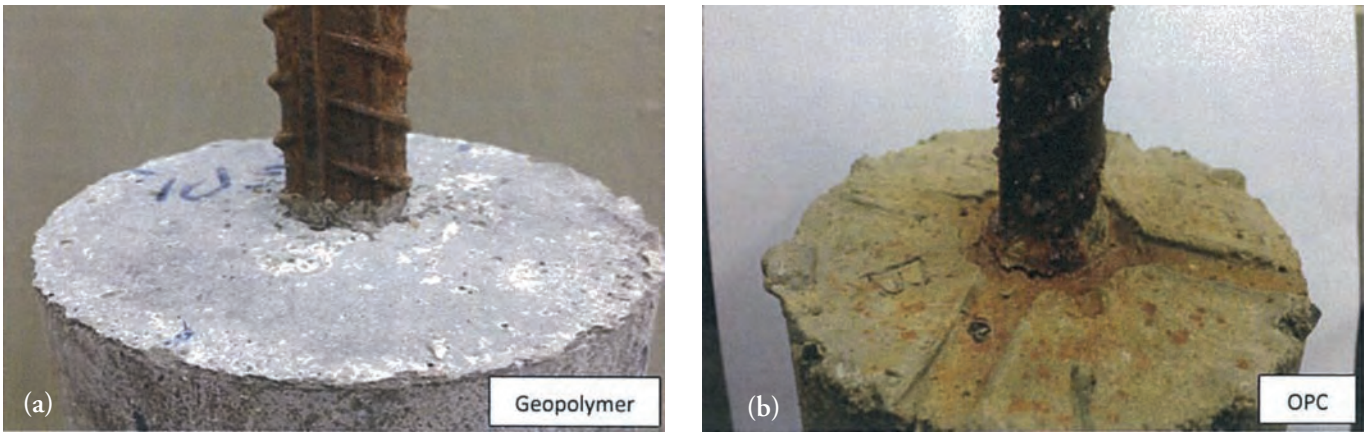


*Figure 7: Corrosion of steel bar in (a) geopolymer concrete and (b) ordinary concrete.*

## 6.0 CONCLUSION

In this study the effects of different molarities of NaOH and contents of $Na_2SiO_3$ on the chloride induced corrosion of geopolymer concrete are evaluated. Within limited variables the following conclusions are made:

- The geopolymer concretes exhibited better corrosion resistance than ordinary concrete.
- The higher the amount of $Na_2SiO_3$ and higher the concentration of NaOH solutions the better the corrosion resistance of geopolymer concrete is.
- Similar behaviour is also observed in sorptivity and chloride penetration depth measurements.
- The geopolymer concretes exhibited lower sorptivity and chloride penetration depth than that of ordinary concrete.
- Correlation between the sorptivity and the chloride penetration of geopolymer concretes is established.

## REFERENCES


1. Duxson P, Fernández-Jiménez A, Provis JL, Lukey GC, Palomo A, van Deventer JSJ. (2007) Geopolymer technology: the current state of the art. *Journal of Materials Science*; 42:2917–33.
2. Davidovits J. (1994) Global warming impact on the cement and aggregates industries. *World Resource Review*; 6(2):263–78.
3. Tempest B, Sanusi O, Gergely J, Ogunro V, Weggel D. (2009) Compressive strength and embodied energy optimization of fly ash based geopolymer concrete. In: World of Coal Ash (WOCA) conference.
4. Miranda, J.M., Jimenez, A.F., Gonzalez, J.A. and Palomo, A. (2005) Corrosion resistance in activated fly ash mortars. *Cement and Concrete Research*, 35:1210-1217.
5. Bastidas, D.M., Jimenez, A.F., Palomo, A. and Gonzalez, J.A. (2008) A study on the passive state stability of steel embedded in activated fly ash. *Corrosion Science*, 50:1058-1065.
6. Olivia, M. and Nikraz, H.R. (2011) Corrosion performance of embedded steel in fly ash geopolymer concrete by impressed voltage method. In: incorporating sustainable practice in mechanics of structures and materials, Taylor and Francis Group, London.
7. Reddy, D.V., Edouard, J.B., Sohban, K. and Rajpathak, S.S. (2011) Durability of reinforced fly ash based geopolymer concrete in the marine environment. In: proceedings of 36th conference on our world in concrete and structures, Singapore, 10pp.
8. Patil, K.K. and Allouche, E.N. (2012) Examination of chloride induced corrosion of reinforced geopolymer concrete. *Journal of Materials in Civil Engineering*, doi:10.1061/(ASCE)MT.1943-5533.0000672
9. Fansuri, H., Prasetyoko, D., Zhang, Z. and Zhang, D. (2012) The effect of sodium silicate and sodium hydroxide on the strength of aggregates made from coal fly ash using the geopolymerisation method. *Asia-Pacific Journal of Chemical Engineering*, 7:73-79.
10. Thompson, J.L., Scheetz, B.E., Schock, M.R., Lytle, D.A., Delaney, P.J. (1997) Sodium silicate corrosion inhibitors: issues of effectiveness and mechanisms, Water Quality Technology Conference, November 9-12, 1997, Denver, Colorado.
11. ASTM C876-09 (2000). Standard Test Method for Half-Cell Potentials of Uncoated Reinforcing Steel in Concrete.
12. Srimahajariyaphong, Y. and Niltawach, T. (2011). Corrosion prevention of rebar in concrete due to chloride. *Journal of Metals, Materials and Minerals*, 21(1):57-66.
13. ASTM C1585-13; Stand test method for measurement of rate of absorption of water by hydraulic cement concrete.
14. ASTM C1543-10a; standard test method for determining the penetration of chloride ions into concrete by ponding.
15. Olivia, M. and Nikraz, H.R. (2011) Strength and water permeability of fly ash geopolymer concrete. *ARPN Journal of Engineering and Applied Science*, 6(7):70-78.
16. He Z. M., Long G. C. and Xie Y. J. (2012) Influence of subsequent curing on water sorptivity and pore structure of steam-cured concrete. *Journal of Central South University*, 19:1155-1162.
17. Asrar, N., Malik, A.U. and Ahmed, S. (1998) Corrosion prevention with sodium silicate. Technical Report N0.TR3804/EVP95013.

# Mechanical properties of geopolymer concrete: Applicability of relationships defined by AS 3600

Kamal Neupane, Ph. D. Student, University of Technology Sydney, NSW

Daksh Baweja, Associate Professor, University of Technology Sydney, NSW

Rijun Shrestha, Lecturer, University of Technology Sydney, NSW

Des Chalmers, Group Product and Process Technology Manager, Cement Australia, Darra, QLD

Peter Sleep, Product Development Manager, Cement Australia, Darra, QLD

*Geopolymers are new inorganic polymer binders, synthesised from aluminosilicate powders such as fly ash and blast furnace slag with alkali activators and producing good binding properties similar to ordinary Portland cement (OPC). This new generation binding material has a potential application in structural and non-structural concretes, fire resistant composites and ceramics. Previous research around the world has suggested that geopolymer binders possess superior engineering, mechanical and durability properties over conventional Portland cement. The process of setting and hardening of geopolymer concrete is based on different chemistry called 'polymerisation' instead of 'hydration' in OPC. The silicon and aluminium oxides in the source materials are activated by a combination of sodium hydroxide and sodium silicate in the presence of water to form a sodium aluminosilicate paste called 'geopolymer' which has binding properties similar to calcium silicate hydrate (CSH) in OPC. In this study, some engineering and mechanical properties of different grades of geopolymer concrete were tested and evaluated according to relevant Australian Standards and compared against the same grade of OPC concrete. AS 3600 has defined some interrelationships between different mechanical properties of Portland cement concrete, such as compressive strength and uniaxial tensile strength, compressive strength and flexural tensile strength etc. From this study, it was found that uniaxial tensile and flexural tensile strengths attained by geopolymer concrete are higher than the prescribed value by AS 3600 for the same grade of concrete. However, modulus of elasticity is found to be almost equal with the calculated value from AS 3600 and similar to the ame grade of OPC concrete.*

## 1.0 INTRODUCTION

Geopolymer is an inorganic polymer cementitious material, first reported by Joseph Davidovits in 1978. Geopolymer binders are generally formed by reaction of an aluminosilicate powder with an alkaline or alkali silicate solution at ambient conditions. Davidovits [1, 2] described the process of setting and hardening of geopolymer concrete as based on a different chemical process called 'polymerisation' which is a synthesis process. The silicon and aluminium oxides in the source materials are activated by a combination of sodium hydroxide and sodium silicate solutions to form a sodium aluminosilicate paste called 'geopolymer' which has a good binding property similar to CSH paste in OPC concrete.

This material can provide better performance than traditional cementitious binders in a range of applications, with the added advantage of significantly reduced greenhouse emissions by utilising industrial waste materials [3, 4]. Depending on the source material, alkali activators and processing conditions, geopolymers can achieve a wide variety of improved characteristics such as better compressive strengths, acid and resistance, fire resistance and low thermal conductivity [5, 6, 7, 8].

Geopolymer binders can be formed using different source materials such as fly ash, blast furnace slag, metakaolin and mine tailings etc. [9, 10, 11]. As fly ash and blast furnace slags are good aluminosilicate materials and available in abundant volume around the world, they can be considered as the predominant source materials for geopolymer binders. Compared to ordinary Portland cement, production of geopolymer binders does not generate a high volume of greenhouse gases [3]; moreover it utilises industrial waste materials and converts them into good binding materials. This energy efficient and low greenhouse gas emitting manufacturing process has made geopolymer a good environmentally friendly construction material.

Based on types of activating material used, geopolymer binders can be classified in two categories – liquid activated geopolymers and powder activated geopolymers [12].

In liquid activated type, the chemical activators, sodium hydroxide and sodium silicate, are in liquid form of different concentrations. In the mixing process, sand, aggregates, source materials and alkali activators are mixed together for a reasonable time as in OPC concrete. Mixing and handling

processes for this binder concrete need skilled manpower. Most of the research works in geopolymer binders are based on liquid activated type geopolymers. This can be considered as a conventional type geopolymer binder.

A powder activated geopolymer binder, as developed by Cement Australia, is physically similar to conventional OPC powder, having all the activators and source material in powder form. The proportions of ingredients in the powder activated type may or may not be similar with the liquid activated type. Mixing and handling processes for concrete using this binder are very similar to conventional OPC concrete, adding required water and mixing until the desired workability is achieved. Development of this type of geopolymer is based on a practical and economical approach which gives a product that can be safely used as a direct substitute for OPC.

Currently, Cement Australia has developed two types of powder activated geopolymer binders according to their purposes [12]. The first one is 'geopolymer I'; powder- activated general purpose geopolymer binder similar to conventional GP (defined by AS 3972). Second is 'geopolymer II': powder activated high early strength geopolymer binder similar to conventional HE (defined by AS 3972). Figure 1 reveals the visual similarity between conventional OPC and powder activated geopolymer binders.

Following the introduction of geopolymer in 1978, significant research work has been carried out to find out engineering, mechanical, thermal and durability properties of this binder. As this is a new material, most of the research work was focused on optimising ingredient proportions i.e. silicon and aluminum oxides and alkali activator to achieve better strength results. Typically researchers used 28 day compressive strength as a performance indicator. Most of the previous research work concentrated on the following area of geopolymer binder's investigation:

- use of different alternative source materials such as Class C & Class F fly ash, blast furnace slag, metakaolin, rice husk ash and mine tailings etc. [9,10, 11].
- different engineering properties of geopolymer binder; concrete compressive strength, indirect tensile strength, water absorption and shrinkage etc. [4, 5, 13].
- effect of ingredients proportion and concentration of activator solution eg ratio of $SiO_2/Al_2O_3$ and concentration of NaOH solution etc. [9, 12, 13, 14].
- influence of calcium content on geopolymer binder in early as well as later strength [15].
- effect of curing at elevated temperature on compressive strength [13, 16].
- durability of geopolymer concrete in sulfate and acid environments [5, 6, 17].

The use of geopolymer binders in Australia as well as around the world is in a trial phase. Geopolymer binders have not been used substantially in the construction industry especially as a structural concrete because of insufficient research and development work in this sector. From the literature review of the previous research work, we can assume that the engineering properties of geopolymer concrete are very similar to OPC concrete. Most of the research outcomes suggest that geopolymer binder concrete possesses superior mechanical and durability properties compared to conventional OPC concrete. However, it is not clear whether the same standards and testing procedure for OPC concrete will be applicable with geopolymer binders or not. Thus extensive R&D of geopolymer binders is necessary to find out their engineering and mechanical properties and their interrelationships.

## 2.0 RESEARCH SIGNIFICANCE

This study aims to find out some important engineering and mechanical properties of powder activated geopolymer binder

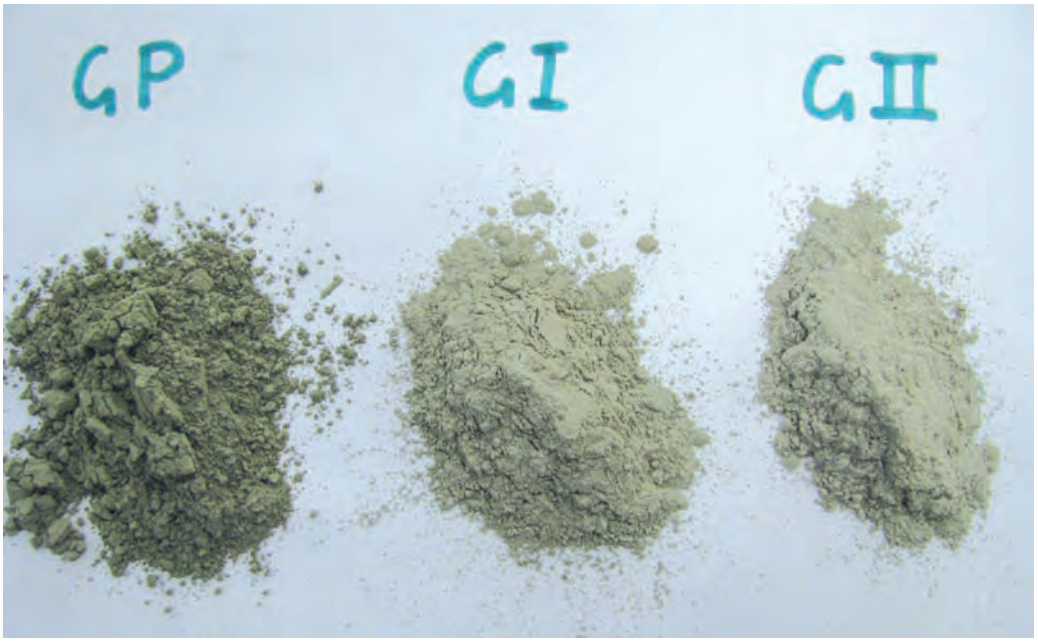


*Figure 1: Colour comparison of binders: GP (General purpose OPC), GI (Geopolymer 1) and GII (Geopolymer 2).*

*Table 1: General properties of concrete mix designs.*

| Concrete Grade (MPa) | Binder Type | Binder Content (kg/m³) | Fine Aggregate/ Total Aggregate Ratio | w/c Ratio | Ave. 28 day Compressive Strength ($f_{cm}$) (MPa) | Average Cylinder density (ρ) (kg/m³) |
|---|---|---|---|---|---|---|
| 50 | Geo I N | 330 | 0.39 | 0.34 | 67.0 | 2420 |
| | Geo II N | 300 | 0.39 | 0.42 | 63.5 | 2420 |
| | Geo II SW | 420 | 0.50 | 0.43 | 59.0 | 2340 |
| | OPC N | 395 | 0.39 | 0.41 | 62.0 | 2380 |
| 65 | Geo I N | 360 | 0.41 | 0.30 | 73.0 | 2420 |
| | Geo I SW | 550 | 0.50 | 0.32 | 73.0 | 2320 |
| | Geo II N | 360 | 0.41 | 0.32 | 82.5 | 2420 |
| | Geo II SW | 520 | 0.50 | 0.36 | 82.0 | 2340 |
| | OPC N | 500 | 0.41 | 0.36 | 78.0 | 2400 |

concrete of different strength grades. Geopolymer concretes of different strength grades were tested and evaluated according to relevant Australian standards, and were compared against the OPC concrete of the same grades. For the same amount of binder content (kg/m³), this experimental investigation showed that geopolymer binder concrete possesses superior compressive strength compared to OPC concrete. However, the interrelationships between different mechanical properties at the same strength grade appear similar in both types of concrete.

## 3.0 EXPERIMENTAL PROGRAM

Two different strength grades (50 MPa and 65 MPa) of concrete were prepared using OPC and geopolymer binders. The engineering and mechanical properties of different concretes were tested at standard ages of maturity (1, 3, 7, 28, 56, 90 days) as prescribed in AS 3600.

All the geopolymer concretes were prepared in Cement Australia's Darra laboratory without any extra chemical or mineral additive and admixtures such as water reducing admixtures and air entraining agents. However, OPC concrete was prepared adding superplasticiser (Grace ADVA 142) and water reducer (Grace PWR) while mixing in order to maintain workability with low w/c ratio.

The relevant concrete mix design information and 28 day cylinder testing data of each concrete are summarised in the table below.

**Notes:**

1. Standard slumped concrete (N): concrete having maximum aggregate size of 20 mm and 80-120 mm slump.
2. Super workable concrete (SW): concrete having maximum aggregate size of 10 mm and 500-700 mm spread.
3. Geo I: geopolymer I (Powder-Activated General Purpose geopolymer binder)
4. Geo II: geopolymer II (Powder-Activated High Early Strength geopolymer binder).

*Table 2: Measured mechanical properties of different concretes.*

| Concrete Grade (MPa) | Binder Type | Ave. 28 days Compressive Strength ($f_{cm}$) MPa | | Measured Ave. Flexural Strength ($f_{ct\cdot f}$) MPa | | Measured Ave. Indirect Tensile Strength ($f_{ct\cdot sp}$) MPa | | Measured Modulus of Elasticity (GPa) | |
|---|---|---|---|---|---|---|---|---|---|
| | | | Sample Nos. | | Sample Nos. | | Sample Nos. | | Sample Nos. |
| 50 | Geo I N | 67.0 | 8 | 6.5 | 3 | 5.4 | 5 | 36.0 | 3 |
| | Geo II N | 63.5 | 8 | 6.3 | 3 | 5.3 | 6 | 35.0 | 3 |
| | Geo II SW | 59.0 | 6 | 5.6 | 3 | 4.4 | 5 | 28.0 | 3 |
| | OPC N | 62.0 | 6 | 6.3 | 3 | 5.0 | 5 | 33.0 | 3 |
| 65 | Geo I N | 73.0 | 6 | 7.0 | 3 | 5.9 | 5 | 37.0 | 3 |
| | Geo I SW | 73.0 | 6 | 6.4 | 3 | 4.9 | 5 | 31.0 | 3 |
| | Geo II N | 82.5 | 7 | 8.7 | 3 | 6.2 | 5 | 39.0 | 3 |
| | Geo II SW | 82.0 | 6 | 7.1 | 3 | 5.2 | 5 | 33.0 | 3 |
| | OPC N | 78.0 | 6 | 8.4 | 3 | 5.9 | 5 | 37.0 | 3 |

*Table 3: Tensile strength properties of different concretes.*

| Concrete Grade (f'c) MPa | Binder Type | Mean in situ Compressive Strength ($f_{cmi}$) MPa (from AS 3600) | Measured Ave. Indirect Tensile Strength ($f_{ct.sp}$) MPa | Uniaxial Tensile Strength ($f_{ct}$) MPa (from AS 3600) | Characteristic Uniaxial Tensile Strength ($f'_{ct}$) MPa (from AS 3600) | Ratio of Tensile to Compressive Strength (percentage) |
|---|---|---|---|---|---|---|
| | | fcmi = 0.9*fcm | | f ct = 0.9*fct.sp | (f'ct) = 0.36√f'c | fct/fcmi |
| 50 | Geo I N | 60.3 | 5.4 | 4.8 | 2.5 | 8.0 |
| 50 | Geo II N | 57.2 | 5.3 | 4.7 | 2.5 | 8.3 |
| 50 | Geo II SW | 53.1 | 4.4 | 4.0 | 2.5 | 7.5 |
| 50 | OPC N | 55.8 | 5.0 | 4.5 | 2.5 | 8.0 |
| 65 | Geo I N | 65.7 | 5.9 | 5.3 | 2.9 | 8.1 |
| 65 | Geo I SW | 65.7 | 4.9 | 4.4 | 2.9 | 6.7 |
| 65 | Geo II N | 74.3 | 6.2 | 5.5 | 2.9 | 7.5 |
| 65 | Geo II SW | 73.8 | 5.2 | 4.7 | 2.9 | 6.3 |
| 65 | OPC N | 70.2 | 5.9 | 5.3 | 2.9 | 7.6 |

## 4.0 RESULTS AND EVALUATION

In this study, four major mechanical properties – compressive strength, indirect tensile strength, flexural tensile strength and modulus of elasticity of each concrete have been measured according to the relevant Australian Standard (AS 1012). The 28 day testing results for those properties are presented in Table 2. Each data point represents the average value of a minimum of three numbers of samples.

### 4.1 Uniaxial tensile strength

Uniaxial tensile strength was determined by indirect (splitting) tensile testing of cylinders at 28 days of maturity which are presented in the table above. Result shows that the tensile strength property of geopolymer concrete is very similar to that of OPC concrete. However, super workable concrete has lower tensile strength likely due to the smaller sized aggregates and higher volume of binder paste. The ratio of uniaxial tensile to compressive strength of geopolymer concrete is similar to OPC concrete for the 80-120 mm standard slumped concretes.

From AS 3600 (Clause 3.1.1.3),

Characteristic Tensile Strength ($f'_{ct}$) can be estimated as:

$$f'_{ct} = 0.36^* \sqrt{f'_c} \quad (1)$$

For 65 MPa geopolymer I N concrete,

$f'_c$ = 65 MPa, i.e. $f'_{ct}$ = 2.9 MPa (compared to the measured value of 5.3 MPa).

The 28 days mean compressive strength and corresponding uniaxial tensile strength are plotted in Figure 2. A line representing the relationship defined in AS 3600 is also plotted here for a reference.

Considering standard slumped concrete only, above data can be represented by a relationship:

*Table 4: Measured flexural strength and evaluation.*

| Concrete Grade (f'c) MPa | Binder Type | Mean in situ Compressive Strength (fcmi) MPa (from AS 3600) | Measured Ave. Flexural Strength ($f_{ct.f}$) MPa | Characteristic Flexural Strength ($f'_{ct.f}$) MPa (from AS 3600) | Flexural Strength Ratio (Measured / Calculated) | Ratio of Flexural to Compressive Strength (percentage) |
|---|---|---|---|---|---|---|
| | | $f_{cmi} = 0.9^*f_{cm}$ | | $(f'_{ct.f}) = 0.6\sqrt{f'c}$ | $f_{ct.f} / f'_{ct.f}$ | $f_{ct.f}/f_{cmi}$ |
| 50 | Geo I N | 60.3 | 6.5 | 4.2 | 1.53 | 10.8 |
| 50 | Geo II N | 57.2 | 6.3 | 4.2 | 1.48 | 11.0 |
| 50 | Geo II SW | 53.1 | 5.6 | 4.2 | 1.32 | 10.5 |
| 50 | OPC N | 55.8 | 6.3 | 4.2 | 1.47 | 11.2 |
| 65 | Geo I N | 65.7 | 7.0 | 4.8 | 1.45 | 10.7 |
| 65 | Geo I SW | 65.7 | 6.4 | 4.8 | 1.32 | 9.7 |
| 65 | Geo II N | 74.3 | 8.7 | 4.8 | 1.79 | 11.7 |
| 65 | Geo II SW | 73.8 | 7.1 | 4.8 | 1.47 | 9.6 |
| 65 | OPC N | 70.2 | 8.4 | 4.8 | 1.74 | 12.0 |

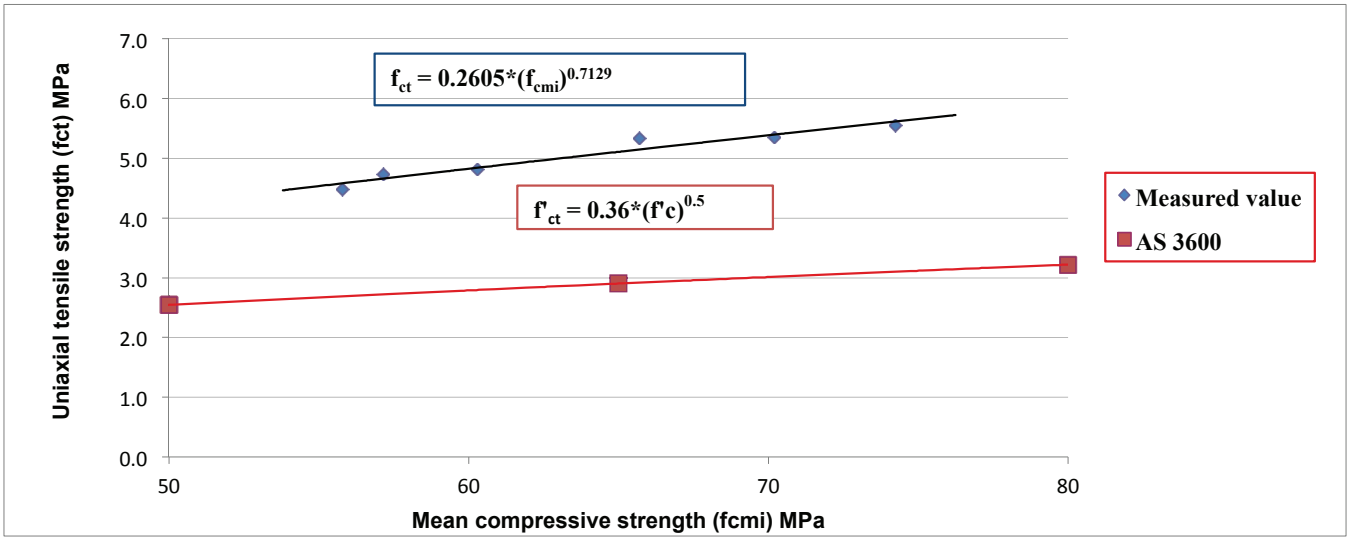


*Figure 2: Relation of tensile strength and compressive strength.*

$f_{ct} = 0.2605*(f_{cmi})^{0.7129}$ (2)

For mean in situ Compressive Strength ($f_{cmi}$) = 65.7 MPa (geopolymer I N, 65 MPa),

Uniaxial Tensile Strength ($f_{ct}$) = 5.15 MPa (close to measured value of 5.3 MPa)

## 4.2 Flexural tensile strength

The flexural tensile strength of concrete was determined by testing of 100 mm x100 mm x 350 mm concrete beams at 28 days of maturity according to AS 1012.11. The data in Table 4 represents the average result from three samples.

This data suggests that standard slumped (80-120 mm slump) geopolymer concrete possesses similar flexural strength to OPC concrete. Similar to the uniaxial tensile strength result, the super workable geopolymer concretes possess lower flexural tensile strength than slumped concrete.

In Table 4, the average Flexural Strength Ratio (measured/calculated) for standard slumped concrete is 1.58 and for super workable concretes is 1.37. The flexural tensile strength attained by geopolymer concrete is found to be higher than the calculated value from AS 3600.

From AS 3600 (Clause 3.1.1.3),

Characteristics flexural Tensile Strength ($f'_{ct.f}$) can be estimated as:

$(f'_{ct.f}) = 0.6* \sqrt{f'_c}$ (3)

For 65 MPa geopolymer I N concrete, $f'_c$ = 65 MPa, ie; ($f'_{ct.f}$) = 4.8 MPa (compared to the measured value of 7.0 MPa).

Using the above data, a graph can be plotted between measured flexural tensile strength ($f_{ct.f}$) and mean in situ compressive strength ($f_{cmi}$). Since super workable concrete behaves in a different way to standard slumped concrete, the graph considers standard slumped concretes only.

The 28 days mean compressive strength and corresponding flexural tensile strength are plotted in Figure 3. A comparison with AS 3600 relationship is also presented here.

Figure 3 can be represented by a relationship:

$f_{ct.f} = 0.0421*(f_{cmi})^{1.2358}$ (4)

For mean in situ Compressive Strength ($f_{cmi}$) = 65.7 MPa (geopolymer I N, 65 MPa),

Flexural Strength ($f_{ct.f}$) = 7.4 MPa (close to measured value 7.0 MPa)

## 4.3 Modulus of elasticity

The modulus of elasticity of different concretes was determined using the static chord modulus of elasticity method (AS 1012.17) at 28 days of maturity. Each data point in Table 5 represents the average result from three samples.

The results show the similarity in modulus of elasticity of geopolymer concretes and OPC concretes. Following the previous trend, super workable concretes possess lower elastic modulus than slumped concrete.

Mean modulus of elasticity ($E_{cj}$) calculated from AS 3600 (Clause 3.1.2),

For 65 MPa, geopolymer I Slumped concrete,

Mean compressive strength ($f_{cmi}$) = 65.7 MPa and density= 2420 kg/m$^3$

$Ecj = \rho^{1.5} (0.024 \sqrt{f_{cmi}} + 0.12)$ MPa; when $f_{mci}$ >40 MPa (5)

Calculated modulus of elasticity (Ecj) = 37.4 GPa (similar to measured value of 37.0 GPa)

According to ACI 318 - 08;

$Ec = 0.043\rho^{1.5}*\sqrt{f'c}$ (6)

Calculated modulus of elasticity (Ec) = 41.3 (higher than measured value of 37.4)

The above data and calculation suggest that AS 3600 can be applied to estimate the modulus of elasticity of both OPC and geopolymer concretes. Another noticeable factor in this relationship is that it is based on average mean in situ compressive strength rather than characteristic compressive strength (in ACI method), which is a practical approach.

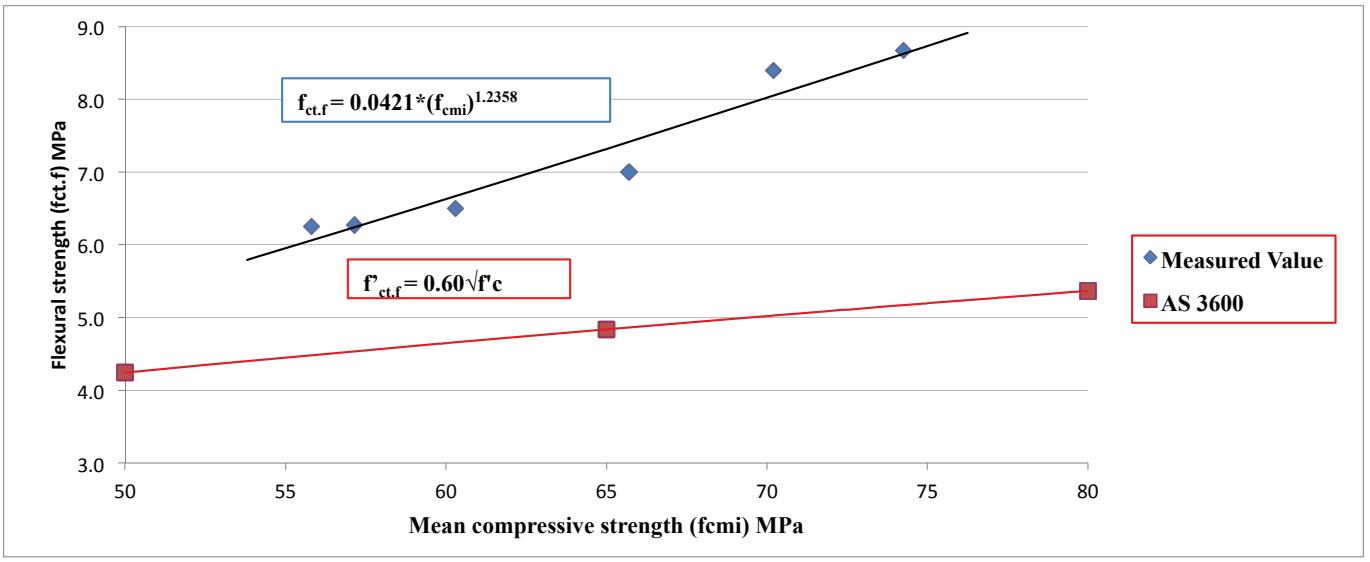


*Figure 3: Relation of flexural tensile strength and compressive strength.*

### 4.4 Poisson's ratio

The Poisson's ratio (v) of different concretes was determined according to AS 1012.17 at 28 days of maturity.

According to AS 3600 (Clause 3.1.5) Poisson's ratio for concrete shall be taken as 0.2 or determined by test according to AS 1012.17.

Unlike other mechanical properties, no equation or relationship is suggested to estimate the Poisson's ratio of concrete from characteristic compressive strength.

The results show the Poisson's ratio of geopolymer concrete is similar to OPC concrete and close to the recommended value by AS 3600 (0.2). In this study, super workable concretes show slightly higher Poisson's ratio value than slumped concrete. However, without enough data of different strength grades of concretes, it is difficult to explain whether or not Poisson's ratio depends on compressive strength of concretes and their type.

## 5.0 CONCLUSION

The main objectives of this study were to examine and evaluate the engineering and mechanical properties of geopolymer binder concrete. As geopolymers are new binding materials, a wide range of research and development work is still necessary to verify this material being as reliable as OPC for the construction industry.

Despite having different chemistry and setting and hardening processes, geopolymer concrete possesses similar engineering and mechanical behaviour to conventional OPC concrete. This work shows major mechanical properties such as indirect tensile strength and flexural tensile strength of geopolymer concretes were found to be higher than calculated value by AS 3600. The modulus of elasticity of geopolymer concrete appears to be able to estimate accurately using the equation defined in AS 3600.

In addition to 50 MPa and 65 MPa strength grade concretes, this research is being expanded to investigate the relevant

*Table 5: Modulus of Elasticity (MoE) testing results and evaluation.*

| Concrete Grade (f'c) MPa | Binder Type | Mean in situ Compressive Strength ($f_{cmi}$) MPa | Measured Average MoE (GPa) | Average cylinder density (ρ) kg/m³ | Calculated mean MoE According to AS 3600 (Ecj) (GPa) |
|---|---|---|---|---|---|
| | | $f_{cmi}$ = 0.9*fcm | | | $(\rho^{1.5})*(0.024\sqrt{f_{cmi}}+0.12)$ |
| 50 | Geo I N | 60.3 | 36.0 | 2420 | 36.5 |
| 50 | Geo II N | 57.2 | 35.0 | 2420 | 35.9 |
| 50 | Geo II SW | 53.1 | 28.0 | 2340 | 33.4 |
| 50 | OPC N | 55.8 | 33.0 | 2380 | 34.7 |
| 65 | Geo I N | 65.7 | 37.0 | 2420 | 37.4 |
| 65 | Geo I SW | 65.7 | 31.0 | 2320 | 35.1 |
| 65 | Geo II N | 74.3 | 39.0 | 2420 | 38.9 |
| 65 | Geo II SW | 73.8 | 33.0 | 2340 | 36.9 |
| 65 | OPC N | 70.2 | 37.0 | 2400 | 37.8 |

*Table 6: Poisson's Ratio (v) of different concretes.*

| Concrete Grade (f'c) MPa | Binder Type | Mean in situ Compressive Strength ($f_{cmi}$) MPa | Samples Number | Average Poisson's Ratio (v) |
|---|---|---|---|---|
| 50 | Geo I N | 60.3 | | |
| 50 | Geo II N | 57.2 | | |
| 50 | Geo II SW | 53.1 | 3 | 0.24 |
| 50 | OPC N | 55.8 | | |
| 65 | Geo I N | 65.7 | 3 | 0.20 |
| 65 | Geo I SW | 65.7 | 3 | 0.23 |
| 65 | Geo II N | 74.3 | 3 | 0.21 |
| 65 | Geo II SW | 73.8 | 3 | 0.21 |
| 65 | OPC N | 70.2 | 3 | 0.21 |

engineering and mechanical properties of 40 MPa and 80 MPa grades of geopolymer as well as OPC concretes for comparison. This final outcome of all 40 MPa, 50 MPa, 65 MPa and 80 MPa strength grades of concretes will give a clearer picture about the interrelationships between different mechanical properties of geopolymer concrete over a broader range of application.

## ACKNOWLEDGEMENT

The authors are grateful to Cement Australia for its financial, technical and other support in this research work and the Faculty of Engineering and Information Technology, University of Technology Sydney for providing guidance in research.

## REFERENCES

1. Davidovits, J., "Geopolymers and Geopolymeric Materials", *Journal of Thermal Analysis,* Vol. 35, 1989, pp. 429-41.
2. Davidovits, J., "Geopolymers – Inorganic Polymeric New Materials", *Journal of Thermal Analysis,* Vol. 37, 1991, pp. 1633-1656.
3. Davidovits, J., "Environmentally Driven geopolymer Cement Applications", Geopolymer 2002 Conference, October 28-29, 2002, Melbourne, Australia.
4. Sagoe, K., Brown, T. et al., "Engineering properties of Si-rich geopolymer binder systems", The 24th Biennial Conference of the Concrete Institute of Australia, 2009, Sydney.
5. Rangan, B.V., Hardjito, D. et al., "Sulfate and Acid resistance of Fly Ash-based Geopolymer Concrete", Curtin University of Technology, 2005, Perth, Australia.
6. McKenzie, C., "A report on Durability Characteristic of Geopolymer Concrete", Griffith University, QLD (Industrial Affiliates Program 2011).
7. Sen, N., "A report on Thermal Characteristic of Geopolymer Concrete", Griffith University, QLD (Industrial Affiliates Program 2011).
8. Lyon R.E., Davidovits, J. et al., "Fire Resistant Aluminosilicate Composites", *Fire and Materials,* Vol. 21, 1997, USA.
9. Rangan, B.V., Hardjito, D., et al., "On the Development of Fly Ash-based Geopolymer Concrete", *ACI Materials Journal,* Vol. 101, No. 6, Nov-Dec 2004.
10. Tippayasam, C., Boonsalee, S. et al., "Geopolymer Development by Powders of Metakaolin and Wastes in Thailand", *Advances in Science and Technology,* Vol. 69, 2010 pp. 63-68.
11. Drechsler, M. and Graham, A., "Geopolymers – An Innovative Materials Technology Bringing Resources Sustainability to Construction and Mining Industries", 48th Institute of Quarrying Conference, 2005, Adelaide SA.
12. Kidd P., "One-Part Dry Mix geopolymer Binder", Ambient Cured Geopolymer Program, 2009, Cement Australia, Darra, QLD.
13. Cement Australia, "Various data about Ingredients and Engineering Properties of geopolymer Binders" provided by Des Chalmers, Peter Sleep and Paul Kidd, 2011, Darra, QLD.
14. Crentsil, K. and Brown T., "Role of oxide ratios on strength development and engineering properties of geopolymer mortars", The 23rd Biennial Conference of the Concrete Institute of Australia, 2007, Adelaide SA.
15. Temuujin, J., Riessen, A. et al., " Influence of Calcium Compounds on The Mechanical Properties of Fly Ash geopolymer Pastes", *Journal of Hazardous Materials,* Vol. 167, 2009.
16. Kong, D. and Sanjayan, G., "Effect of elevated temperate on geopolymer paste, mortar and concrete", Cement and Concrete Research Vol. 40; 2010, pp. 334-339.
17. Bakharev, T., "Resistance of geopolymer materials to acid attack", *Cement and Concrete Research* Vol. 35, 2005, pp. 558-670. Standards Australia; *AS 3972, AS 1379, AS 1012, AS 3582* and *AS 3600* etc.
18. American Concrete Institute, "Building code requirements for Structural Concrete (ACI 318-08)", ACI Committee 318, 2008.

# LATEST TITLES

*Concrete Institute of Australia members are welcome to use the Cement Concrete and Aggregates Australia's library services. The library is located at the CCAA's Sydney office on Level 10, Altitude Corporate Centre, 163-175 O'Riordan Street, Mascot NSW. The databases can be accessed electronically via* **www.concrete.net.au**. *The postal address is PO Box 124, Mascot NSW 1460. Phone: 02 9667 8320 Fax: 02 9693 5234, email:* **library@ccaa.com.au**.

## ACI Physical testing of cement training video (DVD – total running time: 1:42:51)

*ACI COMMITTEE E905, TRAINING PROGRAMS, TASK GROUP, ACI, 2013*

The ACI Physical Testing of Cement Training Video is a resource for new Portland cement testers and a refresher for experienced testers. The video is presented in chapters based on test methods so each can be reviewed individually. Each chapter reviews the equipment specific to the ASTM test, the procedure to follow the test, and calculation of the result. Helpful tips are provided throughout to improve a technician's knowledge and technique.

## *fib* Bulletin No. 69: Critical comparison of major seismic codes for buildings

*THE INTERNATIONAL FEDERATION FOR STRUCTURAL CONCRETE, 2013*

*fib* Bulletin 69 illustrates and compares major buildings seismic codes applied in the US, Japan, New Zealand, Europe, Canada, Chile and Mexico. *fib* Bulletin 69 represents a useful, unique instrument for rapidly gaining an overview of the distinguishing features of major world codes, of their conceptual framework and application rules.

## SP-295: Recent advances in the design of prestressed concrete piles in marine structures in seismic regions

*OSPINA, C. E., FRIZZI, R. P., D'ARGENZIO, DE. (Eds.) ACI, 2013*

This CD consists of eight papers presented at a technical session sponsored by ACI Committees 357, 423, and 543 at the ACI Convention in Minneapolis in the United States in April 2013. The papers cover key aspects which are relevant to seismic analysis, design, detailing and experimental testing of precast prestressed concrete piles as substructure elements of marine structures.

## *fib* Model code for concrete structures 2010 (MC2010)

*THE INTERNATIONAL FEDERATION FOR STRUCTURAL CONCRETE, 2013*

The objectives of the *fib* Model Code 2010 are to serve as a basis for future codes for concrete structures and to present new developments on concrete structures, structural materials and new ideas. The Model Code for Concrete Structures 2010 is now the most comprehensive, focusing on concrete structures, including their complete life cycle: conceptual design, dimensioning, construction, conservation and dismantlement. It is expected to become an important document for both national and international code committees, practitioners and researchers.

## Principles of pavement engineering, 2nd edition

*THOM, N.*

*ICE Publishing, 2014*

The second edition provides an in-depth analysis of the principles underlying material behaviour, pavement design and maintenance for pavement engineers and infrastructure experts faced with practical design issues for which transient standards are insufficient. Covering soils, granular materials, hydraulically-bound materials (including concrete), and asphalt, this publication explains their various properties and the way in which they are affected by compaction, water content and binder content. New information on warm-mix and cold-mix asphalt; design against potholes; and stress absorbing membrane interlayers is included.

## Curing concrete

*TAYLOR, P. C., CRC, 2013*

Curing Concrete explains exactly why curing is so important and shows how it is best done. The book covers the fundamentals behind hydration; how curing affects the properties of concrete, improving its long-term performance; what curing technologies and techniques you can use for different applications; and how to effectively specify, provide, and measure curing in a project. Curing Concrete also explores US and European Standard specifications, making the book applicable for international use.

## 9th RMS Annual Bridge Conference: Bridge journey through partnership, 4-5 December 2013, Sydney. [papers] *NSW Govt, Roads & Maritime Services, 2013*

The RMS Annual Bridge Conference continues to serve the bridge community as a conduit in sharing innovations, sustainable solutions and emerging technologies relevant to the future. Understanding the interests and capabilities of our partners is one of the important challenges faced by us is to deliver effectively "more for less".

## Mathematical excursions to the world's great buildings

*HAHN, A. J., Princeton University Press Oxford, 2012*

This book takes readers on a tour of the elementary mathematics of some of the world's most spectacular buildings and combines this with an in-depth look at their aesthetics, history, and structure. Hahn guides readers through Greek, Roman, Islamic, Romanesque, Gothic, Renaissance and modern styles of architecture, exploring the Pantheon, Hagia Sophia, the Great Mosque of Cordoba, Saint Peter's Basilica, the Duomo in Florence, Palladio's villas, and the Capitol building in the United States. He also introduces some of history's ground-breaking architects.

# New Members

*These companies and individuals recently became members of the Concrete Institute.*

### BRONZE

Mobile Wetbatch Global
Waeger Constructions

### INDIVIDUAL MEMBERS

Jason Birch
Cody Bush
Stephen Foley
Daren King
Sanjay Patel
Darragh Rabbitte
Julian Schlesinger
Warrick Smith
Ozgur Tasyurek
Derek Westerland
Arthur Yencken

### INDIVIDUAL YOUNG MEMBERS

Tian Sing Ng
Rocky Vasile
Keith Wilmoth

### STUDENT MEMBERS

Joseph Bechara
Joshua Buckham
Andre De Villiers
Eloise Gordon
Weijun Huang
Darren Kosh
Rex Lin
Graciela Lopez Alvarez
Asif Maskati
Chris Moore
Nicholas Murphy
Thana Prekpanarut
Samuel Rech
Malindu Sandanayake
Andrew Shehadeh
Kristian Smolic
Jayaprasad Thampi
Michael Thiess
John Yap

# Academic Institutions

**Curtin University of Technology**
**Deakin University**
**Griffith University**
**James Cook University**
**Monash University**
**Northern Melbourne Institute of TAFE**
**Qld University of Technology**
**RMIT University**
**Swinburne University of Technology**
**University of NSW**
**University of Queensland**
**University of Sydney**
**University of South Australia**
**University of Southern Qld**
**University of the Sunshine Coast**
**University of Technology, Sydney**

# Bronze Plus Members

Actech International
Australasian Concrete Repair Association
BAM
BG & E
Bornhorst & Ward
Brenntag Australia
Brisbane City Council
Brown Consulting (WA)
Cairns Industries
Concrete Colour Systems
Concrete Pipe Association of Australasia
Duratec Australia
Engineered Material Solutions
Golik Concrete
Hallett Concrete
Hobson Engineering
Krystol Group
Mahaffey Associates
Main Roads WA
Queensland Rail
Reinforced Earth
Robert Bird Group
Rocla
Structural Concrete Industries
Sunstate Cement
Thiess
VicRoads
Wood & Grieve Engineers

# Bronze Members

ACOR Consultants
Active Minerals Australia
AECOM
ALS Industrial
Amorphous Silica Association of Australia
Ash Development Association of Australia
Ausenco
Austrak
Australasian (Iron & Steel) Slag Association
Baigents
Bonacci Group
Bridge Design
Brown Consulting (VIC)
Building Chemical Supplies
Byrne Bros Concrete
Central Systems
CITI Commercial Maintenance (CCM Group)
Concretus
Concrib
Concrite
Construction Skills Training Centre
Cozens Regan Williams Prove
CSIRO MIT
Dante Constructions
Dept. Construction & Infrastructure (NT)
Donovan Associates
Dr Fixit Institute of Structural Protection & Rehabilitation
Duggans (Tas)
DW Knox & Partners
EB Mawson & Son
Elite Concrete Protection & Repair
Enstruct Group
Ergon Energy Corporation
FormAction Concrete Civils
Freyssinet Australia
Geoff Ninnes Fong & Partners
Gold Coast City Council
Grocon
Halcrow Group
Henry & Hymas
Intelara
Interspan
Intrax Consulting Engineers
irwinconsult
J F Hull Holdings
Jack Hodgson Consultants
Lesa Systems
McVeigh Consulting
Meinhardt
Mobile Wetbatch Global
Monier
Mott MacDonald Australia
Northern Consulting Engineers
Northrop Engineers
O'Neill Group
Poly-Tech Industrial Flooring
Port of Brisbane Corporation
Postenco
Precast Concrete (Qld)
Pritchard Francis
Prompt Engineering
Ramset
Reinforced Concrete Pipes Australia (WA)
Richmond & Ross
Robertson's Building Products
RSA
Sedgman
Sellick Consultants
Si Powders
Solid Concrete Services
Structerre Consulting Engineers
Structerre WBA
Sunwater
Synergy Pigments (Australia)
TA Taylor (Aust)
Taylor Thomson Whitting
The Construction Store
Turner Builders
Ultrafloor
Vital Chemical
W&G Engineers
Waeger Constructions
Water Corporation (WA)
Westkon Precast Concrete
Whittens
Woolacotts Consulting Engineers

MASTER®
BUILDERS
SOLUTIONS


# 30 BRANDS BECOME ONE: MASTER BUILDERS SOLUTIONS

With more than 100 years of experience, BASF can help you to realise nearly every project you plan. To simplify things further, all brands of construction chemicals by BASF have been combined into one: Master Builders Solutions. Innovative products, long-term experience, specific solutions – finding reliable support for your projects has never been easier.

**Call us today on 1300 227 300 (1300 BASF 00)**
**or visit us at www.basf-cc.com.au**

BASF
The Chemical Company